

Global control of host antiviral responses by rotavirus NSP1

By

Kaitlin A. Davis

A dissertation submitted to Johns Hopkins University in conformity with the
requirements for the degree of Doctor of Philosophy

Baltimore, Maryland

November, 2017

© Kaitlin Davis 2017

All rights reserved.

Abstract

Rotaviruses are a leading cause of severe, life-threatening diarrhea worldwide, primarily in infants and young children. Interferon induction is a key protective host defense mechanism triggered during viral infection, and to combat this response, rotaviruses encode the primary interferon antagonist non-structural protein 1 (NSP1). Expression of NSP1 proteins from diverse rotavirus strains is associated with a decrease in interferon induction, and depending on host species and virus strain, may achieve this result by facilitating the degradation of various host signaling proteins. Most human and porcine strains, including the rotavirus strain OSU, encode an NSP1 capable of facilitating the degradation of β -TrCP, a key regulator of NF- κ B-mediated interferon induction. β -TrCP acts as a substrate adaptor protein of cellular E3 ubiquitin ligases, and by directing degradation of I κ B (inhibitor of kappa B), allows NF- κ B to translocate to the nucleus to induce interferon responses. β -TrCP recognizes and binds a phosphorylated degron (phosphodegron) motif (DSG ϕ xS) within I κ B, and other cellular proteins, to facilitate degradation. The C-terminus of OSU NSP1 harbors a mimic of this motif (DSGIS) that allows for binding and sequestration of β -TrCP. In our studies, we have found that like I κ B, NSP1 is phosphorylated and requires phosphorylation for β -TrCP engagement. Unlike I κ B, NSP1 is a substrate of casein kinase II (CKII). NSP1 is a substrate adaptor protein of cullin-RING ligases (CRLs), and while NSP1 appears to engage cullin 3 via an N-terminal RING domain, C-terminal degron phosphorylation is required for NSP1 incorporation into CRLs. Interestingly, NSP1 proteins that engage interferon response factor (IRF) proteins are able to engage these substrates without phosphorylation. These data suggest that NSP1 proteins may inhibit interferon induction

through binding and sequestration alone, without the specific need for degradation of substrates. Furthermore, many viruses are known to encode proteins that directly engage and direct β -TrCP activity. β -TrCP regulates stability of proteins involved in a number of pathways beyond simply interferon induction, including mTOR. Our studies indicate that OSU infection results in accumulation of DEPTOR, a β -TrCP substrate and negative regulator of mTOR complexes. Analysis of mTOR signaling cascades suggests that control of β -TrCP may result in a pro-viral cellular environment with benefits to viruses beyond promoting rotavirus replication.

Readers:

Advisor: John T. Patton, PhD

Second Reader: Karen Beemon, PhD

Acknowledgments

I've thought often of what I would write for everyone who deserves to be on this page, and the words that come never seem to be quite enough. So many have supported and believed in me throughout these endeavors, and I wouldn't be here without you. Accordingly, it would be near impossible to do you all justice.

First and foremost, this dissertation would not have been possible without the dedication and support of Dr. John T. Patton. Dr. Patton has been an ideal mentor, leader, example, and ally. He has provided the space, environment, and support for me to find myself as a scientist. With just enough eye-rolls, he has encouraged me to think harder and reach higher. He has pushed me to earn respect with my efforts, and has shown me what it means to embody dedication and hard work as life's work. Above all, he has invested himself in my education and my future. I know you hate clichés, and I mean it when I say I can't possibly thank you enough.

Thank you to my committee members Dr. Sarah McDonald, Dr. Karen Beemon, Dr. Xioaping Zhu, and Dr. Kyle Cunningham. You have been inspiring examples of what it means to dedicate yourself, and your support has been transformative. Thank you to Marco Morelli for being a model postdoc in the lab, and for being so visionary (and methodically organized) in your pursuit of NSP1.

I am so grateful to my friends for the integral role they have played in this phase of my life and personal journey. You all are the best distractions and the best cheerleaders I could ask for. Thank you for reminding me what life can be and what it is all for, both inside and outside of science. Christopher J. Obara, I hope you know you will always be family.

And above all, thank you to my parents and my brother. This body of work is for you. You have led me by example, and have never wavered in your support and belief in my success. Thank you for infusing in me the desire to ask boundless questions, and for fanning the flames of my inquisitive nature. Thank you for showing me what independence means and what it feels like. Thank you for seeing me when others didn't, and for reminding me what I am made of. You have taught me so much more than could be contained in any dissertation. I could never have done this without you.

Table of Contents

Abstract	ii
Acknowledgments	iii
Table of Contents	vi
Index of Figures & Tables	x
Chapter 1: Introduction	1
Public health considerations of rotavirus	2
Rotavirus classification	4
Rotavirus particle structure	4
Rotavirus genome structure and organization	8
Rotavirus replication cycle	11
Overview	11
Adsorption	11
Entry	14
Transcription	15
Viroplasm and assortment	18
Replication intermediates	19
Virion morphogenesis, maturation	20
Innate immune responses to rotavirus infection	21
Rotavirus proteins with roles in innate immune evasion, antagonism	26
VP3	26
dsRNA binding protein	26

NSP3	27
NSP4	28
NSP1: A key modulator of cellular immune pathways	29
Research program overview	34
Hypothesis	34
Summary of experimental aims and approaches	34
Significance of study	35
 Chapter 2: Cullin-RING ligases and viral adaptors: novel repurposing of a familiar tool	 38
Abstract	39
Introduction	39
Cullin-RING E3 ubiquitin ligase construction and regulation	41
CRLs as targets of viral manipulation	44
Perspectives and conclusions	52
 Chapter 3: OSU NSP1 as a phosphorylated adaptor protein of cellular E3 ubiquitin ligases	 55
Abstract	56
Introduction	57
Materials and Methods	61
Results	66
Discussion	80

Chapter 4: Shutdown of interferon signaling by a viral-hijacked E3 ubiquitin ligase	87
Main text	88
Chapter 5: Biochemical exploration of human and animal NSP1 proteins	95
Part 1: The pLxIS motif does not require phosphorylation for substrate engagement	96
Abstract	96
Introduction	96
Materials and Methods	100
Results	101
Discussion	105
Part 2: Non-RVA NSP1 proteins harbor interferon antagonist activity	108
Abstract	108
Introduction	109
Materials and Methods	111
Results	114
Discussion	122
Part 3: OSU rotavirus infection affects mTOR signaling through DEPTOR accumulation	124
Abstract	124
Introduction	125
Material and Methods	127

Results	129
Discussion	135
Chapter 6: Conclusion & Discussion	137
References	145
Appendix	182
Curriculum vitae	189

Index of Figures & Tables

Table 1-1. Rotavirus proteins and protein-function nomenclature	5
Table 1-2. Rotavirus non-structural proteins	7
Table 1-3. Rotavirus structural proteins	7
Figure 1-1. Rotavirus particle structure	10
Figure 1-2. Overview of rotavirus life cycle	12
Figure 1-3. A model for rotavirus transcription	17
Table 1-4. PRRs and associated ligands	22
Figure 1-4. Innate immune responses to RNA virus infection	23
Table 1-5. NSP1 C-terminal alignment	30
Figure 2-1. The SCF ^{β-TrCP} ligase targets many cellular proteins to control a myriad of cellular processes	42
Figure 2-2. Schematic depiction of CRLs with viral adaptor proteins	45
Figure 2-3. A model of NSP1 CRL incorporation.	47
Figure 3-1. Targeting of the interferon activation pathway by rotavirus NSP1	60
Figure 3-2. Phosphorylation of transiently expressed OSU NSP1	68
Figure 3-3. Effect of priming loop mutations on NSP1 phosphorylation	70
Figure 3-4. Phosphorylation of NSP1 in rotavirus infected cells	72
Figure 3-5. Effect of CKII inhibition on NSP1 phosphorylation	74
Figure 3-6. Influence of NSP1 phosphorylation on interactions with β -TrCP	76
Figure 3-7. Effect of phosphorylation on interactions with Cul3	79

Figure 3-8. Accumulation of p-NSP1, β -TrCP, and p-I κ B during viral infection	81
Figure 3-9. Predicted steps in the CKII-dependent incorporation of NSP1 into a Cul3-CRL	83
Figure 4-1. NF- κ B induction of interferon	91
Figure 4-2. A model of NSP1-CRL assembly	93
Figure 5-1. Activation of immune adaptor proteins and IRF3	98
Figure 5-2. C-terminal alignment of SA11-like NSP1 proteins	99
Figure 5-3. Effect of NSP1 expression on IRF3 promoter activity	102
Figure 5-4. Effect of pLxIS truncation on NSP1-mediated IRF3 inhibition	104
Figure 5-5. Non-group A NSP1 predicted structural architecture	110
Figure 5-6. Effect of NSP1 expression on NF- κ B activation	115
Figure 5-7. Quantification of NSP1 protein ability to facilitate degradation of β -TrCP or IRF3	117
Figure 5-8. Effect of non-RVA NSP1 expression on ISRE activation	119
Figure 5-9. Effect of non-RVA NSP1 expression on JAK/STAT activation	121
Figure 5-10. Accumulation of DEPTOR during OSU infection	130
Figure 5-11. Effects of drug treatment on DEPTOR accumulation	131
Figure 5-12. Effects of drug treatment and viral infection on mTOR signaling proteins	133

Figure A-1. Long exposure of immunoblot for proteins in infected cell lysate	185
Figure A-2. Detection of ubiquitinated substrates in complex with β -TrCP	187

Chapter 1:

Introduction

Public health considerations of rotavirus

Acute viral gastroenteritis is a major public health concern worldwide, and illness is associated with high annual mortality. Gastroenteritis is associated with diarrhea, vomiting, and severe dehydration, and can be particularly serious for young children in developing countries. A main cause of viral gastroenteritis is rotavirus, a genus of non-enveloped double-stranded RNA (dsRNA) viruses from the *Reoviridae* family.

Rotaviruses were initially recognized as a major cause of gastroenteritis in humans in 1974 (1), but their discovery as animal pathogens predates this finding by a full decade (2). Since their initial identification, rotaviruses of human and veterinary concern have been discovered in the young of many mammalian species, including mice, rats, pigs, cows, dogs, and bats, in addition to some bird species. Rotavirus infection predominantly occurs in the young of affected species, and symptoms can lead to severe debilitating malnourishment or death. An estimated 1.3 million children under the age of five die annually because of diarrheal disease (3), and rotavirus is predicted to account for 37% of deaths due to gastroenteritis in young children (4). Over two million children have died as a result of rotavirus infection in the last 10 years alone, and infections are estimated to cause upwards of 125 million symptomatic human infections each year (5, 6).

Vaccines have recently been made available for both human and veterinary use; however the efficacy of prophylactic vaccination has been met with variable results and with apparent geographical inconsistency. Severe disease occurs disproportionately in underdeveloped countries, with 90% of human deaths occurring in Asia and Africa, and over half in four specific countries (Democratic Republic of Congo, India, Nigeria, and

Pakistan). Almost 22% of these deaths occur in India alone (4). Accordingly, since the introduction and continued use of vaccines in developing countries, it is estimated that the number of global rotavirus-related deaths has declined between 2000 and 2013 to 215,000 annually (4).

Prior to the introduction of rotavirus vaccines in the US in 2006, rotavirus-related medical costs totaled near \$300 million each year (7). The use of a pentavalent human-bovine reassortant vaccine (RotaTeq, RV5; Merck & Co) and a monovalent vaccine (Rotarix, RV1; GSK) has been successful in reducing this burden in the US and other developed countries (8, 9). In clinical trials, vaccines decreased hospitalizations and emergency room visits by almost 95% (9), and vaccine effectiveness approaching 100% (10, 11) has been reported in similar higher-income countries. However, similar results for vaccine programs in developing countries have not been observed, and specifics contributing to these differences remain unclear. In low-income countries, where vaccines offer the greatest lifesaving potential, vaccine efficacy remains at only 40-60% (6).

Symptoms and pathology associated with rotavirus infection have been well described in infected hosts of diverse species. Rotavirus is transmitted primarily via the fecal-oral route, and incubation periods are typically 1-2 days following initial exposure. Infection spreads from the small bowel to the ileum over 1-2 days (12), and most infection and viral replication occurs within mature enterocytes at villus tips of the small intestine. This infection cycle is rapidly lytic and leads to disruption of the gut epithelium, as well as shortening of villi and crypt hyperplasia (13). In addition to compromised absorption within the small intestine, hypersecretion caused by the

rotavirus enterotoxin (NSP4; see page 28) is thought to contribute to diarrheal disease phenotypes (14). Vomiting may precede symptoms of diarrhea, which together, may last for 5 days. Death of infected individuals most often occurs because of severe dehydration and cardiovascular failure. Symptoms can be easily treated and alleviated in developed countries, largely because of access to medical intervention and rehydration measures, but deaths are a common outcome in less developed areas of the world.

Rotavirus classification

The genus *Rotavirus* is one of 15 genera of the *Reoviridae* family. Within this genus, rotaviruses are genetically and antigenically diverse, and can be divided into at least eight groups or species, A-H (15, 16). Rotavirus group A (RVA) is the major cause of pathogenic human infections, and includes genotypes specified by the primary antigenic proteins of the virus. These include the surface and spike proteins of the virus, VP4 (P-type, for protease sensitive protein) and VP7 (G-type, for glycoprotein). A more extensive genotyping system has been developed that incorporates all 11 genome segments of the virus and is based on nucleotide sequence diversity, rather than serotype or genotype (17-19). Table 1-1 demonstrates the nomenclature utilized to denote each genome segment and associated protein(s).

Rotavirus particle structure

The architecture of rotavirus virions reflects the close relationship between replication cycle and the structure of these particles. Mature, infectious particles consist of three concentric protein layers encasing 11 distinct dsRNA genome segments. These

Protein	Acronym	Function
VP7	G	Glycosylated
VP4	P	Protease-sensitive
VP6	I	Inner capsid
VP1	R	RNA-dependent RNA polymerase
VP2	C	Core protein
VP3	M	Methyltransferase
NSP1	A	Interferon antagonist
NSP2	N	NTPase
NSP3	T	Translation enhancer
NSP4	E	Enterotoxin
NSP5	H	Phosphoprotein

Table 1-1. Rotavirus proteins and protein-function nomenclature.

segments code for six non-structural proteins (NSP1-NSP6) (Table 1-2) that aid in viral replication, assembly, and evasion of host antiviral defense mechanisms, and six structural proteins (VP1-VP4, VP6-VP7) (Table 1-3) that form the icosahedral, triple-layered particles (TLPs) (Fig. 1-1, A). TLPs are non-enveloped and by cryo-EM, have a wheel-like appearance that gives rise to the name of the genus (latin, rota) (1). The outermost layer of the particle is formed by trimers of VP7 (780 molecules) arranged with T=13 symmetry, and is studded with protruding VP4 multimeric spikes (60 molecules). Upon trypsin activation, VP4 is cleaved into VP8* and VP5*, the latter which anchors the spike in the shell of the virion. Both VP5* and VP7 make contacts with the intermediate layer, formed by trimers of VP6 (green, Fig. 1-1, B). Below this layer is the inner core shell (blue, Fig. 1-1, B), consisting of 60 VP2 capsid protein dimers (one each of conformation A and B) organized with T=1 symmetry (20).

VP2 dimers are arranged as decamers at each axis of five-fold symmetry (Fig. 1-1, C), with flexible N-terminal arms (~100 residues) that protrude into the center of the particle. Within the VP2 core shell and associated with each decamer is one copy each of the VP1 RNA-dependent-RNA-polymerase (RdRp) and the VP3 capping enzyme (Fig. 1-1, D) (21). Data suggests that VP1 sits slightly off center from the five-fold axis (22); the structure of VP3, which is suggested to sit adjacent to VP1, remains largely unsolved. VP2 N-terminal arms (Fig. 1-1, E, red arrows), too, are structurally unresolved, but their flexibility and non-specific ssRNA binding affinity, in addition to their requirement for activation of VP1 (23), suggest a role in assembly, encapsidation, or mediation of RNA synthesis events. VP1 and VP3, in addition to contacts with VP2, form functional replication complexes.

Genome segment	Size (bp)	Protein	Size (aa; kDa)	Localization	Function
5	1519	NSP1	486; 58	Cytoplasm	Interferon antagonist, RNA binding
7	1016	NSP3	313; 35	Cytoplasm	Translation inhibitor
8	1003	NSP2	317; 35	Cytoplasm, viroplasm	RNA binding/folding, viroplasm formation, assortment & assembly
10	700	NSP4	175; 28	ER	Enterotoxin, DLP ER translocation
11	631	NSP5	197; 21	Cytoplasm, viroplasm	Viroplasm formation
(11)	(631)	(NSP6)	(51; 12)	(Cytoplasm)	(RNA binding)

Table 1-2. Rotavirus non-structural proteins, adapted for rotavirus strain OSU (RVA/Pig-tc/USA/LS00005_OSU/1975). Only some rotavirus strains are reported to encode NSP6.

Genome segment	Size (bp)	Protein	Size (aa; kDa)	Localization	Molecules per virion	Function
1	3271	VP1	1088; 125	Core	12	RdRp
2	2683	VP2	890; 100	Core	120	Core shell, RdRp regulation
3	2529	VP3	835; 98	Core, cytoplasm	12	Guanylyltransferase, methyltransferase, interferon antagonist
4	2336	VP4	776; 85	Outer layer	180	Receptor attachment, cleaved to VP4 and VP8
6	1315	VP6	397; 45	Intermediate layer	780	Structural integrity
9	1023	VP7	326; 37	Outer layer	780	Structural integrity, receptor binding

Table 1-3. Rotavirus structural proteins, adapted for rotavirus strain OSU (RVA/Pig-tc/USA/LS00005_OSU/1975).

By close examination, the rotavirus virion shell is perforated with pores and channels that align with axes of symmetry. Virions have 132 channels that constitute three classes. Twelve of these channels (Class I) are located at axes of five-fold symmetry, in alignment with VP1 and VP3 in the inner core shell (24, 25). Class II channels pass through axes of three-fold symmetry (60 channels) and Class III channels exist at axes of two-fold symmetry (60 channels). Because rotavirus particles do not entirely disassemble in the cytoplasm of infected cells, these channels likely play valuable roles in nucleotide exchange and extrusion of nascent positive-sense RNAs (+RNAs) from transcriptionally active particles.

Rotavirus genome structure and organization

The segmented, dsRNA genome of rotavirus is approximately 18.5 kilobases (kb) in total, and is comprised of segments ranging in size from 0.5 to 3.3 kb. Within the rotavirus particle, the genome segments form contacts with replication complexes, with each segment interacting with an individual VP1 RdRp. RNAs produced by VP1 from individual genome segments within the particle exit through Type I channels, and data suggests each channel is specific for a single mRNA (26). These assignments are thought to be consistently arranged and maintained between particles (26). This inter-particle genomic organization is likely shared with other dsRNA viruses within the *Reoviridae* family, such as blue tongue virus (27).

It has been postulated that genome segments within the particle are arranged to form conical cylinders, increasing in diameter from the center of the particle to the distal interior boundary where contacts can be made with VP1 (20, 28). The genomic RNA in

TLPs is thought to be held in a rigid, peri-crystalline state, as the preferred geometry of dsRNA is to form a rigid rod. By cryo-EM, curved, concentric layers of RNA can be observed in the interior of actively transcribing particles (Fig. 1-1, E) (29). While atomic resolution structures of double- and triple-layered particles (DLPs, TLPs) have revealed in fine detail the organization within and between capsid protein layers, much less information is available describing the organization of the dsRNA within these particles.

While genome segments vary in length and composition, they share prototypical organization. Each segment is arranged as a central ORF with conserved 5' and 3' untranslated regions (UTR) terminal sequences. These ORFs are monocistronic, except for some RV strains which encode a second protein from genome segment 11 (30). The UTR sequences range from 9-48 nucleotides at the 5' end and 17-182 nucleotides at the 3' terminus. These ends are partial inversions with complementarity and likely facilitate long-range interactions in single-stranded (ss) +RNAs, which fold to form panhandle-like structures (31). The 3' UTR sequence UGUGACC engages the VP1 RdRp and VP3 (32, 33), and likely interacts with NSP3 during translation (34). During replication, segments are modified through the addition of a 5' cap structure (m^7GppG) mediated by the VP3 capping enzyme (guanylyltransferase-methyltransferase) (35).

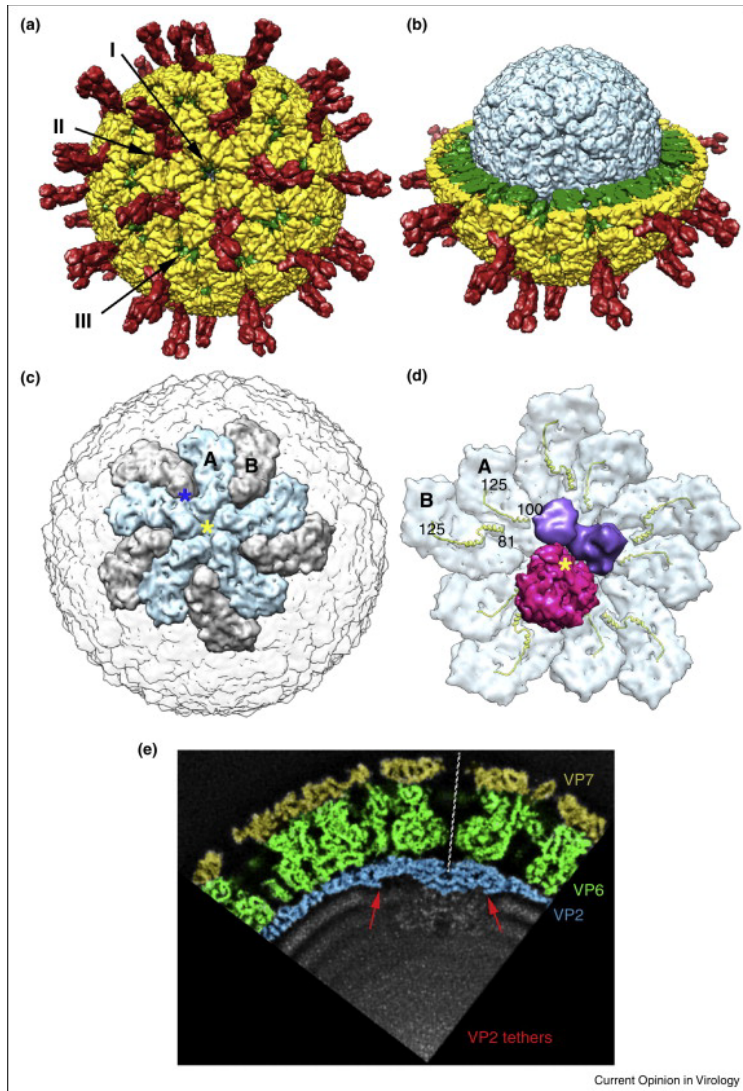


Figure 1-1. Rotavirus particle structure, adapted from Gridley & Patton (29).
 (a) A mature rotavirus virion (TLP), with VP7 in yellow, VP4 in red. Arrows point to Type I, II, and III channels. (b) Under the outer VP4/VP7 layer is the intermediate VP6 layer (green), and the innermost VP2 core shell (blue). (c) The inner core shell is formed by 12 decamers of VP2, each constructed of 5 copies each of VP2 folded in conformation A and B. Type I channels run through the center of each decamer, the center of five VP2-A molecules (yellow asterisk), and Type II channels sit at the inner tip of VP2-B molecules (blue asterisk). (d) On the underside of each decamer, within the core, one VP1 RdRp (pink) and one VP3 molecule (purple) associate with VP2 proteins. Unstructured VP2 tethers are shown as yellow ribbons, and extend 80-100 residues. (e) A slice of a cryo-EM image of a mature TLP, colored to reflect individual protein layers (yellow VP7, green VP6, blue VP2). dsRNA density appears as concentric rings within the particle. A portion of the VP2 tethers can be observed (red arrows). Additional density at the five-fold axis corresponds to VP1 and VP3.

Rotavirus replication cycle

Overview

In the gastrointestinal tract, exposure of virions to trypsin-like proteases cleaves VP4 spikes (red, Fig. 1-2) into VP5* and VP8* to yield infectious virions capable of entry into target cells. The outer shell capsid proteins facilitate virion attachment to cells via sialic acid and other specific cellular surface receptors. Most rotavirus strains enter cells by clathrin-mediated endocytosis (36). Low calcium concentrations in endosomes trigger membrane penetration and shedding of the outer virion shell to yield double-layered particles (DLPs), activating the encapsidated replication complexes to transcribe from dsRNA genome segments. Transcripts (+RNAs) are translated to produce viral proteins, or accumulate in viroplasms with other viral components to act as templates for minus-strand (-RNA) replication. Replication occurs as the +RNA strands interact with VP1 and VP3 via the conserved 3' UTR, and commences as the VP2 core shell engages the VP1 RdRp. The intermediate VP6 layer assembles on the core to form a DLP, which buds into the ER and acquires a VP4/VP7 layer before egress via lysis or in exosomal membrane bound packets. This has been observed for other RNA viruses to enhance transmission and reassortment (37).

Adsorption

Rotavirus infection occurs primarily in mature enterocytes at the epithelial tips of intestinal microvilli, and adsorption and entry into these cells is a complex, multistep process. Both VP7 and VP4 play roles in binding to cells, but rotavirus particles must

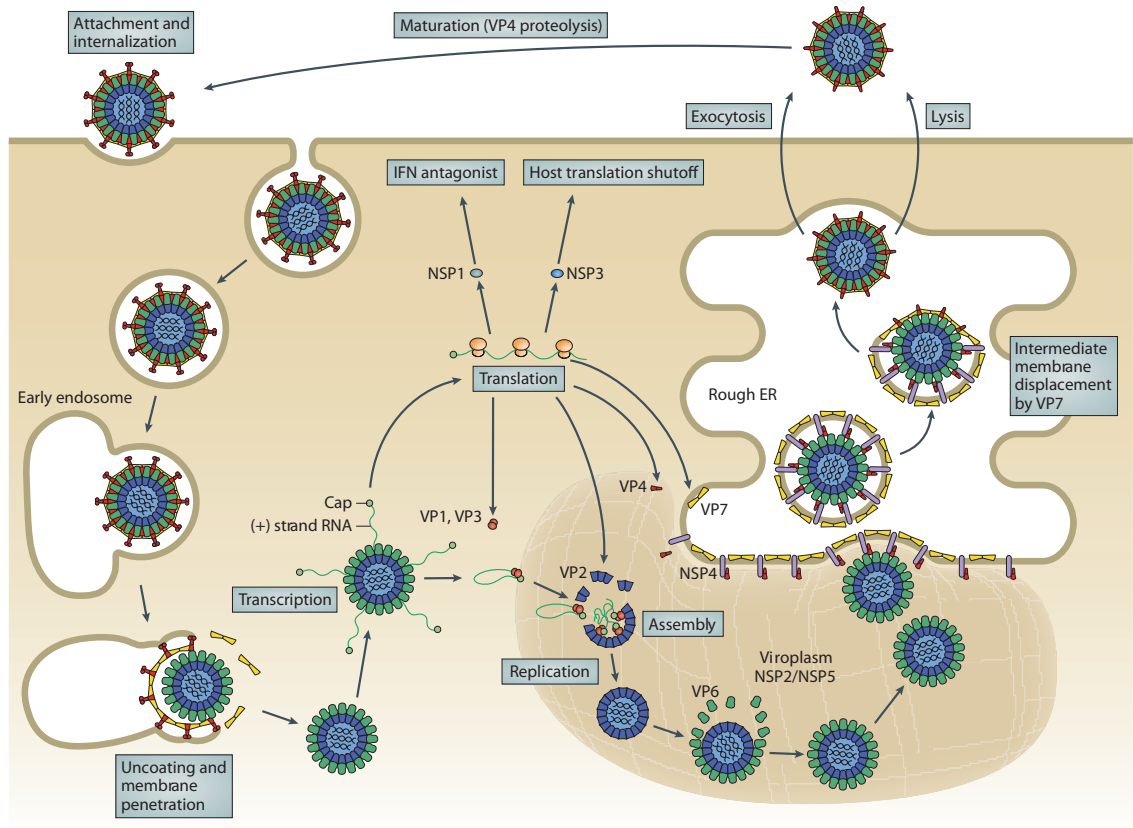


Figure 1-2. Overview of rotavirus life cycle, from Trask, et al. (24). Rotavirus virions attach to target cells through VP8* (red) interactions with surface receptors such as sialic acid. Virions enter through various endocytic processes, and in early endosomes, low calcium concentrations allow uncoating of VP7 (yellow), and subsequent membrane penetration. Released DLPs are transcriptionally active, and ssRNAs produced by VP1 and capped by VP3 serve as templates or replication (minus strand synthesis). Proximal to the ER, NSP2 and NSP5 form viroplasm where replication, assortment, and assembly take place; VP1, VP2, and VP3 interact with RNAs during the assortment process (mediated by NSP2), and assemble into viral cores coated by VP6, forming DLPs. DLPs bind NSP4 on the ER surface, mediating entry into the ER lumen, where they acquire a VP4 and VP7 layer. Assembled TLPs are released from cells by exocytosis or lysis, and encounter trypsin, which cleaves VP4, resulting in a mature particle.

encounter trypsin-like proteases in order to be infectious; trypsin cleavage of VP4 yields VP5* and VP8*. This cleavage process uncovers a shallow groove on the surface of VP8* that can bind sialic acid residues, and rotaviruses can be divided based on preference for a terminal or internal sialic residue. Internal sialic acid is insensitive to neuraminidase treatment, thus resulting in “neuraminidase-resistant” classification for some strains, such as human DS-1 and Wa (38). Most human strains are neuraminidase resistant, whereas some animal strains require sialic acid for attachment (39). Some VP8* additionally bind to non-sialic acid containing histo blood group antigens via a Gal β 1-GlcNAc motif (40-42). These strains have either H-type or A-type glycan binding specificity (40). Some strains also require a functioning FUT2 enzyme (43), which is crucial in mediating entry of other enteric pathogens, such as norovirus.

VP5* and VP7 glycoproteins mediate interactions with most co-receptors, such as integrins (α 2 β 1, α v β 3, α x β 2, α 4 β 1) (39). Rotavirus may also interact with the heat shock cognate protein hsc70, although the order of events mediating coreceptor interaction and their roles in attachment and entry are less defined (36, 44, 45). All known co-receptors are associated with lipid rafts, and these detergent resistant membrane regions are required to facilitate rotavirus entry (39, 46). The relative importance of the various receptors and coreceptors continues to be addressed (47). It is of particular interest that silencing, blocking, or inhibiting all known receptors and cofactors reduces rotavirus infectivity by less than 1 log (48), suggesting there may be additional pertinent factors that have yet to be described.

Entry

The process by which rotavirus particles enter cells is contentious, but many studies have emphasized the importance of VP4 trypsin cleavage in entry (49, 50). Prior to cleavage, VP4 spikes are flexible, but their structure is nearly identical to the more rigid post-cleavage VP4 (49). Following binding to cellular receptors, spikes undergo conformational changes to expose lipophilic domains of VP5* (51), a transition favored by the post-cleavage VP4 (49). Following binding and conformational transition, entry steps are less clear. Rotavirus was initially thought to enter cells through direct penetration (52), although more recent data suggests that diverse endocytic pathways are recruited for this process and vary by virus strain. Most human and animal strains enter cells via clathrin-mediated endocytosis (36) (53), but the simian virus RRV, an integrin-dependent neuraminidase-sensitive strain, uses an alternative endocytic pathway and is independent of clathrin and caveolin (36, 54). VP4 is likely responsible for observed endocytic pathway preference differences (36) (53). Regardless of strain and pathway, however, RNAi screens confirm the role of multiple endosomal sorting complex required for transport (ESCRT) pathway machinery in rotavirus entry processes (55).

Upon internalization, and regardless of the entry pathway utilized, rotavirus particles enter maturing endosomes. Virus strains require the formation of intraluminal vesicles (ILVs), characteristic structures of maturing endosomes, that are formed by ESCRT machinery (56). While RRV only requires maturing endosomes, those viruses that enter via clathrin-mediated endocytosis must also migrate to late endosomes to establish infection (57). In this cellular compartment, low Ca^{2+} ion concentrations lead to solubilization of the outer capsid layer, yielding double-layered particles (DLPs) (58).

Beyond this change in virion composition, the precise mechanism of membrane penetration remains unclear, but it appears to be a rapid process associated with membrane disruption and gross morphological changes (59).

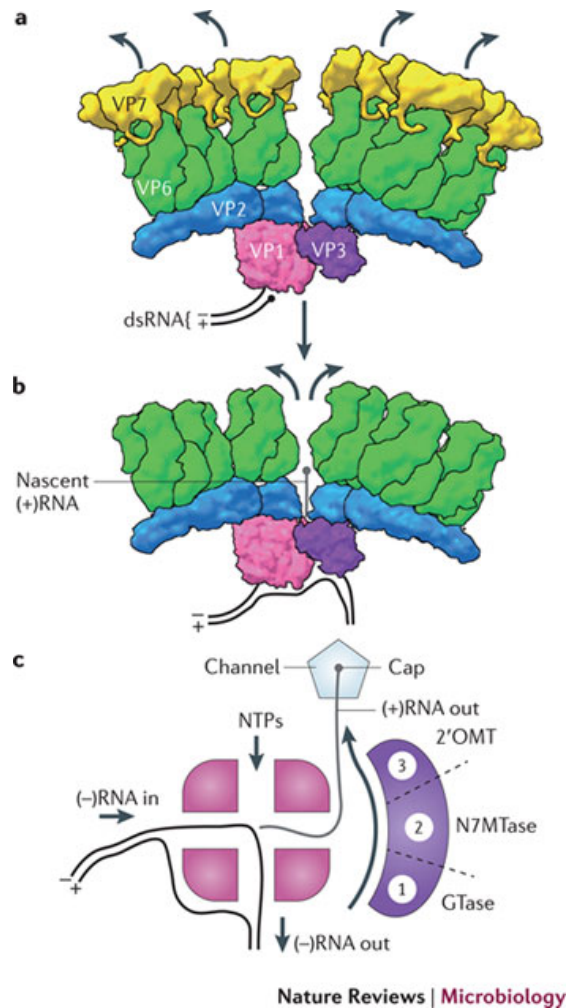
Transcription

Loss of the outer capsid proteins during particle entry leads to membrane penetration and the release of transcriptionally active double-layered particles (DLP) into the cytoplasm. These particles rapidly diffuse inward, away from the site of initial entry. Dissociation of the outer VP4 and VP7 capsid layer allows for expansion of the particle and of the Type I channels (60), through which nascent RNAs are extruded. DLPs are transcriptionally active both in the cytoplasm and *in vitro*, and these particles are capable of generating large amounts of RNA, within the mg range (60, 61). Experiments with fluorescently-tagged particles suggest that the uncoating efficiency of membrane-bound virions can reach up to 50%, and that RNA synthesis can be detected as early as 15 minutes post infection (p.i.) (62); RNA synthesis by even a single particle is sufficient to initiate infection.

Within DLPs, each VP1 polymerase, paired with a VP3 methyltransferase, interacts with a VP2 decamer to initiate transcription (24, 63). Each of these transcription complexes interacts with a single dsRNA genome segment (26) to produce positive sense ssRNAs with a 5' cap structure (m^7GppG) that are not poly-adenylated (35) (Fig. 1-3, a, b, c). Newly generated ssRNAs serve as templates for translation and as templates for replication upon packaging into newly forming particles (32).

The VP1 polymerase is a hollow, channeled, globular enzyme with a conserved right-handed polymerase domain. The N- and C-terminal domains associated with this protein are well-conserved and are unique to the RdRp enzymes of the *Reoviridae*. Four channels lead to the catalytic center of the enzyme, and serve as entry and exit sites for nucleotides, template RNAs, and for nascent RNA products (Figure 1-3, c). VP1 transcription is a conservative process; negative-sense genomic RNA enters through one channel towards the catalytic center and exits through a second channel towards the particle core where it reanneals with genomic positive-sense RNA. Nascent positive-sense ssRNAs are directed out a third channel towards VP3 (61). The fourth channel serves as an entry site for NTPs.

Despite advances in research describing transcriptionally active rotavirus particles, it remains uncertain how structural changes within entering virions and the transition from TLP to DLP induce transcription. It is clear that removal of the outer capsid shell has structural consequences resulting in the expansion of the DLP and its exit channels in a process that can be reversed through in vitro recoating of these particles (64, 65). Retention of the VP6 intermediate layer is crucial for VP1 transcriptional activation (66), and antibodies that bind to this layer can be inhibitory for transcriptional activity (67). It is currently unknown whether additional changes are required to initiate transcription within the particle, or if initiation results simply due to the increase in particle diameter. Interestingly, the amount of ssRNA made per dsRNA template is not equimolar (68, 69), and the relationship or coordination between replication complexes within particles has not been fully explored. Whether active complexes are synchronized or may operate independently is unknown. It has also been suggested that there may be



Nature Reviews | Microbiology

Figure 1-3. A model for rotavirus transcription, from Trask, et al. (24). During the entry process, particles lose the outer VP7 layer (yellow) (a), releasing a DLP (b) into the core. Loss of this layer allows for expansion of the particle and of exit channels through the VP2 (blue) and VP6 (green) layers, permitting extrusion of nascent RNA transcripts, generated by VP1 from the dsRNA templates within the core. (c) Four channels run through the RdRp, allowing for entry of a minus strand template, entry of NTPs, exit of newly formed ssRNAs, and exit of the template strand to reanneal with its positive-sense pair. New ssRNAs are capped by VP3 prior to extrusion from the particle through the Type I channel at the center of each VP2 decamer (blue pentagram). VP3 has domains that accomplish the activities of a guanylyltransferase, N-7-methyltransferase, and a 2'-O-methyltransferase.

additional rounds of transcription that occur during particle formation, not just from post-entry DLPs (69).

Viroplasms & Assortment

Little is known about the processes that govern rotavirus assortment and packaging intermediates, in part because these processes take place in electron-dense structures called viroplasms (70). Viroplasms are formed through the activities of NSP2 and NSP5, and while colocalization of these proteins and structures is clear, details outlining their formation processes are scarce. NSP2 is an octameric, RNA-binding protein (71) that interacts directly with the NSP5 phosphoprotein (72, 73), which is largely disordered and remains unsolved. Exogenous expression of NSP2 and NSP5 in the absence of active infection is sufficient to drive formation of viroplasm structures (74). Because it is hypothesized that the location of nascent viral ssRNAs determines their role as either translation or replication templates, it has been suggested that viroplasms function to sequester viral RNAs and proteins to drive assembly; indeed, viral ssRNAs associated with these structures are selectively packaged and replicated within newly assembling viral cores (75). Additionally, the number and size of viroplasms increase in a manner that correlates with multiplicity of infection (MOI) (76), but whether these structures form directly at points nucleated by entering virions or form independently by another process remains unclear.

Genome replication is known to be coupled with assembly, but the lack of *in vitro* packaging assays and only recent availability of a reverse genetics system (77) has made these processes difficult to study. Studies with other members of the *Reoviridae* suggest

that assortment is governed by RNA-RNA interactions, and data supporting this model may be valid for rotavirus as well (78). It is hypothesized that rotavirus ssRNAs form complexes through cis-acting elements to form a supramolecular complex that engages structural proteins of the inner core shell, including VP1, V2, and VP3 (32). These RNA-RNA interactions are facilitated through conserved sequences within the 5' and 3' termini, which likely harbor RNA structural elements that act as assortment and packaging signals (79, 80). More recently, Borodavka, et al. have demonstrated that folding of the ssRNA segments mediated by NSP2 is a major factor in determining interactions between specific RNAs (81).

Replication intermediates

While viroplasm and their contents are difficult to observe or purify by traditional approaches, subviral particles capable of *in vitro* genome replication can be isolated via biochemical techniques (82). By EM (83), these particles are heterogenous, and are thought to represent replication intermediates that demonstrate a stepwise assembly process. Small, smooth surfaced particles may be forming viral cores, consisting of viral RNAs bound to VP1 and VP3 in assembling VP2 cores. Larger, honeycomb surfaced particles may be indicative of assembling cores that have acquired the VP6 intermediate layer. Both particle types, however, are very fragile and are sensitive to RNases, suggesting they have not fully formed intact, complete capsid layers. Together with biochemical studies assessing protein activity and RNA binding affinities, this data supports a consensus model of assembly (24, 84). In this model, ssRNAs associate with each other, and individually, with a VP1 polymerase and VP3 methyltransferase. VP2

begins to associate with the complex, and interactions between VP2 and VP1 trigger the initiation of replication, synthesis of the minus-strand of the dsRNA genome. Each polymerase functions independently, but the process is synchronized between each replication unit such that replication of each segment is concurrent with replication of the others (85). During this process, the VP2 core shell assembles and acquires the VP6 intermediate layer to form a DLP.

Virion morphogenesis, maturation

To form a fully infectious virion, particles formed during replication must next acquire the outer capsid layer. DLPs must exit the viroplasm and bud through the endoplasmic reticulum (ER), by a process in which they encounter VP4, NSP4, and VP7. VP4 is a cytoplasmic protein, and DLPs associate with this protein en route to the ER. NSP4 is associated with the ER membrane, and in binding to VP6, acts as a receptor to facilitate movement of the DLP into the ER compartment (86). DLPs bud into the ER, and thus they are enveloped, but only briefly; breaching this membrane allows the DLP to associate with VP7, an ER-resident glycoprotein, and for full assembly of the VP4-VP7 capsid layer. It is likely that VP4 spikes form contacts with the VP6 layer first, which is then filled in with a continuous layer of VP7 trimers (87). Binding of the outer layer is Ca^{2+} dependent, and NSP4 plays an additional role as a viroporin, facilitating release of Ca^{2+} from intercellular stores (88) by interacting with the Ca^{2+} -sensing protein STIM (89). This Ca^{2+} release facilitates stabilization of the outer capsid layer, but also triggers kinase cascades that lead to autophagy (90, 91). Virions are then released from cells by lysis (92), or through a budding process that is not immediately lethal to infected

cells (93). Following release, virions must encounter trypsin to mature to fully infectious particles (94).

Innate immune responses during rotavirus infection

Rotavirus infection rapidly triggers broad innate immune responses within infected cells, prior to the activation of rotavirus-specific immune cell responses (95). Hosts have evolved a number of pattern recognition receptors (PRRs) (Table 1-4, Fig. 1-4) by which they detect the presence of an invading pathogen and trigger responses that lead to induction of interferon and anti-viral interferon stimulated genes (ISGs). Regardless of strain, interferon responses appear to be a dominant host response to rotavirus infection, particularly in pigs and humans (96, 97). This response is largely triggered by the detection of viral RNA that is recognized as non-self during replication (98, 99). However, specific activation of innate immune response signaling cascades appears to vary by strain and by cell type (100), and the approaches by which rotavirus combats these responses also diverges by strain and host species specificity. Viruses may evade detection through sequestration of key viral elements, disrupt expression or activation of transcription factors required for innate immune response induction, or inhibit downstream signaling cascades involved in transduction of amplifying responses (101).

Interferon induction is triggered by an initial detection of a pathogen associated molecular pattern (PAMP) by a dedicated PRR. During RNA virus infections, these can include Toll-like receptors (TLRs), nucleotide-oligomerization domain (NOD)-like receptors (NLRs), retinoic acid-inducible gene 1 (RIG-I)-like receptors, and more

PRR	Canonical molecular pattern	Putative rotavirus ligand
TLR2/TLR6	Bacterial lipoprotein	None
TLR4	Bacterial lipopolysaccharide	None
TLR3	dsRNA	dsRNA
TLR7	ssRNA	ssRNA
RIG-I	Capped dsRNA	Capped dsRNA, hairpin ssRNA
MDA5	dsRNA	dsRNA
NOD2	Bacterial peptidoglycan	None
PKR	dsRNA	dsRNA

Table 1-4. PRRs and associated ligands.

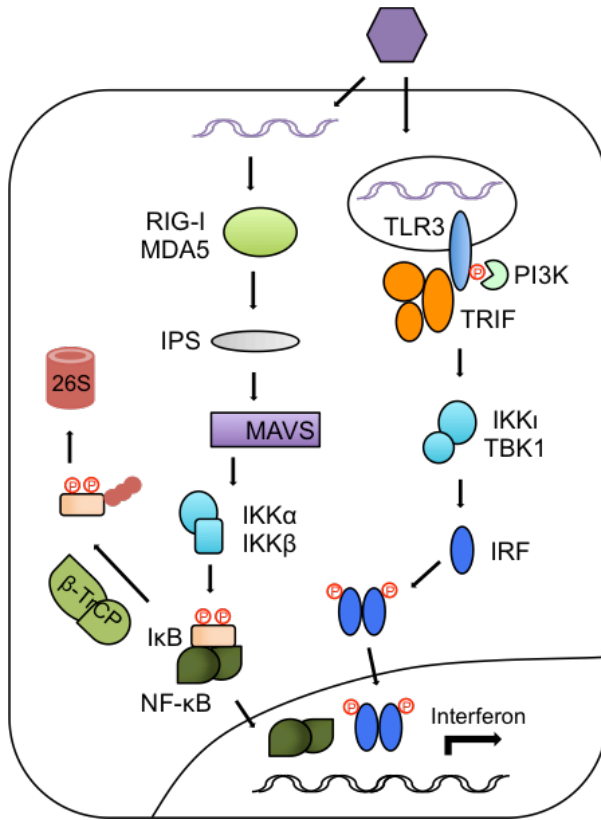


Figure 1-4. Innate immune responses to RNA virus infection. Upon virus entry, dsRNA (purple) is detected by PRRs such as RIG-I or MDA5 in the cytoplasm, or TLR3 in endosomes. Cytoplasmic PRRs signal through IPS at the mitochondria to MAVS, which results in activation of IKK α and IKK β (IKK complex). Activated IKK phosphorylates a degron sequence of I κ B, the inhibitor of NF- κ B, allowing for recognition by B-TrCP and subsequent I κ B ubiquitination and degradation by the 26S proteasome. NF- κ B that has been freed of its inhibitor translocates to the nucleus to induce interferon. Similarly, TLR3 detection of dsRNA also results in interferon induction. TLR3 interacts with PI3K and TRIF, activating IKKi and TBK1, resulting in IRF phosphorylation, dimerization, and nuclear translocation.

recently, even receptors classically associated with DNA, such as cGAS (cyclic GMP-AMP Synthase) (99, 102). These PRRs are expressed in distinct areas of the cell as membrane-associated or as cytosolic proteins, resulting in broad surveillance that can result in specific activation of individual focused responses. Ultimately, detection of a PAMP by an associated PRR can result in interferon expression. Expressed interferon binds to receptors on the infected cell, triggering amplified autocrine interferon signaling, and to adjacent cells, triggering paracrine responses.

Triggering through MAVS (mitochondrial antiviral signaling protein, also known as VISA or Cardif) is known to be crucial for innate immune response activation during rotavirus infection (103). MAVS signaling is initiated through the activation of RIG-I or of MDA-5 (melanoma differentiation-associated protein 5). Both of these PRRs appear to be crucial to build an effective response to rotavirus (103, 104). This response is dependent on active replication, as no response can be observed upon infection with UV-inactivated virus (103). This finding suggests that the relevant PAMP during rotavirus infection is a product of replication, rather than the entering viral genome contained in DLPs (104).

RLRs sense the presence of rotavirus replication products or intermediates in the cytoplasm and recruit MAVS in order to activate cytosolic transcription factors. Transcription factors like interferon regulatory factors (IRFs) and nuclear factor-kappa B (NF- κ B) are promoters of interferon expression and rely on specific kinases in the I-kappa-B kinase (IKK) complex (IKK α , IKK β) or the IKK-related kinases (TKB1, IKK- ϵ) for activation. NF- κ B and IRF transcription factor families are activated simultaneously (105), but they are responsible for activating distinct groups of downstream target genes;

most pro-inflammatory cytokines signal through NF- κ B, whereas type 1 interferon activation relies primarily on IRFs (106-108). Cytoplasmic IRFs are directly activated by phosphorylation of their C-termini by TBK1 or IKK- ϵ (109). This modification leads to dimerization of IRFs and their subsequent translocation to the nucleus where interferon induction proceeds.

In contrast to activation of IRFs, where phosphorylation occurs directly on the transcription factors themselves, phosphorylation within NF- κ B signaling cascades occurs instead on a conserved phosphodegron motif of I κ B, the inhibitor of NF- κ B. Prior to PRR signaling induction, NF- κ B dimers exist in a sequestered state in the cytoplasm, bound to their inhibitors. When upstream signaling has commenced and the IKK complex is activated, the I κ B phosphodegron motif, DSGIS, is phosphorylated on two serine residues by IKK α and IKK β , the catalytic units of the IKK complex. Dual modification of I κ B is detected and bound by β -TrCP, an F-Box-containing adaptor protein of cellular E3 ubiquitin ligases, leading to subsequent ubiquitination and degradation of I κ B. By degrading the inhibitory protein, NF- κ B transcription factors are free to relocate to the nucleus. In addition to I κ B phosphorylation, some reports suggest that the p65 subunit of NF- κ B also undergoes phosphorylation for optimal activity (110).

Evidence also supports roles for membrane-associated or endosomal PRRs during rotavirus infection (111, 112). Specific preference for detection pathways and associated PRRs may be cell-type specific, and the role of TLRs has not been extensively studied. TLR7 and TLR9 have been implicated in antiviral signaling in plasmacytoid dendritic cells (pDCs), however this cell type is not a primary target of rotavirus infection (113). Despite limited permissiveness to rotavirus infection, pDCs contribute a significant

interferon response during infection (113). Further research is required to uncover the intricacies of interplay between rotavirus specialized immune cells during infection.

Rotavirus proteins with roles in innate immune evasion, antagonism, and activation

VP3

VP3 is an 835 amino acid protein that is the product of genome segment 3. While the role of VP3 as a structural protein with methyltransferase activity has been studied extensively, VP3 has also been shown to influence virulence in mice and piglets, suggesting a role for this protein in host range restriction (114, 115). Capping and methylation by VP3 may result in shielding of viral RNAs from host PRRs (116), but for reasons that remain unclear, a small percentage of rotavirus RNAs have been found to lack these modifications. More recently, VP3 has been shown to directly influence signaling through the OAS/RNase L pathways through a different activity, (117-119). VP3 cleaves 2',5'-oligoadenylates (2-5As) produced by oligoadenylate synthetase (OAS), a cytoplasmic dsRNA PRR that activates RNase L to cleave RNAs. The RNase L response disrupts viral infection by directly attacking viral and cellular RNAs, but also produces ssRNAs to activate other interferon-inducing RLRs. Few structural details are available for VP3, but by homology modeling, it bears striking similarities to viral enzymes from bluetongue and vaccinia viruses (120).

dsRNA binding protein

Some RVC strains encode two separate proteins on genome segment 6: NSP3 and a small dsRNA binding protein (dsRBP). The rotavirus dsRBP has predicted homology

with dsRBP domains used by many cellular proteins to bind dsRNA, including protein kinase R (PKR), an interferon induced protein with pro-apoptotic functions. PKR binds to dsRNA through tandem N-terminal dsRNA binding motifs, which facilitates dimerization and autophosphorylation reactions, activating the protein. Once active, PKR phosphorylates the eukaryotic translation initiation factor eIF2a. This phosphorylation inhibits mRNA translation, thus preventing both cellular protein production but also any production of viral or pro-viral proteins. By mimicking PKR, the RVC dsRBP sequesters viral RNA from PKR binding and activation, or any other accessible PRRs.

NSP3

Many RNA viruses harbor the ability to alter the activity of host translational machinery such that viral replication and protein production is favored over production of host proteins (121). This feature allows viruses a broad approach to bolster their own replication systems while also impeding host antiviral responses, including expression of interferon and any interferon signaling molecules or stimulated genes that may have detrimental outcomes.

NSP3 is a 313 amino acid protein encoded by genome segment 7, and one of its primary functions is to enhance translation of viral mRNAs and impair host translation during infection (122). NSP3 forms dimers in infected cells, and the N-terminus of dimerized NSP3 has strong affinity for the 3' consensus sequence of viral ssRNAs (123). The C-terminus interacts strongly with eIF4G, a component of the eukaryotic eIF4F cap-binding complex that aids in recruiting ribosomes to mRNAs. Host mRNAs are polyadenylated and bound by poly-A binding protein (PABP) during the initiation of

translation; eIF4G bridges PABP and the 5' cap-binding complex, circularizing RNAs during translation initiation. NSP3 mimics the activities of PABP for rotavirus ssRNAs, which are not polyadenylated. By binding eIF4G and the 3' end of rotavirus ssRNAs, NSP3 circularizes viral mRNAs, evicts PABP from eIF4G complexes, and aids in recruitment of ribosomes. This process sequesters crucial components of translation machinery and inactivates PABP, inhibiting translation of host mRNA templates. In line with this activity, NSP3 must have a functional RNA binding motif in order to disrupt host translation (124). This model however, may be incomplete, as RNAi silencing of NSP3 does not inhibit generation of viral proteins or reduce viral yields from infected cells (125). Similarly, productive, high-yield mutant viruses exist that encode defective NSP3 (126). Interestingly, NSP3 has a long coiled-coil domain that is responsible for dimerization of the protein, and also for binding to heat shock protein 90 (HSP90), a process that precedes its acquisition of function (127, 128).

NSP4

NSP4 is a 175 amino acid protein encoded by genome segment 10. Three individual populations of NSP4 are produced during the course of rotavirus infection: transmembrane NSP4 in the ER (129), secreted soluble NSP4 (130, 131), and viroplasm localized NSP4 (129). In these different cellular compartments, NSP4 plays distinct roles during rotavirus infection, including aiding in virion morphogenesis and as the only rotavirus protein known to function as an endotoxin. Secreted NSP4 may account for early onset diarrhea, or diarrhea in individuals in the absence of any observable histopathological changes within the small intestine (132). Expression of NSP4 alone has

been shown to induce significant pro-inflammatory cytokine expression from murine macrophages and appears to induce signaling through interactions with TLR2 (133). It has also been reported that children produce antibodies against NSP4 early in infection or upon vaccination (134, 135), but it is unclear what role specifically this interaction may play in modulating infection.

NSP1: A key modulator of cellular immune pathways

NSP1 is encoded by genome segment 5 and remains the best-characterized rotavirus innate immune antagonist to date (136). NSP1 proteins from diverse strains have been shown to be associated with the degradation of IFN signaling proteins within both the IRF and NF- κ B signaling cascades (137). Examination of rotavirus species from diverse hosts and their innate immune targets has yielded a classification system based upon the C-terminal sequences of NSP1 proteins. These viruses fall into three primary groups based on this categorization: IRF targeting NSP1s, NF- κ B targeting NSP1s, and those which fall somewhere between and share features with both previous groups (138) (Table 1-5). The C-terminus is a key determinant in host range restriction and in determining which innate immune pathway is primarily targeted during infection (138, 139); motifs within this region of the protein are often termed substrate recognition sequences. NSP1 proteins have been reported to interact with numerous cellular proteins, including p53 (140), TRAF2 (141), and MAVS (142); however, most evidence suggests the proteins have a targeted approach to facilitate β -TrCP or IRF3/IRF7 degradation. Despite target diversity and significant sequence variation between strains, evidence suggests that NSP1 proteins retain a similar predicted structure and domain organization

OSU-like	Porcine	OSU	CTGS-KTVDYDSGISDVE
	Human	WI61	CIEP-KTVDYDSGISDVE
	Human	Wa	HTEL-KTAEYDSGISDVE
	Human	DS-1	YEKD-RTAEHDSGISDIE
UK-like	Bovine	UK	NKRNELIDEYDLELSDVE
	Human	AK-13	NKRNDLMDEYSYELSDTE
SA11-4F-like	Simian	SA11-4F	KNSGTLTEEFELLISNSEDNE
	Simian	RRV	EEEGKLSEYELLISDSEDDD
	Human	B4106	EEEGKLAEEYELLISDSEDDD
	Lapine	30-96	EEEGRLAEEYELLISDSEDDD
	Human	Ro1845	EEEGKISEYELLISDSEDDD
	Canine	K9	EEEGKISEYELLISDSEDDDQ
	Equine	L338	YEQGELSEYELLISDSGDDE
	Equine	FI14	EKQGKLSEYDLLISDSDDD
	Murine	ETD	QEHGDLAEEFDLLLSSSDSDDED

Table 1-5. NSP1 C-terminal alignment, grouped into OSU-like β -TrCP targeting strains, SA11-4F-like IRF-targeting NSP1s, and UK-like NSP1 proteins that share features and activities of both groups.

(138), supporting the hypothesis that common mechanisms may be utilized in their activities. Full-length NSP1 localizes throughout the cytoplasm in a punctate manner, and NSP1-induced degradation of targets has been shown to be dependent on proteasome activity (136-138, 143). As a result of these findings, NSP1 has been hypothesized to modulate and redirect components of the cellular ubiquitin-proteasome pathway to facilitate degradation of cellular targets within antiviral immune signaling pathways (138, 144, 145).

The prediction of a putative RING domain within the N-termini of NSP1 proteins (146) initially supported the hypothesis that NSP1 proteins functioned as viral-encoded, single protein E3 ubiquitin ligases (138). Functional E3 ligases must interact with an E2 ubiquitin-conjugating enzyme in order to facilitate transfer of an ubiquitin moiety to their targets; this interaction is facilitated through a RING domain. However, direct evidence supporting NSP1-facilitated poly-ubiquitination of known targets in the absence of cellular machinery is currently insufficient. It is possible for a small protein to act singly as an E3, such as the cellular TRIM family of proteins (147), however, given the known role of the C-terminal 10-20 amino acids of NSP1 in conferring substrate specificity, this hypothesis seems unlikely. Furthermore, new data supports a model in which NSP1 interacts directly with Cullin3 scaffold proteins of cullin-RING E3 ubiquitin ligases (CRLs) (144, 145, 148).

Because of the abundance of cellular CRLs and their adaptable nature, it is hardly novel that viruses may adopt strategies to inhibit or redirect CRLs to their own advantage. Other viral proteins (Epstein-Barr virus LMP1, HIV-1 Vpu, vaccinia virus A49) (149-151) are known to utilize mimicry to interact with β -TrCP and inhibit NF- κ B

interferon signaling without facilitating the degradation of cellular E3 ligase machinery. Notably, Vpu directly appropriates the E3 ubiquitin ligase activity of SCF ^{β -TrCP} to target host proteins for proteasomal degradation (152). To this end, Vpu behaves as an added adaptor protein to shift targeting from I κ B to instead include CD4 and tetherin as ubiquitination substrates. Recently, HBV X protein, too, was reported to hijack a cellular CRL; to direct degradation of Smc5/6, X protein acts as an adaptor to shift targeting towards cellular substrates (153).

Like Vpu, NSP1 recruits the F-box protein β -TrCP, disrupting NF- κ B signaling and preventing interferon expression (138). However, the precise mechanism of NSP1 activity has remained controversial, particularly with respect to proposed ubiquitination and degradation of targets. Recently, three studies identified a novel role for NSP1 as an adaptor protein of a modified, hijacked CRL, similar to the mechanism employed by Vpu or X protein. The indication that NSP1 fosters a direct, functional interaction with the amino-terminus of CUL3 (144, 145) suggests an added role for NSP1 in the repurposing of cellular degradation machinery to favor viral replication and survival.

NSP1 proteins from OSU and Wa strains, both specific β -TrCP targeting antagonists, associate directly with cullins, and with components of assembled CRLs, including Rbx1 and Nedd8 activating proteins (144, 145). Furthermore, NSP1-induced innate immune antagonism and degradation of substrates does not occur when the association of these components (CUL3, Rbx1) is impeded chemically or through mutagenesis (144). This reliance on the functioning of components within CRL complexes represents the first evidence to directly dispute the hypothesis that NSP1 may act on its own as a single-polypeptide E3 ligase. Moreover, this finding can be expanded

and applied to the IRF-targeting NSP1 proteins, fostering a uniting link between classes of NSP1 antagonists (145). That NSP1 appears to interact with multiple cullin types remains especially intriguing, and as suggested by Lutz, et al., NSP1 may be using cullin-containing complexes to interfere with an as yet unidentified cellular process.

Furthermore, NSP1 may only require a small number of repurposed CRLs in order to effectively inhibit innate immune signaling (145). Lutz, et al. posit that neither dominant negative use nor siRNA knockdown of either Cul1 or Cul3 interrupted NSP1-mediated degradation of targets, suggesting that the small proportion of the cytoplasmic cullin population remaining unaffected is sufficient for NSP1 to exert control over IFN signaling pathways. Ding, et al. instead support that cullins are a necessity for NSP1 innate immune antagonism to occur. It may also be possible that binding alone is sufficient for inhibition.

Research program overview

Hypothesis

To extend our understanding of the functional role of NSP1 in rotavirus infection and its contribution to control of innate immune responses, the following hypothesis was proposed:

Human and porcine NSP1 proteins are known to interact with β -TrCP through a conserved C-terminal motif. We propose that this region of the protein, a mimic of the phosphodegron of I κ B, is phosphorylated by a cellular kinase and that phosphorylation is an activating event that regulates NSP1 activity. We propose to evaluate the phosphorylation status of NSP1, to identify cellular kinase(s) responsible for the modification, to examine the role that phosphorylation plays in NSP1 control of cellular CRLs, and to assess how phosphorylation regulates NSP1 control of host responses to infection.

Summary of experimental aims and approaches

Specific Aim 1: To determine the phosphorylation status of the C-terminal NSP1 I κ B-like motif. Utilizing phospho-specific antibodies generated against the phosphorylated I κ B degron, we will assess the phosphorylation status of NSP1 by immunoblot. We will probe the cross reactivity of this antibody by incorporating mutant NSP1 proteins, and validate our findings with the incorporation of protein phosphatase treatment.

Specific Aim 2: To determine the identity of cellular kinases responsible for NSP1 phosphorylation. By *in silico* analysis, we will assess the surrounding degron

context within the NSP1 C-terminus to identify consensus sequences of cellular kinases. We will validate or dismiss hits through directed mutagenesis of kinase priming motifs, the use of kinase specific small molecule inhibitors, and RNAi.

Specific Aim 3: To assess the role of phosphorylation in regulation of NSP1 activity. By immunoprecipitation assay, we will address NSP1 binding to both targets and CRL machinery, for wildtype NSP1 and phospho-deficient NSP1 proteins.

Specific Aim 4: To characterize the ability of NSP1 to antagonize cellular responses to infection, and how this response is affected by NSP1 phosphorylation status. In addition to NF- κ B signaling and interferon induction, β -TrCP regulates numerous pathways. We will address the effect of phosphorylated NSP1 on signaling through these cascades, with particular emphasis on mTOR and pro-apoptotic signaling.

Significance of study

To date, there has been remarkably little data to support the notion that NSP1 proteins from various strains utilize common mechanisms to target host innate immune pathways. However the development of new technologies, including the use of sequence-searching motif databases, has uncovered previously unknown similarities between NSP1 proteins of diverse strains to support this hypothesis. While primary sequence varies significantly between strains, and even within classes of NSP1 proteins, new data suggests the retention of similar predicted structures, as well as a common role for the C-terminal motifs of these proteins, much like what has been described for the OSU NSP1 phosphodegron. Descriptions of the precise requirements of NSP1 antagonistic mechanisms describe a role for NSP1 as a novel adaptor protein of CRL3 complexes, and

these new data elaborate on exciting interactions between NSP1s and host ubiquitination machinery.

In this thesis, NSP1 has been classified as a novel substrate adaptor protein of cellular E3 ubiquitin ligases, particularly those incorporating a Cullin 3 scaffold. This finding is built upon studies integrating assessment of protein-protein interactions and biochemical analysis of both exogenously expressed protein and for viral proteins produced during the course of infection. Also included are assessment of both up- and down-stream effects and effectors of these interactions and protein modifications. An activating modification of NSP1 has been identified as a crucial, integral event that precedes antagonistic activity of the protein: NSP1 must be phosphorylated on a conserved, I κ B-like motif within the C-terminus, and this modification is mediated by the cellular kinase CKII. To our knowledge, no other known kinases are able to fulfill this role in the absence of CKII activity or expression. Analogous modifications are observed for numerous NSP1 proteins that contain similar motifs, and data suggests that this activating event occurs regardless of host species. Following phosphorylation, NSP1 is able to bridge interactions with its primary target, β -TrCP, acting as a mimic of the I κ B degron. This initial interaction is likely the limiting step in hijacking of Cullin-RING ligases; phosphorylation precedes interaction with targets, but also precedes any integration of NSP1 proteins into commandeered cellular ligases. Interestingly, while recruitment of β -TrCP into hijacked Cullin-RING ligases leads to ubiquitination and degradation, the activity of β -TrCP appears to be inhibited prior to the terminal steps of this pathway. This finding suggests that interaction alone is sufficient to inhibit activity,

an activity with significant effects on interferon induction pathways, as well as other cellular pathways that rely upon β -TrCP mediated activities, such as mTOR.

Chapter 2:

Cullin-RING ligases and viral adaptors: novel repurposing of a familiar tool

Kaitlin A. Davis, John T. Patton

This article is in preparation for submission to the Journal of General Virology.

KAD and JTP generated figures.

KAD and JTP wrote the manuscript.

Abstract

Viruses commandeer the use of cellular machinery to support their replication and to down-regulate antiviral host pathways. Recent studies continue to highlight the importance of the ubiquitin proteasome system in viral replication processes, and in particular, highlight enzymes of the cullin-RING E3 ubiquitin ligase (CRL) family. CRLs facilitate a critical step in the ubiquitination process, in which substrate proteins are modified with the addition of small ubiquitin moiety tags. Ubiquitin tags affect target proteins by altering protein activity or localization, or by inducing protein turnover via proteasomal degradation. Pathogens interact with CRL machinery by a number of complex approaches, and many viruses encode proteins that incorporate into CRLs by acting as substrate adaptor proteins. Viral adaptor proteins shift the specificity of CRL machinery resulting in ubiquitination of novel targets, including host antiviral factors. This review describes the organization and function of CRLs, mechanisms of viral CRL adaptor proteins, and the types of host proteins targeted by hijacked CRLs.

Introduction

As obligate intracellular parasites, viruses seize control of existing cellular machinery to support their replication. Co-opted or repurposed host proteins perform numerous essential roles during viral replication, including aiding in adsorption and entry (154), expression of viral proteins (155), and antagonism of antiviral immune responses (156). Such hijacking of host proteins benefits viral replication by promoting a cellular environment that is favorable to specific aspects of the viral lifecycle. For example, maintenance of a pro-viral cellular environment often requires the degradation of cellular

proteins that have antiviral activity. This degradation is of particular importance in suppressing interferon (IFN) expression within infected cells (156). To this end, the ubiquitin proteasome system (UPS), a key regulator of protein degradation and recycling, has been identified as a common target for viral hijacking.

The UPS is a degradation pathway integral to the regulation of many normal cellular processes, including cell growth and cell cycle regulation, DNA damage repair, and response to infection or other stressors (157). The UPS utilizes ubiquitin, a small 76 amino acid polypeptide, to target substrates at accessible lysine residues via covalent peptide linkages. The addition of a single ubiquitin tag alters cellular function or localization, whereas Lysine-48 linked poly-ubiquitin chains (158) mark substrates for proteasomal degradation (159). Ubiquitination is an ATP-dependent process and requires the involvement of three distinct classes of enzymes (160), including a ubiquitin-activating enzyme (E1), a ubiquitin-conjugating enzyme (E2), and a target-specific ubiquitin ligase (E3). E1 enzymes catalyze the first step of the process by binding free ubiquitin. E1 enzymes transfer ubiquitin proteins to E2 enzymes, which associate with E3 ubiquitin ligases. E3 ubiquitin ligases are responsible for conferring specificity of substrate proteins, and by bridging bound substrates and ubiquitin-charged E2 enzymes, facilitate transfer of ubiquitin moieties from E2 to substrate (Figure 1). Humans have two E1 proteins and approximately 40 known E2 enzymes, but hundreds of E3 ubiquitin ligases exist and specify thousands of targets with a great degree of selectivity.

Some E3 ubiquitin ligases function as large modular complexes of several subunits whereas others are single-protein enzymes (147). Distinct families can be characterized by conserved structural motifs or the mechanism by which ubiquitin is

transferred from E2 to target. The vast majority of E3 ubiquitin ligases include a RING (really-interesting-new-gene) domain in their construction that mediates interactions with ubiquitin-charged E2s (161, 162). Classic RING domains consist of a conserved zinc-binding Cys₃-His-Cys₄ motif; however, variations of this motif exist and can also include Cys₃-His₂-Cys₄ and Cys₄-His-Cys₃ domains (157), among others.

Cullin-RING E3 ubiquitin ligase construction and regulation

Cullin-RING ligases (CRLs) comprise the most populous group of E3 ubiquitin ligases. CRLs function as large multi-subunit assemblages and are the paradigms for modular ubiquitin ligase construction (163, 164). CRLs are minimally comprised of a cullin scaffold protein (Cul1, 2, 3, 4a, 4b, 5, or 7) with a RING-box protein subunit (Rbx1, Rbx2) at the cullin C-terminus, and at the cullin N-terminus, an adaptor complex of one or two proteins, sometimes including a bridging protein and a substrate adaptor protein (an F-box protein). Archetypal CRLs are built on a Cul1 scaffold, and are known as S phase kinase-associated protein 1 (SKP1)–cullin 1 (Cul1)–F-box protein (SCF) complexes (Fig. 2-1). Substrate specificity of SCFs is primarily determined through the F-box proteins or by additional adaptor proteins that bind a variable region of the F-box protein (165). There are approximately 70 known cellular F-box proteins that can interchangeably bind the SKP1 bridging subunit on SCFs, conferring an enormous degree of flexibility in the selection and targeting of substrates (160). Cul2-, Cul3-, and Cul5-containing CRLs (CRL2s, CRL3s, CRL5s) also incorporate a diverse range of substrate adaptors and bridging proteins, but utilize alternatives to F-box family proteins. CRL3s

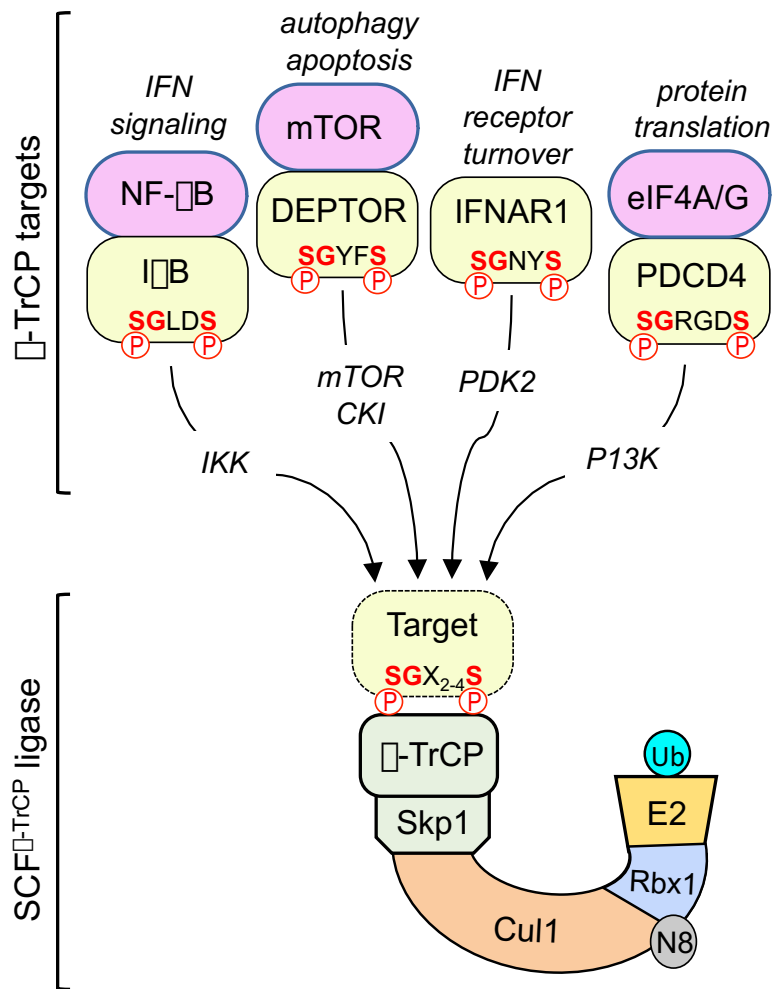


Figure 2-1. The SCF^{β-TrCP} ligase targets many cellular proteins to control a myriad of cellular processes. The SCF^{β-TrCP} ligase is a CRL1, and contains a Cullin 1 scaffold protein that bridges Rbx1 and ubiquitin-charged E2 enzymes at its C-terminus, and adaptor proteins Skp1 and β-TrCP at its N-terminus. β-TrCP binds target proteins that contain a phosphodegron sequence that can be activated cellular kinases. Through neddylation, the addition of a Nedd8 moiety to the cullin scaffold, ubiquitin is transferred from the E2 enzyme to the target protein, leading to modification and degradation of the target. Many β-TrCP targets exist, and their turnover is directly regulated by activation of the phosphodegron sequence. The phosphodegron sequence of IκB (SGLDS), a key regulator of NF-κB and interferon signaling, is modified by IKK. mTOR and CKI activate the DEPTOR phosphodegron (SGYFS). DEPTOR is a component of mTORC1 and mTORC2, and as a regulator of both complexes, control autophagy and apoptosis. Similarly, the PDCD4 phosphodegron (SGRGDS) is activated by P13K, and turnover of this protein effects protein translation mediated by eIF4A/G. IFNAR1 contains a phosphodegron that is activated by PDK2, leading to IFN receptor turnover.

utilize BTB (broad complex, tramtrack, bric-a-brac fold) (166) whereas CRL2s and CRL5s incorporate VHL-box bridging proteins with an Elongin B/C adaptor (167).

Flexibility is integral to the plasticity of the UPS and its ability to rapidly gain control of complex processes, such as cellular homeostasis and cell cycle functioning (168). Despite CRL diversity in both structure and composition, conserved mechanisms regulate their specificity and activity. Modular construction coupled with dynamic assembly and disassembly enables one core E3 complex to ubiquitinate numerous individual substrates through successive cycling (164). Exchange of CRL subunits is subject to various levels of regulation, including processes that affect covalent attachment of assembly factors, such as Nedd8, in a process known as neddylation (169). Neddylation promotes the activity of CRLs, and involves cyclic attachment of a Nedd8 modification to trigger conformational changes within the Cul scaffold protein. This process closes a 50 Å gap between the ubiquitin-charged E2 and bound substrate, catalyzing ubiquitin transfer (170, 171). Conversely, Nedd8 removal, regulated by the COP9 Signalosome (CSN), acts as a signal for SCF complex dissociation and recycling (172, 173). In the absence of substrates, unneddylated cullins can exchange substrate adaptor proteins through the activity of cullin-associated and neddylation dissociated 1 (Cand1), an exchange factor for adaptor proteins that biases assembly towards adaptors for which substrates are available (174). CRLs do not intrinsically have catalytic activity, but catalyze ubiquitination by increasing the local concentration of reactants and positioning them physically to optimally favor ubiquitin transfer (175).

CRLs as targets of viral manipulation

Taken together, the flexibility of CRL regulation, combined with versatility in construction and final composition, makes these complexes viable targets for viral manipulation. Their sensitivity to the availability and concentration of reactants makes them easily exploited by pathogens; data supports that these structures are hijacked and repurposed by viral proteins that interfere with normal targeting at varying levels (176). Some viral proteins act by obstructing binding faces [e.g. SV40 LTag (177), poliovirus P0 (178)] or sequestering crucial modular units of CRLs [e.g. vaccinia virus A49 (151), Epstein Barr virus LMP1 (149)], to halt complex assembly. Other viruses encode proteins that function as substrate adaptor proteins (rotavirus NSP1, HIV Vpu; see below); like their cellular counterparts, these viral proteins bind on one end to a substrate to be targeted for proteasomal degradation, and bind on an opposing face to the remainder of the CRL assemblage. By taking the place of a cellular substrate adaptor protein or by binding to an existing adaptor as a secondary adaptor, these proteins redirect the targeting activity of CRLs (Fig. 2-2). This tactic can be particularly instrumental in modulating innate immune responses by targeting signaling molecules necessary for IFN expression. Hijacking of this system by viral proteins serves a myriad of additional roles, some of which we will describe below.

Suppression of IFN signaling (Rotavirus, RVFV)

Viral-E3 interplay can be illustrated by our understanding of the innate immune antagonist protein of rotavirus, NSP1, and its interactions with CRL3s. This protein behaves as a viral adaptor of hijacked CRL3s to target the F-box protein β -transducin

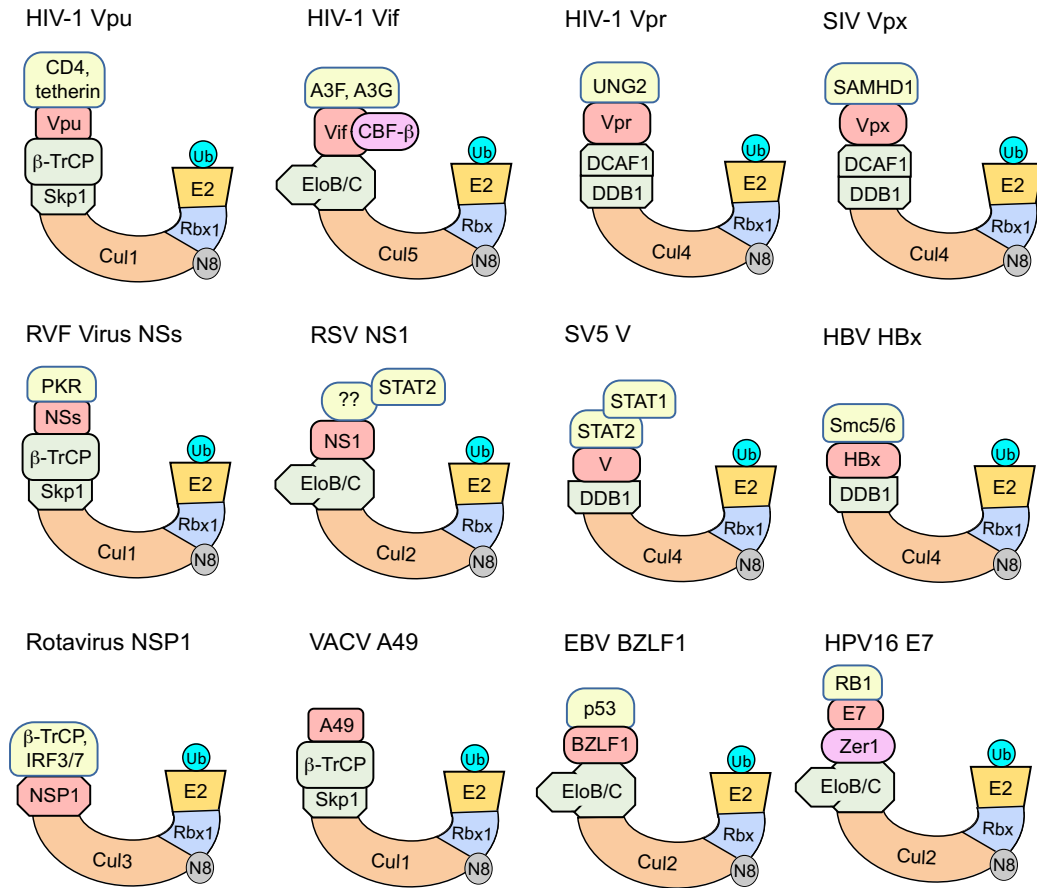


Figure 2-2. Schematic depiction of CRLs with viral adaptor proteins. In each image, cullin scaffold proteins are shown in orange, Rbx proteins are shown in periwinkle, E2 enzymes are shown in goldenrod, and ubiquitin moieties are depicted in turquoise. Cellular adaptor components are shown in light green, viral proteins are red, and target proteins are light yellow. (A) HIV-1 Vpu, shown assembled with CRL1, targets CD4 and tetherin for ubiquitination. (B) HIV-1 Vif assembles with CRL5, and binds EloB/C and CBF- β to target A3F and A3G for ubiquitination. (C) HIV-1 Vpr binds DCAF1 and DDB1 proteins in a CRL4A to target UNG2. (D) Like Vpr, SIV Vpx assembles on a CRL4A, but instead targets SAMHD1 for ubiquitination. (E) RVF virus NSs binds β -TrCP adaptor proteins, which together with Skp1, bind a CRL1. NSs binds PKR proteins as substrates. (F) RSV NS1 assembles with a CRL2 and binds the EloB/C components. NS1 targets STAT2 for ubiquitination, but does not directly bind this target protein and likely requires an additional protein adaptor. (G) SV5 V binds DCAF1 and DDB1 proteins of both CRL4A and CRL4B to target STAT1 for degradation. (H) HBV HBx binds DDB1, displacing DCAF1, to direct CRL4A and CRL4B to facilitate ubiquitination of Smc5/6. (I) Rotavirus NSP1 assembles directly on the Cul3 scaffold of CRL3 without any known cellular adaptor proteins. NSP1 proteins direct degradation of β -TrCP, IRF3, and IRF7. (J) VACV A49 binds the β -TrCP adaptor component of CRL1 and sequesters the complex in an inactive state. (K) EBV BZLF1 EBV BZLF1 binds the EloB/C component of CRL2 to specify p53 as a ubiquitination target. (L) HPV16 E7 assembles on Zer1 to bind EloB/C of CRL2. E7 binds RB1 to facilitate its ubiquitination.

repeat-containing protein (β -TrCP) for degradation, the substrate adaptor component of cellular SCF ^{β -TrCP} (137, 143) (148). β -TrCP is a necessary component of the NF- κ B signaling cascade and is crucial for the induction of IFNs and IFN-stimulated genes (ISGs), leading to an antiviral state in affected cells (179). In an uninfected cell, the inhibitor of kappa B (I κ B) is bound to NF- κ B transcription factors, sequestering them in an inactive state in the cytoplasm. Sensing of double-stranded RNA (dsRNA) by retinoic acid-inducible gene 1 (RIG-I)-like receptors, or other pathogen associated molecular signatures, induces signals that activate the I κ B kinase complex (IKK) (180). This kinase complex phosphorylates a conserved degron motif on I κ B, enabling its targeting by the SCF ^{β -TrCP} E3 ubiquitin ligase. This interaction facilitates the ubiquitination of I κ B and its subsequent proteasomal degradation, freeing NF- κ B (181) to translocate to the nucleus and stimulate induction of IFN (182). By mimicking the I κ B degron, NSP1 selectively recruits β -TrCP, disrupting NF- κ B signaling (138, 148) (Fig. 2-3). As a substrate adaptor, NSP1 then recruits the remainder of the CRL3 assembly to facilitate ubiquitination and proteasomal degradation of its β -TrCP target. The mechanism employed by rotavirus NSP1 is particularly intriguing because this activity involves two distinct cellular CRLs. NSP1 disrupts the activity of the Cul1 CRL SCF ^{β -TrCP} by sequestering its substrate-binding adaptor component (148), and utilizes hijacked CRLs of a different family (CRL3s) that to direct the degradation of the SCF component, β -TrCP (144, 145). Notably, NSP1 appears to take the place of a two-protein BTB-F-Box protein complex typically bound to the N-terminus of Cul3.

The NSP1 proteins of most human and porcine rotavirus strains target their activity towards the degradation of β -TrCP, but the NSP1 proteins of most animal species

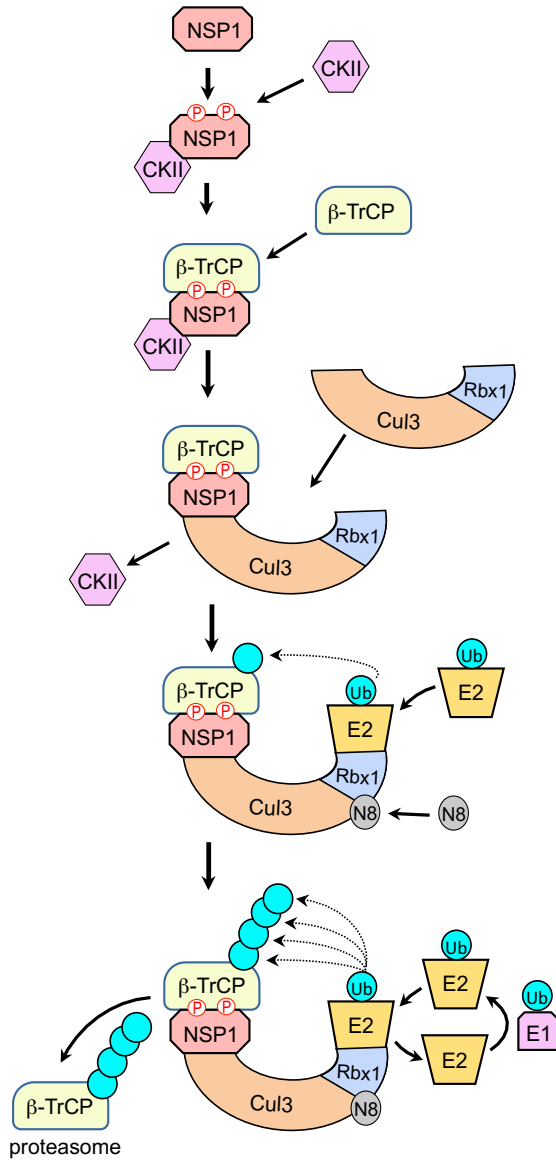


Figure 2-3. A model of NSP1 CRL incorporation. Upon expression, NSP1 is bound by the cellular kinase CKII, which facilitates phosphorylation of serine residues within the NSP1 C-terminal phosphodegion. Phosphorylated NSP1 is bound by β -TrCP, forming an adaptor-substrate complex. Binding of NSP1 to CUL3 facilitates release of CKII and incorporation of a ubiquitin-charged E2 enzyme, resulting in a large CRL complex that includes β -TrCP, NSP1, Cul3, Rbx1, and an E2. Neddylation of the Cul3 scaffold triggers ubiquitin transfer from the E2 to the β -TrCP substrate. Through subsequent rounds of assembly and disassembly, NSP1-hijacked CRLs facilitate poly-ubiquitination of β -TrCP, leading to its proteasomal degradation.

target other innate immune signaling proteins, such as the IFN regulatory proteins (IRFs) (137). Like human and porcine NSP1 proteins, expression of animal NSP1 proteins induces the degradation of target proteins in a proteasome- and Cul3-dependent manner (144, 145). IRFs and β -TrCP represent vital targets of rotavirus innate immune antagonism. Similarly, viruses of other families also require degradation of components of the IFN response network for propagation. Like rotavirus, Rift Valley fever virus (RVFV) encodes the nonstructural protein NSs which directly associates with β -TrCP (183). NSs does not contain a phosphodegron motif, and so likely interacts with β -TrCP through an alternate mechanism as a secondary adaptor. This interaction shifts the targeting of SCF ^{β -TrCP} to facilitate degradation of protein kinase R (PKR), a viral dsRNA sensor that triggers IFN responses. Influenza A virus (IAV) targets IFN signaling pathways by inducing ubiquitination and proteasomal degradation of Type I IFN receptor 1 through actions of the hemagglutinin protein (184), but the precise mechanism or role of a CRL has not yet been fully explored.

Immune cell evasion (HIV)

At least four proteins encoded by human immunodeficiency virus (HIV) are known to interact with host CRL assemblies to support viral replication. Among these proteins, Vpu supports HIV replication by facilitating evasion of immune cells to protect infected cells from NK-mediated death (185). Like rotavirus NSP1, HIV-1 Vpu binds β -TrCP through a phosphorylated degon-like motif (Fig. 2-2), but like RVFV NSs, Vpu functions as a secondary adaptor protein. Both NSs and Vpu-driven complexes utilize the natural β -TrCP CRL complex, SCF ^{β -TrCP}. Vpu binding to β -TrCP shifts affinity of SCF ^{β -}

TrCP to target ICAM-1 surface marker proteins for ubiquitination and subsequent degradation (186). During HIV infection, increased intercellular adhesion molecule 1 (ICAM-1) surface expression on infected cells aids in NK cell targeting of infected cells. By reducing surface levels of ICAM-1, HIV prevents NK cell-mediated cell death, maintaining cellular support of viral replication and virion generation. It has been shown that incorporation of ICAM-1 into progeny virions can increase particle infectivity, and Vpu-induced reduction of this protein to protect infected cells may represent an evolutionary compromise that results in reduced virus infectivity.

Vpu adaptor proteins are also able to induce the CRL-dependent degradation of the surface receptor CD4. CD4 is required for infection of T-cells by HIV, a process that prevents superinfection, and by inhibiting gp120-CD4 binding prior to assembly within cells and at the plasma membrane, also promotes particle release (187, 188). Decreased CD4-surface expression likely also weakens antiviral innate immune responses (189). CD4 interacts with major histocompatibility complex class II on antigen presenting cells, and is an important stimulatory factor of receptor-mediated T-cell activation (190). It has been reported that CD4 surface expression interferes with particle infectivity, and that nascent particles from CD4-negative cells are more infectious than those produced from CD4-expressing cells (191). Thus, targeting of CD4 increases longevity of infected cells by preventing immune-mediated cell death, but also enhances the infectivity of progeny virions.

Increased infectivity of nascent particles (HIV, IAV)

Some viruses are known to package host proteins during budding and assembly processes. Incorporation of host proteins into nascent particles can serve pro-viral purposes to support subsequent rounds of infection, or conversely, antiviral proteins can be packaged as a result of host defense mechanisms. Proteins in the APOBEC family of enzymes (apolipoprotein B mRNA editing enzyme, catalytic polypeptide-like 3) are cytidine deaminases whose activity catalyzes hypermutation of viral genomes, blocking viral spread by inducing lethal mutations. When HIV-1 lacks a functional viral infectivity factor (Vif) protein, APOBEC proteins A3G and A3F are packaged into virions, resulting in lethal editing of viral cDNA in subsequent rounds of infection. To combat this host defense mechanism, the Vif protein recruits Cul5 CRLs as a substrate adaptor protein. Vif directly binds CBF- β proteins (192) and Elongin B/C adaptor proteins (193), enabling hijacked CRL5s to facilitate targeting of A3F and A3G for degradation (194). Hijacking of the CRL system thereby protects the functional integrity of newly formed particles and the propagation of HIV infection.

IAV also utilizes host ubiquitination machinery to promote infectivity of nascent particles. IAV ribonucleoproteins are ubiquitinated during the course of infection, resulting in enhanced polymerase activity, and it has been shown, that the host proteasome is required for IAV virus polymerase function (195). While the E3 ubiquitin ligase activity of Nedd4 and Itch play roles in modulating viral entry and release from the endosome (196, 197), a process that also requires Cul3 (198), the E3 ubiquitin ligase responsible for RNP modification has not yet been identified.

Replication and transcription (HIV, SIV, Hepatitis B)

CRL4s play significant roles in DNA damage control and cancer, and as such, viral proteins that hijack these CRL complexes often do so to support replication and protection of viral genomes. Vpr proteins of HIV-1 and HIV-2, as well as the SIV proteins Vpr and Vpx all act by recruiting CRL4s. Vpr likely plays a role in nucleic acid integrity, as its preferred CRL4 complexes (with a Cul4A scaffold) function in UV-DNA damage recognition. Vpr expression halts cell cycle progression in G2 (199), a DNA damage checkpoint, and Vpr binding to CRL4s directs degradation of cellular substrates, including minichromosome maintenance complex component 10 (MCM10), a known target of cellular CRL4s (200). Vpr also bridges interactions between the Cul4A CRL complex and UNG2 and SMUG1 uracil DNA glycosylases (201). Like Vpu, Vpr binds an existing substrate adaptor protein as a secondary adaptor to redirect CRL specificity. To attract UNG2, Vpr utilizes a variable loop for molecular mimicry of DNA, and engages the adaptor protein DCAF1 to recruit an active CRL4 (202). The Vpx protein of HIV-2 and SIV, however, facilitates the degradation of SAMHD1, a nuclear deoxynucleoside triphosphohydrolase (203). SAMHD1 is an antiviral factor that restricts HIV replication by depleting intracellular deoxynucleotides below levels that can be utilized by the viral reverse transcriptase. Cul4A and Cul4B differ in intracellular distribution and in structure, but are interchangeable for Vpr and Vpx activity (204). Vpx requires both Cul4A and Cul4B for degradation of SAMHD1 in primary macrophages, however, so there may be additional levels of regulation in place that have not yet been described.

Recently, the X protein of Hepatitis B Virus (HBx), whose primary role is to promote transcription of the viral genome, was reported to hijack a CRL4 (153). The Hepatitis B genome exists as an extrachromosomal DNA circle in infected cells, and HBx expression enhances transcription from these extrachromosomal DNA templates exclusively. To this end, HBx hijacks CRL4s as an adaptor protein to facilitate the degradation of the structural maintenance of chromosomes (Smc) complex Smc5/6. Smc5/6 has roles in cell cycle progression and recombinational DNA repair, and was found to bind episomal DNA templates and to the Hepatitis B Virus genome. This binding is an inhibitory sequestration step that prevents viral replication, and by facilitating its ubiquitination and proteasomal degradation, HBx supports Hepatitis B genome replication by allowing productive gene transcription.

Perspectives and conclusion

CRLs are responsible for facilitating up to 20% of routine proteasomal degradation (205). These complexes are capable of targeting substrates with marked specificity to regulate numerous processes within cells. Flexibility of this system largely hinges on exchange of substrate adaptor proteins that bind to the N-terminus of cullin scaffold proteins or their bridging proteins in order to specify individual substrates. Viral proteins are known to interact with CRL machinery in a variety of ways, as more extensively described by Mahon et al (176), and many viruses have adopted strategies to redirect CRLs by encoding their own CRL adaptor proteins.

While direct CRL interactions can be described *in vitro*, we lack a thorough understanding of how CRL complexes are regulated *in vivo*. Many studies suggest that

proximity and local concentration are driving factors in regulation, consistent with a model that is rapidly adaptive to subtle changes in the intercellular milieu but difficult to replicate *in vitro*. In line with this hypothesis, *in vitro* data suggests that cullin scaffold proteins can be neddylation at a variety of assembly steps, rather than as a final activation step. Similarly, Cand1 appears to regulate CRLs *in vitro* with diverse effects on function (206-208), and CRLs are reported to retain their activity *in vitro* even without neddylation (209-211). These results may also suggest that diverse CRLs with varied composition are subject to different levels of regulation. For example, a recent study (148) identified an ordered sequence of events required for integration of rotavirus NSP1 adaptor proteins into hijacked CRL3s in a process highly reliant on phosphorylation steps; not all adaptor proteins are known to require phosphorylation to engage substrates, even when comparing NSP1 proteins from diverse rotavirus strains (212).

Within the last decade, research into mechanisms employed by HIV proteins has made this group of viral proteins archetypal in control and hijacking of CRLs. In particular, the diverse mechanisms employed by Vpu make this protein a model for viral control of host responses (213). Vpu is reported to facilitate degradation or down-regulation of ICAM-1, ICAM-3, BST2/tetherin, CD4, HLA-C, and many others (214, 215). This list of targets has grown dramatically in recent years, and our understanding of the mechanisms through which Vpu exerts this control has diversified. The multi-pronged approaches utilized by a single protein, and better understanding of the balance Vpu must employ in execution, makes this protein a seminal model for our understanding of other viral proteins. Rotavirus NSP1, for example, appears both to require Cul3 scaffold proteins for its activity (144, 148), and to perform its antagonistic control of innate

immune responses in the absence of this protein (145). As we continue to uncover mechanisms employed by these viral proteins and others, and as the range of described mechanisms continues to grow, the multi-faceted approach of Vpu may be revealed as a widely employed tool set. NSs of Rift Valley may employ similar tactics, as this protein is known to interact with at least two distinct F-box proteins to direct degradation of distinct cellular targets (183, 216). Furthermore, an increasing numbers of viral proteins are reported to immunoprecipitate or directly interact with proteins from this family [e.g. Rice black streaked dwarf virus P7-2 (217), human T-cell leukemia virus type 1 bZIP (218), adenovirus E4orf6 (219)]. It will be no surprise if many more viral proteins identified as novel CRL adaptors in coming years.

Chapter 3:

OSU NSP1 as a phosphorylated adaptor protein of cellular E3 ubiquitin ligases

Kaitlin A. Davis, Marco Morelli, John T. Patton

The published manuscript may be accessed as follows:

<http://mbio.asm.org/content/8/4/e01213-17.full>

All data and figures were generated by KAD.

KAD, MM, and JTP wrote the manuscript.

Abstract

The rotavirus nonstructural protein NSP1 repurposes cullin-RING E3 ubiquitin ligases (CRLs) to antagonize innate immune responses. By functioning as substrate adaptors of hijacked CRLs, NSP1 causes ubiquitination and proteasomal degradation of host proteins essential for expression of interferon (IFN) and IFN-stimulated gene products. The target of most human and porcine rotaviruses is β -TrCP, a regulator of NF- κ B activation. β -TrCP recognizes a phosphorylated degron (DSG Φ XS) present in inhibitor of NF- κ B (I κ B); phosphorylation of the I κ B degron is mediated by I κ B kinase (IKK). Because NSP1 contains a C-terminal I κ B-like degron (ILD) (DSGX Φ S) that recruits β -TrCP, we investigated whether the NSP1 ILD is similarly activated by phosphorylation and whether this modification is required to trigger the incorporation of NSP1 into CRLs. By mutagenesis and phosphatase treatment, we found that both serine residues of the NSP1 ILD are phosphorylated, a pattern mimicking phosphorylation of I κ B. A three-pronged approach using small molecule inhibitors, siRNAs, and mutagenesis assays demonstrated that NSP1 phosphorylation was mediated by the constitutively active casein kinase II (CKII), rather than IKK. By co-immunoprecipitation assays, we found that this modification was essential for NSP1 recruitment of β -TrCP and induced changes involving the NSP1 N-terminal RING motif that allowed formation of Cul3-NSP1 complexes. Taken together, our results indicate a highly regulated stepwise process in the formation of NSP1 Cul3-CRLs that is initiated by CKII-phosphorylation of NSP1, followed by NSP1-recruitment of β -TrCP, and ending with incorporation of the NSP1- β -TrCP complex into the CRL via interactions dependent on the highly conserved NSP1 RING motif.

Importance

Rotavirus is a segmented double-stranded RNA virus that causes severe diarrhea in young children. A primary mechanism used by the virus to inhibit host innate immune responses is to hijack cellular cullin-RING E3 ubiquitin ligases (CRLs), redirecting their targeting activity to the degradation of cellular proteins crucial for interferon expression. This task is accomplished through the rotavirus nonstructural protein NSP1, which incorporates itself into a CRL and serves as a substrate recognition subunit. The substrate recognized by NSP1 of many human and porcine rotaviruses is β -TrCP, a protein that regulates the transcription factor NF- κ B. In this study, we show that formation of NSP1 CRLs is a highly regulated stepwise process initiated by CKII-phosphorylation of the β -TrCP recognition motif in NSP1. This modification triggers recruitment of the β -TrCP substrate and induces subsequent changes in a highly conserved NSP1 RING domain that allow anchoring of the NSP1- β -TrCP complex to a cullin scaffold.

Key words. Rotavirus, NSP1, β -TrCP, CKII, viral E3 ubiquitin ligase

Introduction

Rotaviruses, members of the family Reoviridae, are a leading cause of severe life-threatening diarrhea in infants and children under five years of age (136), (134). The segmented double-stranded RNA of these viruses encode six structural (VP1-VP4, VP6-VP7) and six nonstructural (NSP1-NSP6) proteins (134). Rotaviruses antagonize the expression of interferon (IFN) and IFN-stimulated gene (ISG) products chiefly through the action of NSP1, the sole protein product of viral genome segment (gene) 5 (115). NSP1 is the least conserved of the twelve rotavirus proteins, including VP4 and VP7, the

outer capsid proteins of the virus under immunological pressure (137). However, the NSP1 proteins of group A rotaviruses (the subject of this article) have a similar predicted secondary structure and share the same N-terminal RING domain motif (137). The C-termini of NSP1 proteins have variable C-terminal substrate recognition domains that recruit and induce the proteasomal degradation of host proteins involved in IFN and ISG expression (137, 138). The NSP1 C-terminal domain of most human and porcine rotaviruses target β -transducin repeat-containing protein (β -TrCP) for degradation (143), a protein critical for activation of the transcription factor, nuclear factor- κ B (NF- κ B) (Fig. 3-1A). In contrast, the target of many animal rotaviruses, including simian, bovine, equine, and murine strains, are the IRF regulatory factors (e.g., IRF3 and IRF7) (136-138).

Human and porcine NSP1 proteins recognize β -TrCP through the presence of a DSGXS motif in their C-terminal substrate recognition domain (Fig. 3-1B, C). This motif mimics the DSG Φ XS degron present in inhibitor of NF- κ B (I κ B) (138). When bound to NF- κ B, I κ B prevents movement of the NF- κ B p65-p50 heterodimer from the cytoplasm to the nucleus where the transcription factor stimulates IFN and ISG promoter activity (Fig. 3-1A) (179). Induction of upstream innate immune signaling cascades by viruses and other pathogens triggers phosphorylation of the I κ B degron by the I κ B kinase (IKK) complex (171). Recognition of I κ B's phosphorylated degron (phosphodegron) by β -TrCP, a substrate adaptor of an E3 ubiquitin ligase, triggers I κ B ubiquitination and proteasomal degradation, allowing nuclear translocation of the NF- κ B heterodimer (171). By recruiting β -TrCP to its C-terminal I κ B-like degron (ILD), NSP1 is able to interfere with the interaction of β -TrCP with phosphorylated I κ B, thus thwarting β -TrCP-mediated

degradation of I κ B and NF- κ B activation. Indeed, mutagenesis and deletion analyses have indicated that the NSP1 C-terminal ILD has an essential role in the formation of NSP1- β -TrCP complexes and in the degradation of β -TrCP in infected cells (138).

Recent studies by Lutz et al (145) and Ding et al (144) suggest that NSP1 induces β -TrCP degradation by functioning as a substrate adaptor subunit of hijacked E3 cullin-RING ligases (CRLs). CRLs are large multicomponent assemblages that coordinate the activities of many cellular processes, including innate immune responses to viral infection (157), by facilitating directed degradation of substrates. Central to CRL function, a cullin scaffold protein bridges ubiquitin-charged E2 conjugating enzymes to substrates anchored to substrate adaptor proteins. Modification of the cullin component by neddylation activates the CRL, resulting in the transfer of ubiquitin from the E2 onto the substrate (157, 163). NSP1 is believed to be a component of a cullin-3 CRL (Cul3 CRL) with specificity for β -TrCP. In contrast, the E3 ligase responsible for targeting I κ B for proteasomal degradation is assembled on a cullin-1 (Cul1) scaffold that anchors a substrate recognition complex consisting of Skp1 and the F-box adaptor protein β -TrCP; this E3 is termed the Skp1-Cul1-F-box (SCF ^{β -TrCP}) CRL (165, 179).

Because of its critical role in innate immune responses, the function of the SCF ^{β -TrCP} CRL and its components are primary targets of viral proteins made by viruses in addition to rotavirus (220). For example, through its interaction with β -TrCP, HIV Vpu redirects the activity of the SCF ^{β -TrCP} CRL, causing the ubiquitination and degradation of CD4 (150, 185). Similarly, by sequestering β -TrCP, the vaccinia virus A49 protein prevents the SCF ^{β -TrCP} CRL from targeting I κ B for degradation (151). Unlike NSP1, the

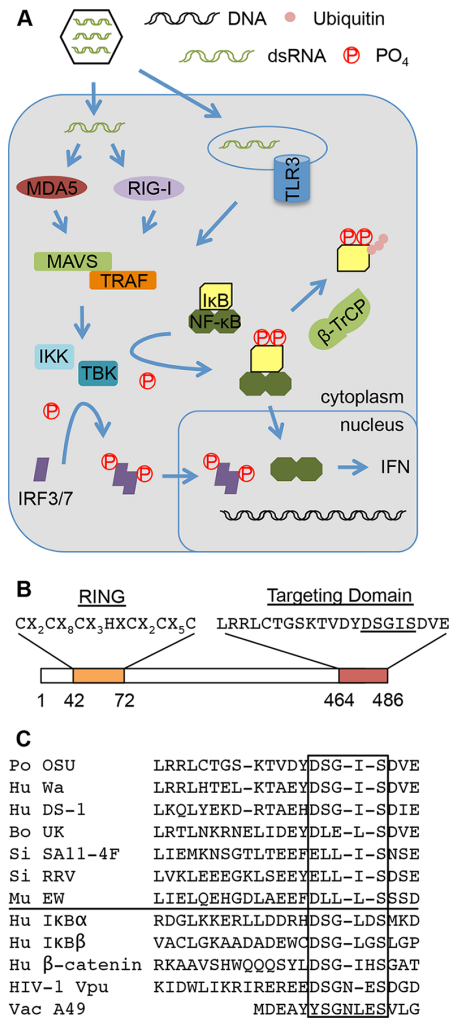


Figure 3-1. Targeting of the interferon activation pathway by rotavirus NSP1. (A) Recognition of viral dsRNA causes host RNA sensors RIG-I, MDA5 and/or TLR3 to interact with MAVS and TRAF adaptor proteins, activating the kinases IKK and TBK1. IKK directs the phosphorylation of serine residues in the DSG ϕ XS motif of inhibitor of NF- κ B (I κ B), generating a phosphodegron that is recognized by β -TrCP, a substrate adaptor of an E3 cullin-RING ligase. β -TrCP mediates the ubiquitination and degradation of I κ B, freeing the NF- κ B subunits to translocate to the nucleus and promote IFN expression. TBK1 directs phosphorylation of the interferon-regulatory factors IRF3/7, inducing their dimerization and nuclear translocation and further stimulating IFN expression. (B) Key features of NSP1 proteins include a conserved N-terminal RING-like domain and a variable C-terminal substrate targeting domain. The C-terminal targeting domain of OSU NSP1 includes an ILD motif (underlined). (C) Above line: Alignment revealing the presence of ILDs in the NSP1 proteins of common porcine (OSU) and human (Wa and DS1) virus strains, but absence in the NSP1 proteins of bovine (UK), simian (SA11-4F, RRV), and murine (EW) virus strains. Below line: I κ B-like degron sequences within other known binding partners of β -TrCP, including the HIV Vpu and vaccinia A49 proteins. Regions that include I κ B degron and degron-like sequences are boxed.

A49 protein does not function as part of an E3 ligase and is not associated with β -TrCP degradation.

Phosphorylation of the I κ B degron by the IKK kinase complex triggers a sequence of events leading to the assembly of the SCF ^{β -TrCP} CRL that induces I κ B degradation and promotes NF- κ B activation (181). Whether rotavirus NSP1 relies on a similar pathway to assemble Cul3 CRLs targeting β -TrCP for degradation is unknown. In this study, we determined that the NSP1 ILD is phosphorylated and that the kinase responsible for this modification is the constitutively active casein kinase II (CKII), rather than the kinase (IKK) that phosphorylates the I κ B degron. Moreover, we have found that phosphorylation of the NSP1 ILD not only enables formation of a stable NSP1- β -TrCP complex, but also triggers changes involving the NSP1 N-terminal RING domain that result in Cul3 interaction. Thus, CKII phosphorylation is a critical initiating event not only in the ability of NSP1 to recruit β -TrCP, but also in its ability to incorporate itself into a CRL that induces the ubiquitination and degradation of β -TrCP.

Materials & Methods

Cells and viruses. Human embryonic kidney HEK293T cells were grown in Dulbecco's modified Eagle's medium (DMEM) containing 10% fetal bovine serum (FBS) (Gibco), 2 mM glutamine, and 1,000 units per ml each penicillin and streptomycin. Human colorectal HT29 cells were grown in McCoy's 5A (modified) medium containing 10% FBS and penicillin-streptomycin. African green monkey fetal kidney (MA104) cells were grown in Medium M199 containing 10% FBS and penicillin-streptomycin. Porcine PK15 cells were grown in EMEM containing 10% FBS and penicillin-streptomycin.

Rotaviruses were propagated and titered by plaque assay on MA104 cells as described by Arnold et al (221). Prior to infection, rotaviruses were activated by treatment with 5 μ g per ml of porcine pancreas trypsin (type IX-S; Sigma-Aldrich) for 1 h at 37°C. The monoreassortant rotavirus strains SOF, SKF, SDF, and SRF were a kind gift of Nobumichi Kobayashi (222).

Antibodies. Rabbit polyclonal antibodies to simian SA11-5S and porcine OSU NSP1 proteins (137) and PCNA (Santa Cruz Biotech [SCB], sc-7907), rabbit monoclonal antibody to β -TrCP (Cell Signaling Technology [CST], #11984S), and mouse monoclonal antibodies to $\text{I}\kappa\text{B}$ (CST, #4814), p- $\text{I}\kappa\text{B}$ (CST, #9246), and CKIIa (SCB, sc-373894) were used at 1:5,000 dilution. Mouse monoclonal antibody to Halo tag (Promega, #G928A) and rabbit polyclonal antibodies to Cull1 (Bethyl Lab [BL], #A303-373A), cyclophilin B (CST, #D1V5J), and Cul3 (BL, #A301-109A) were used at 1:1000 dilution. Rabbit polyclonal anti-enterokinase cleavage (DDDDK) antibody (BL, #A190-102A) was used at 1:10,000 dilution to detect FLAG tags. HRP-conjugated goat anti-rabbit IgG antibody (CST, #7074) and horse anti-mouse IgG antibody (CST, #7076) were used at 1:10,000 dilution.

Inhibitors. The protein kinase CKII inhibitor, 4,5,6,7-tetrabromobenzotriazole (TBB) (Tocris Bioscience) and the small molecule inhibitor of Nedd8-activating enzyme, MLN4924 (Cayman Chemical), were prepared as 1 mM stocks in dimethyl sulfoxide (DMSO), which were stored at -20°C. TBB and MLN4924 were diluted in cell culture medium to final concentrations of 80 and 1 μ M, respectively, immediately prior to use.

TNF- α (Sigma) was dissolved in water at a concentration of 25 mg/ml and diluted in media to a final concentration of 25 ng/ml. MG132 (Sigma) was dissolved in DMSO and diluted in media to a final concentration of 15 μ M.

Plasmids. The construction of CMV-expression vectors, pLIC6 and pLIC6F, used for transient expression of wild type and mutant forms of NSP1 or FLAG-tagged β -TrCP, were described previously (138). pcDNA3-DN-hCUL3-FLAG was a gift from Wade Harper (Addgene plasmid # 15820). pHTN-NSP1(OSU) was kindly provided by Michelle Arnold (145). Plasmids were grown in TOP10 E. coli (ThermoFisher), purified using NucleoBond Xtra endotoxin-free plasmid purification kits (Clontech), and verified by sequencing.

Transfections. For transient protein expression, transfection mixtures containing 94 μ l Opti-MEM [Gibco], 1 mg vector DNA, and 2 μ l Lipofectamine 2000 [Invitrogen] were placed in wells of a 12-well cell-culture plate. Afterwards, 0.9 ml HEK293T cell suspension (1.3×10^6 cells per ml) in DMEM containing FBS was added to each well. At 24 h p.t., cell monolayers were rinsed with phosphate-buffered saline (PBS, pH 7.4) and lysed in a 200- μ l solution of 1 \times radioimmunoprecipitation assay (RIPA) buffer (150 mM NaCl, 50 mM Tris-HCl, pH 8.0, 1% Nonidet P-40, 0.5% sodium deoxycholate, 0.1% sodium dodecyl sulfate) containing 1 \times phosphatase inhibitor cocktail (1 mM each sodium fluoride, sodium orthovanadate, β -glycerophosphate, and sodium pyrophosphate), and 1 \times Complete EDTA-free protease inhibitor cocktail (Roche). Lysates were incubated on ice

for 30 min with vortexing every 10 min, and clarified by centrifugation for 10 min at 15,000 x g at 4°C.

For RNAi experiments, CKII-directed siRNA (Dharmacon SMARTpool ON-TARGETplus CSNK2A1 siRNA, #L-003475-00) or scrambled control siRNA (ON-TARGETplus non-targeting pool, #D-001810-10) was added to siLentFect (BioRad, #1703360) immunoblot assay.

Viral infection. Nearly confluent monolayers of HT29 cells in 10 cm² tissue-culture dishes were infected at an MOI of 5 with trypsin-activated rotavirus. After a one-hour adsorption period, virus inoculum was removed and cell monolayers rinsed with PBS. Cell monolayers were then maintained in serum-free McCoy's 5A (modified) medium until time of harvest. Cell lysates were prepared by washing monolayers with cold PBS and scraping cells into 0.5 ml RIPA lysis buffer. Lysates were incubated on ice for 10 min, gently mixed, and clarified by centrifugation for 10 min at 15,000 x g at 4°C.

Immunoblot assay. Protein samples were mixed with NuPAGE LDS sample buffer (Invitrogen) containing 50 mM dithiothreitol (DTT), denatured by heating to 70°C for 10 min, and resolved by electrophoresis on pre-cast 10% Tris-glycine polyacrylamide gels (Novex). Molecular weight markers (SeeBlue Plus2, Invitrogen; EZ-Run, Fisher Scientific) were resolved in parallel to determine protein sizes. Proteins were transferred from gels onto nitrocellulose membranes using an iBlot dry transfer apparatus (ThermoFisher). Membranes were blocked by incubation in 5% Carnation dry milk dissolved in PBS-0.2% Tween-20 (PBST) prior to incubation with primary antibody

diluted in milk-PBST solution. Membranes were washed with PBST before incubating with HRP-conjugated secondary antibody diluted in milk-PBST solution. Membranes were washed with PBST and developed using Super Signal West Pico chemiluminescent substrate (Pierce). Signal was detected by exposing membranes to BioExcell X-ray film or using the Azure Series c500 Infrared Imaging System. Bands of interest were normalized to the loading control PCNA.

In-blot phosphatase treatment. Protein samples were resolved by electrophoresis on 10% polyacrylamide gels and transferred onto nitrocellulose membranes, as described above. Membranes were blocked by incubation at room temperature in 5% BSA dissolved in PBST. Afterwards, membranes were incubated overnight at room temperature in a solution containing 100 units per ml of calf alkaline intestinal phosphatase (CIP, NEB M0290S), 100 mM NaCl, 50 mM Tris-HCl (pH 7.9), 10 mM MgCl₂, and 1 mM DTT. Following an additional 30-min incubation at 37°C, membranes were rinsed with PBST and probed by immunoblot assay.

Immunoprecipitation. Nearly confluent monolayers of HEK293T cells in 10-cm² dishes containing 10 ml of media were transfected by adding plasmid DNA mixtures prepared from 1.4 ml Opti-MEM, 7.5 µg each pLIC6-NSP1 and pLIC6F-β-TrCP or pcDNA3-DN-hCUL3-FLAG, and 29 µl Lipofectamine 2000. Transfected cells were incubated for 24 h at 37° C, harvested by resuspending into media, and recovered by low speed centrifugation (5 min at 500 x g). Cell pellets were rinsed twice with cold PBS and disrupted by resuspension in IP lysis buffer (150 mM NaCl, 50 mM Tris-HCl, pH 7.4,

1% Triton X-100, with 1× Complete EDTA-free protease inhibitor cocktail). After incubation on ice for 1 h, cellular debris were removed by centrifugation at 14,000 x g for 10 min. Fifty µl of a slurry of anti-FLAG M2 magnetic beads (Sigma, #M8823), pre-rinsed 3-times with IP wash buffer (150 mM NaCl, 50 mM Tris-HCl, pH 7.4), was added to clarified cell lysates. After overnight incubation at 4°C with nutation, M2 beads were recovered using a BioRad Surebeads magnetic stand and rinsed 3 times with IP wash buffer. Protein was released from M2 beads by nutation in IP elution buffer (0.1 M glycine, pH 3.0) for 5 min at 4°C. Eluted proteins were examined by gel electrophoresis and immunoblot analysis.

Results

The NSP1 ILD is phosphorylated. The interaction of β-TrCP with IκB requires phosphorylation of the two serine residues in the IκB degron, DSGΦXS(8). By extrapolation, interaction of β-TrCP with NSP1 may similarly require phosphorylation of the two serine residues in the NSP1 C-terminal ILD, DSGXS. To determine whether NSP1 was phosphorylated, we transiently expressed various untagged forms of NSP1 in HEK293T cells including wild type OSU NSP1 (WT) and a C-truncated form of OSU NSP1 lacking the ILD (DC13) (Fig. 3-2A, B). Also expressed were two chimeras produced by combining portions of the OSU and SA11-4F NSP1 proteins. The OSU-4F chimera is identical in sequence to OSU NSP1 except that its last 8 residues have been replaced with the corresponding region of SA11-4F NSP1. Thus, the OSU-4F NSP1 chimera lacks an ILD. In contrast, the 4F-OSU chimera is identical in sequence to SA11-4F NSP1 except that its last 12 residues have been replaced with the corresponding

region of OSU NSP1. Thus, the 4F-OSU NSP1 chimera contains an ILD. The phosphorylation status of transiently expressed WT and DC13 NSP1 and OSU-4F and 4F-OSU chimeras was examined by immunoblot assay using a monoclonal antibody (p-I κ B) that specifically recognizes the fully phosphorylated form of the I κ B degron (DpSG Φ XpS). The assay showed that only those NSP1 proteins containing an ILD (WT, 4F-OSU) were recognized by p-I κ B antibody (Fig. 3-2B). These results suggest that OSU NSP1 is a phosphoprotein and that its ILD undergoes phosphorylation.

To further evaluate the possibility that the ILD of OSU NSP1 was phosphorylated, blots of transiently expressed WT and DC13 NSP1 and OSU-4F and 4F-OSU chimeras were incubated with calf intestinal alkaline phosphatase (CIP) prior to probing with p-I κ B antibody. The analysis demonstrated that CIP pre-treatment reduced recognition of WT and 4F-OSU NSP1 by p-I κ B antibody (Fig. 3-2B). Similar results were obtained utilizing HALO-tagged OSU NSP1 (H-NSP1) in place of untagged NSP1 (Fig. 3-2C). CIP pre-treatment reduced recognition of H-NSP1 by p-I κ B antibody, even though the protein remained present as determined using anti-HALO antibody. Likewise, in control experiments, CIP treatment reduced recognition of p-I κ B formed in cells treated with tumor necrosis factor alpha (TNF- α), a cytokine that upregulates IKK and activates NF- κ B (Fig. 3-2B). The importance of the ILD in recognition of NSP1 by p-I κ B antibody was also investigated by mutagenesis. This analysis showed that alanine replacement of serine residues in the I κ B-like DSGXS motif, either individually or in combination, prevented p-I κ B antibody from recognizing OSU NSP1 (Fig. 3-3A).

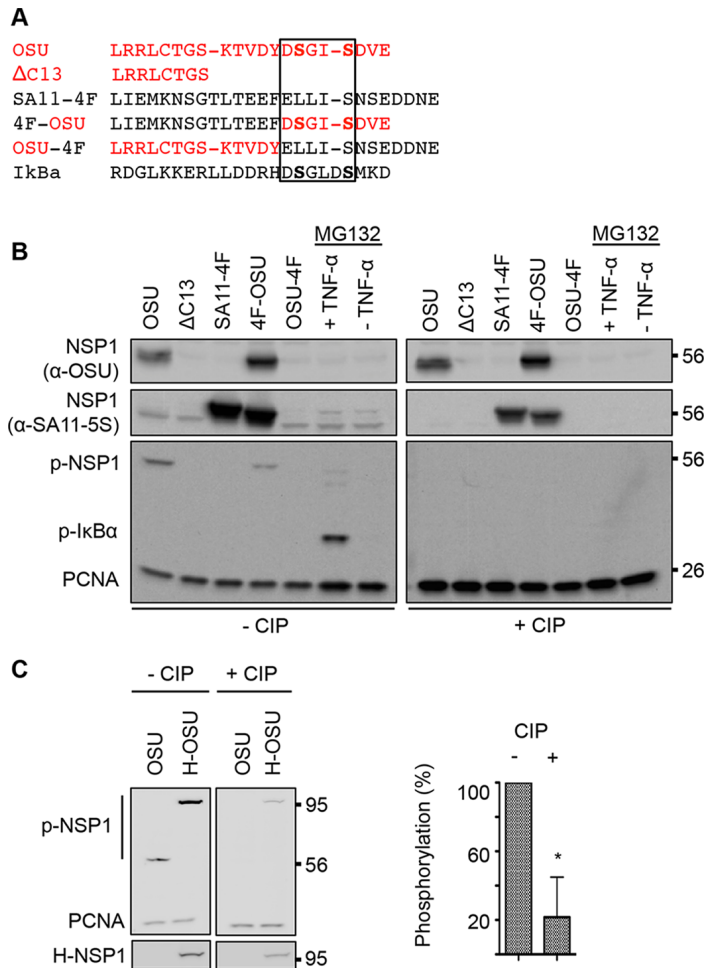


Figure 3-2. Phosphorylation of transiently expressed OSU NSP1. (A) Alignment of C-terminal NSP1 sequences and a portion of IkB containing the DSGΦXS phosphodegron. Red lettering indicates OSU-specific residues. The phosphodegron region is boxed. (B) HEK293T cells were transfected with NSP1 expression vectors or maintained in the presence of MG132 with or without TNF-α beginning at 20 h p.t. Lysates prepared from cells at 24 h p.t. were resolved by gel electrophoresis, in duplicate, and blotted onto nitrocellulose membranes. Membranes were mock treated (-CIP) or treated with calf alkaline intestinal phosphatase (+CIP) in parallel. Mock- and CIP-treated membranes were probed with PCNA antibody, p-Ik B antibody to detect phosphorylated NSP1 (p-NSP1) and Ik B (p-Ik B), OSU NSP1 antibody to detect OSU and 4F-OSU NSP1, and SA11-5S antibody to detect SA11-4F and 4F-OSU NSP1. (C) Lysates prepared from HEK293T cells transfected with expression vectors for OSU NSP1 (OSU) or HALO-tagged OSU NSP1 (H-OSU) were resolved by gel electrophoresis and blotted onto nitrocellulose membranes, in duplicate. Mock- and CIP-treated membranes were probed with p-Ik B antibody to detect p-NSP1 and with antibodies to the HALO tag and PCNA. Levels of phosphorylated H-OSU were calculated relative to PCNA levels and normalized to 100% for the untreated sample. Data are from two independent experiments (mean ± SD, $p < 0.05$) are shown.

Together, these findings indicate that the ILD of OSU NSP1 is phosphorylated in a manner mimicking the I κ B degron, with both serine residues of the DSGXS motif phosphorylated.

NSP1 encoded by various rotavirus strains is phosphorylated. To assess whether NSP1 proteins expressed during infection were phosphorylated, human HT29 cells were infected with rotavirus strains OSU, SA11-4F, and SA11-5S, and with a panel of mono-reassortant rotaviruses containing various segment 5 RNAs in an SA11-L2 background. The reassortant viruses included SOF, SKF, SDF, and SRF, which express the NSP1 proteins of porcine OSU, human KU, human DS-1, and simian RRV strains, respectively. Of these NSP1 proteins, only those encoded by OSU, KU, and DS1 viruses contain an ILD (Fig. 3-4A). Rotavirus-infected HT29 cells were harvested at 10 h p.i., and proteins in HT29 lysates were analyzed by immunoblot assay using p-I κ B antibody. The results showed that those NSP1 proteins containing an ILD were recognized by p-I κ B antibody (Fig. 3-4B). Thus, NSP1 proteins with ILDs undergo phosphorylation in rotavirus-infected cells and this protein modification occurs for rotavirus strains isolated from a variety of animal species (e.g., human, simian, porcine). OSU, KU, and DS1 NSP1 proteins produced in rotavirus-infected simian MA104 and porcine PK15 cells were similarly recognized by p-I κ B antibody suggesting that phosphorylation of the ILD takes place regardless of the species origin of the host cell line (data not shown). While our results showed that SA11-4F and RRV NSP1 proteins were not recognized by the p-I κ B antibody, these data do not exclude the possibility that these proteins are phosphorylated at sites other than an ILD motif.

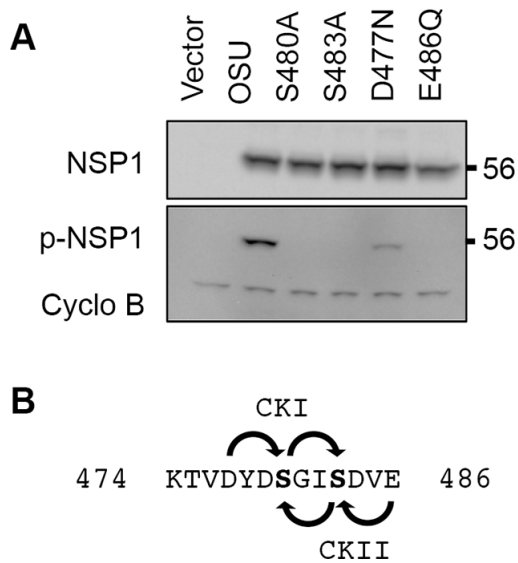


Figure 3-3. Effect of priming loop mutations on NSP1 phosphorylation. (A) Lysates prepared from HEK293T cells expressing wild type (WT) OSU NSP1 and forms of the protein with the indicated mutations were analyzed by immunoblot assay using p-Ik B antibody to recognize p-NSP1, OSU NSP1 antibody, and PCNA antibody. **(B)** Predicted phosphorylation patterns of the OSU NSP1 ILD by CKI and CKII using D477 and E486 as priming residues, respectively.

NSP1 is phosphorylated by CKII. Interaction of β -TrCP with I κ B is dependent on phosphorylation of the I κ B degron by the IKK β subunit (223). To determine whether the NSP1 ILD motif was phosphorylated by the same kinase, or a different one, the Eukaryotic Linear Motif resource (elm.eu.org) (224) was used to identify potential kinase recognition motifs in NSP1 protein. The analysis indicated that NSP1 proteins with an ILD lack a recognition site for IKK β kinase. Instead, the NSP1 ILD was found to be situated within recognition motifs for casein kinase I (CKI) and II (CKII) (Fig. 3-3B) (138). CKI and CKII direct phosphorylation after priming at a negatively charged amino acid residue (e.g., aspartic acid, glutamic acid) located three positions upstream or downstream of a target serine residue, respectively (225-227). Examination of NSP1 proteins indicates that such amino acids are present at the putative priming positions for CKI and CKII in the NSP1 ILD motif [(D/E)YDSGISDVE] (priming positions are underlined, phosphoserines are in bold). Whether CKI or CKII was involved in NSP1 phosphorylation was examined by transient expression of OSU NSP1 proteins in which the putative priming residues had been mutated. The results showed Glu>Gln mutation of the putative CKII priming residue prevented recognition of OSU NSP1 by p-I κ B antibody, whereas Asp>Asn mutation of the putative CKI priming residue did not (Fig. 3-3A). These mutagenesis data indicate that CKII is responsible for phosphorylation of the NSP1 ILD.

To further evaluate the importance of CKII activity on NSP1 phosphorylation, HEK293T cells were transfected with a vector expressing HALO-tagged OSU NSP1 and either siRNA specific for CKII RNA or a scrambled control siRNA pool (Fig. 3-5A-C). Immunoblot analysis showed that treatment with CKII siRNA significantly reduced

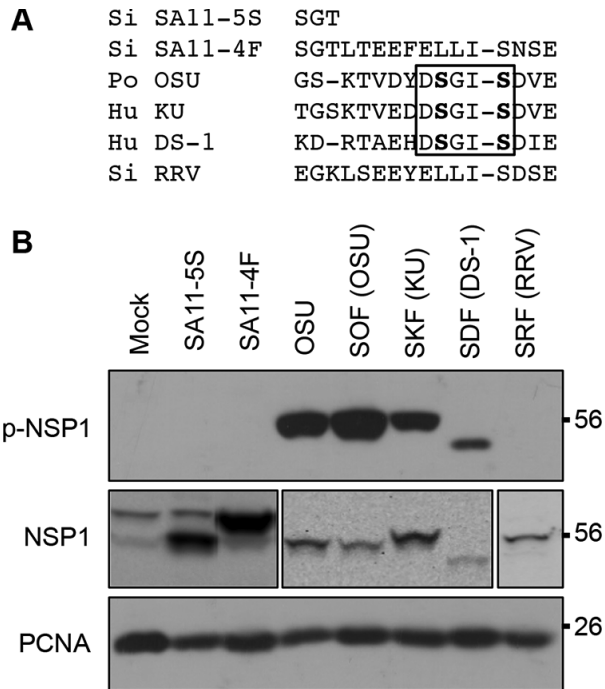


Figure 3-4. Phosphorylation of NSP1 in rotavirus-infected cells. (A) Alignment of C-terminal sequences of NSP1 proteins with the ILD boxed. (B) HT29 cells were infected with SA11-4F, SA11-5S, or OSU virus strains or mono-reassortant SA11-L2 virus strains expressing OSU (SOF), KU (SKF), DS-1 (SDF), or RRV (SRF) NSP1. SA11-5S expresses a mutant form of NSP1 that lacks the 13-terminal residues of wild type SA11-4F NSP1. Lysates prepared from the infected cells at 15 h p.i. were analyzed by immunoblot assay using p-Ik B antibody to detect p-NSP1 and PCNA antibody. To detect total NSP1, lysates from mock-, SA11-4F-, and SA11-5S-infected cells were probed with antibody made against SA11-5S NSP1, lysates from OSU-, SOF-, SKF-, and SDF-infected cells were probed with antibody made against OSU NSP1, and the lysate from RRV-infected cells was probed with antibody made against RRV NSP1 (137).

levels of CKII expression and phosphorylated NSP1 (Fig. 3-5B, C), relative to treatment with scrambled siRNAs, supporting the hypothesis that CKII mediates phosphorylation of the NSP1 ILD. The contribution of CKII to NSP1 phosphorylation was also examined by treating OSU-infected human HT29 and porcine PK15 cells with 4,5,6,7-tetrabromobenzotriazole (TBB), a highly-specific cell-permeable nucleoside inhibitor of CKII (228). Whole-cell lysates prepared from the infected cells at 4 and/or 9 h p.i. were analyzed by immunoblot analysis using an antibody specific for the OSU NSP1 RING domain (anti-RING antibody) to detect total NSP1 and the p-I κ B antibody to detect nucleoside inhibitor of CKII (228). Whole-cell lysates prepared from the infected cells at 4 and/or 9 h p.i. were analyzed by immunoblot analysis using an antibody specific for the OSU NSP1 RING domain (anti-RING antibody) to detect total NSP1 and the p-I κ B antibody to detect phosphorylated NSP1 and I κ B proteins (Fig. 3-5D, E). The results showed that TBB inhibited the accumulation of phosphorylated NSP1 in both HT29 and PK15 infected cells. The detection of NSP1 in TBB-treated cells with the anti-RING antibody ruled out the possibility that the inhibitor prevented NSP1 expression. Taken together, the results obtained using CKII siRNAs and TBB demonstrate that CKII is responsible for phosphorylation of the NSP1 ILD.

NSP1 phosphorylation is required for NSP1- β -TrCP interactions. Because I κ B must undergo phosphorylation for interaction with β -TrCP (171), we predicted that NSP1 may likewise require phosphorylation for interaction with β -TrCP. To examine this

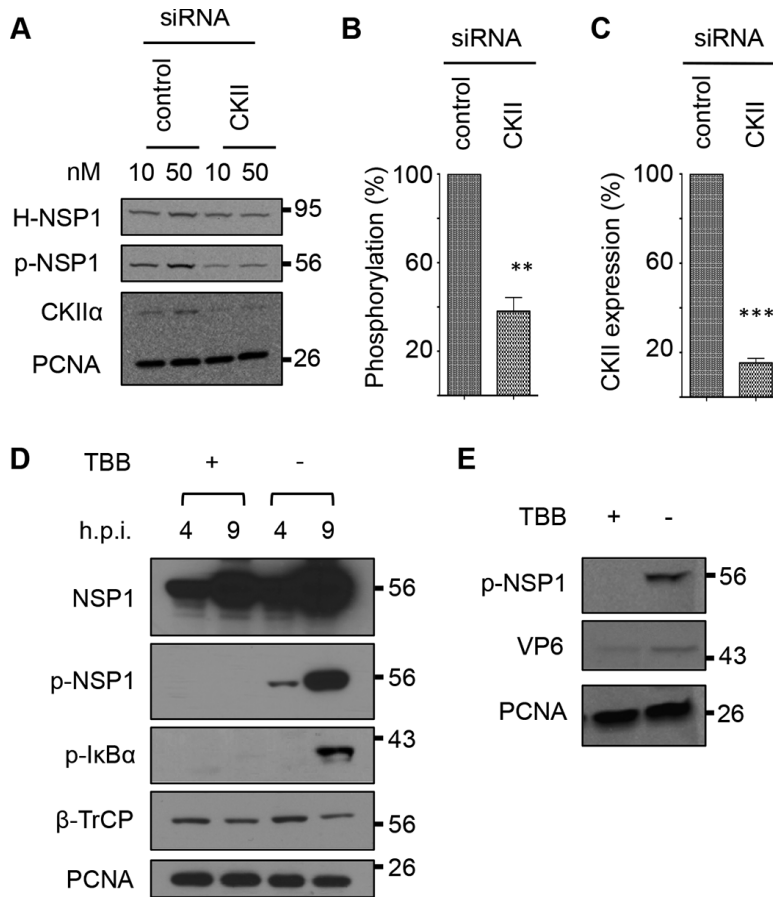


Figure 3-5. Effect of CKII inhibition on NSP1 phosphorylation. (A) HEK293T cells were co-transfected with a vector expressing HALO-tagged NSP1 (H-NSP1) and a 10 or 50 mM siRNA pool targeting the CKII RNA or representing a scrambled siRNA control pool. At 48 h p.t., cells were collected and proteins samples analyzed by immunoblot assay with antibodies specific for HALO tag, p-NSP1, CKII α , and PCNA. Band intensities from two independent experiments using 50 mM concentration of siRNA pools were determined with an Azure digital imager. (B) Levels of OSU NSP1 phosphorylation were calculated by dividing p-NSP1 intensity values by those for H-NSP1 and normalizing the results to 100% for the control siRNA sample. (C) CKII levels were calculated by dividing CKII intensity values by those for PCNA and normalizing the results to 100% for the control siRNA sample. (D) HT29 cells were infected with OSU at an MOI of 5, and treated with TBB or DMSO at 2 h p.i. At 4 and 9 h p.i., cells were collected and lysed, and proteins in the samples were resolved by electrophoresis and examined by immunoblot assay using antibodies recognizing OSU NSP1, p-NSP1, p-I κ B, β -TrCP, and PCNA. (E) PK15 cells were infected with OSU at an MOI of 5, and mock treated or treated with TBB. Cells were harvest at 9 h p.i., and proteins in the samples examined by immunoblot assay with antibodies to p-NSP1, rotavirus VP6, and PCNA.

possibility, FLAG-tagged β -TrCP was transiently expressed in HEK293T cells with WT NSP1 or mutant forms of NSP1 that lacked either an ILD (dC13) or the CKII priming residue (E486Q), or that contained a mutation of a conserved cysteine residue in the N-terminal RING domain (C42A). FLAG-tagged β -TrCP (F- β -TrCP) was recovered from lysates prepared from the transfected cells by affinity purification with anti-FLAG resin, and proteins co-purifying with β -TrCP were identified by immunoblot assay. The results indicated that WT NSP1 and NSP1 with a mutated RING domain (C42A) interacted with F- β -TrCP (Fig. 3-6). In contrast, NSP1 that lacked an ILD motif (DC13) or that was unable to undergo CKII phosphorylation (E486Q) did not form complexes with F- β -TrCP (Fig. 6). These data indicate that NSP1 must contain a phosphorylated ILD for stable interaction with β -TrCP. Interestingly, the data also suggest that the NSP1 RING domain may not have a role in modulating NSP1- β -TrCP interactions, since the NSP1 RING mutant C42A retained binding activity for β -TrCP.

NSP1 phosphorylation is required for incorporation into CRLs. Previous reports have indicated that NSP1 functions as a substrate adaptor of Cul3 CRLs (144, 145). To address whether incorporation of NSP1 into Cul3 CRLs is influenced by the phosphorylation status of the NSP1 ILD, we transiently expressed F- β -TrCP with WT NSP1 or mutant NSP1 proteins C42A or E486Q in HEK239T cells. We stabilized CRLs that formed in transfected cells by the addition of MLN4924, a NEDD8-activating enzyme inhibitor that inhibits cullin neddylation and CRL disassociation (229). Immunoprecipitates containing F- β -TrCP were recovered from transfected-cell lysates using anti-FLAG affinity resin and analyzed by immunoblot assay (Fig. 3-7A).

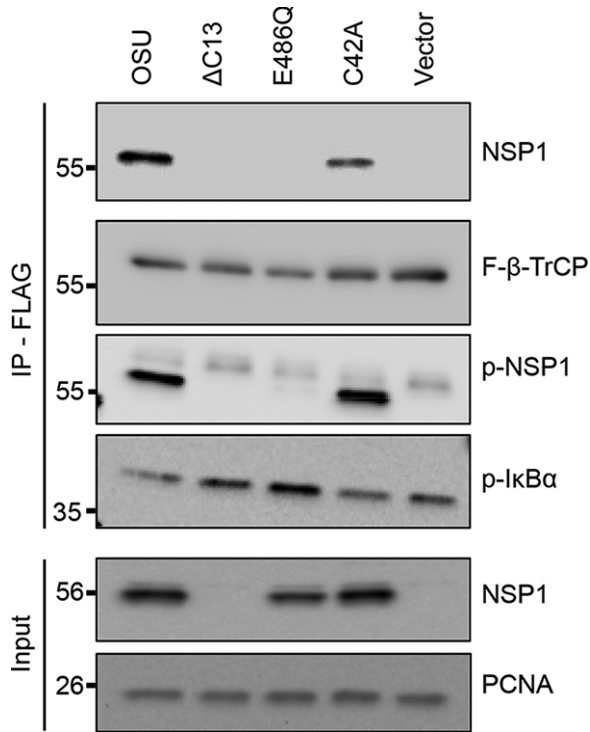


Figure 3-6. Influence of NSP1 phosphorylation on interactions with β -TrCP. HEK293T cells were transfected with vectors expressing FLAG- β -TrCP and WT or mutant OSU NSP1. Lysates prepared from the cells at 24 h p.t. were incubated with anti-FLAG resin to immunoprecipitate (IP) complexes containing FLAG- β -TrCP. Input fractions and eluted proteins were analyzed by immunoblot assay with antibodies specific for NSP1, FLAG, p-NSP1, p-I κ B, and PCNA. The OSU NSP1 antibody was generated using a peptide representing the C-terminus of the OSU NSP1 proteins (137). As a result, the OSU NSP1 antibody is not able to recognize the product of the OSU DC13 expression vector (138).

Characterization of the immunoprecipitates indicated that F- β -TrCP interacted with neddylated and non-neddylated forms of Cul1, consistent with previous reports showing that β -TrCP is a component of the SCF ^{β -TrCP} E3 ligase (Fig. 3-7A). The analysis also indicated that F- β -TrCP interacted with WT and C42A p-NSP1, but not with E486Q NSP1 (Fig. 3-7A). This finding argues that the interaction of β -TrCP with NSP1 is dependent on phosphorylation of the NSP1 ILD, consistent with data presented in Fig. 3-6. Surprisingly, analysis of F- β -TrCP immunoprecipitates recovered from cells expressing C42A NSP1 indicated that C42A NSP1- β -TrCP complexes were formed that contained CKII, the kinase responsible for phosphorylation of the NSP1 ILD (Fig 3-7A). In contrast, relatively little CKII was detected in F- β -TrCP immunoprecipitates recovered from cells in which F- β -TrCP was co-expressed with WT NSP1 or a mutant form of NSP1 that cannot undergo phosphorylation (E486Q). These data suggest that CKII has affinity for NSP1 and that the interaction between the two proteins requires the CKII E486 priming residue and/or phosphorylation of the NSP1 ILD. Moreover, these data suggest that CKII interaction with the NSP1- β -TrCP complex does not require a WT RING domain in the NSP1 protein.

More Cul3 appeared to be present in F- β -TrCP immunoprecipitates recovered from transfected cells in which F- β -TrCP was co-expressed with WT NSP1 than with C42A or E486Q NSP1 (Fig. 3-7A). To further evaluate this possibility, we transiently expressed FLAG-tagged dominant negative Cul3 [F-(DN)Cul3] with WT, C42A, or E486Q NSP1 in HEK293T cells (Fig. 3-7B). (DN)Cul3 is a carboxyl truncated form of Cul3 that forms stable complexes with F-box adaptor proteins and substrates but is unable to interact with Rbx1 and the E2 ubiquitin-conjugating enzyme (166).

Immunoblot analysis of F-(DN)Cul3 immunoprecipitates indicated that WT NSP1, but neither NSP1 with a mutated RING motif (C42A) nor a phosphorylation-defective ILD motif (E486Q), interacted with Cul3 (Fig. 3-7B). These results suggest that the NSP1 RING domain plays an important role in NSP1-Cul3 interactions, and consequentially, the incorporation of NSP1 into Cul3 CRLs. However, the fact that E486Q NSP1 did not bind Cul3, despite the presence of a WT RING domain, argues that the CKII E486 priming residue and/or phosphorylation of the NSP1 ILD motif precedes the activity of the RING domain in promoting NSP1-Cul3 interactions. Taken together, this data suggests an ordered association of NSP1 with CRLs and its protein target; NSP1 interactions with CKII lead to phosphorylation of its C-terminal ILD and binding to β -TrCP targets, followed by CKII release and Cul3 binding.

Relationship between NSP1 phosphorylation and β -TrCP degradation. The results presented above indicate that the interaction of phosphorylated NSP1 with β -TrCP is not dependent on the incorporation of NSP1 into a CRL, raising the question of whether NSP1 could inhibit NF- κ B-activation simply sequestering by β -TrCP away from its I κ B target. To examine this possibility, HT29 cells were mock infected or infected with OSU rotavirus. Lysates prepared from the cells at 2, 4, 6, 8, and 10 h p.i. were analyzed by immunoblot assay using antibodies recognizing phosphorylated NSP1 and I κ B, and β -TrCP (Fig. 3-8). The analysis showed that NSP1 was initially detected by 4 h p.i., with levels sharply increasing by 6 h p.i. Phosphorylated NSP1 was first observed by 6 h p.i., with levels further increasing until 8 h p.i. Phosphorylated I κ B was initially detected by 4 h p.i., indicating activation of the IKK signaling cascade. The level of phosphorylated I κ B

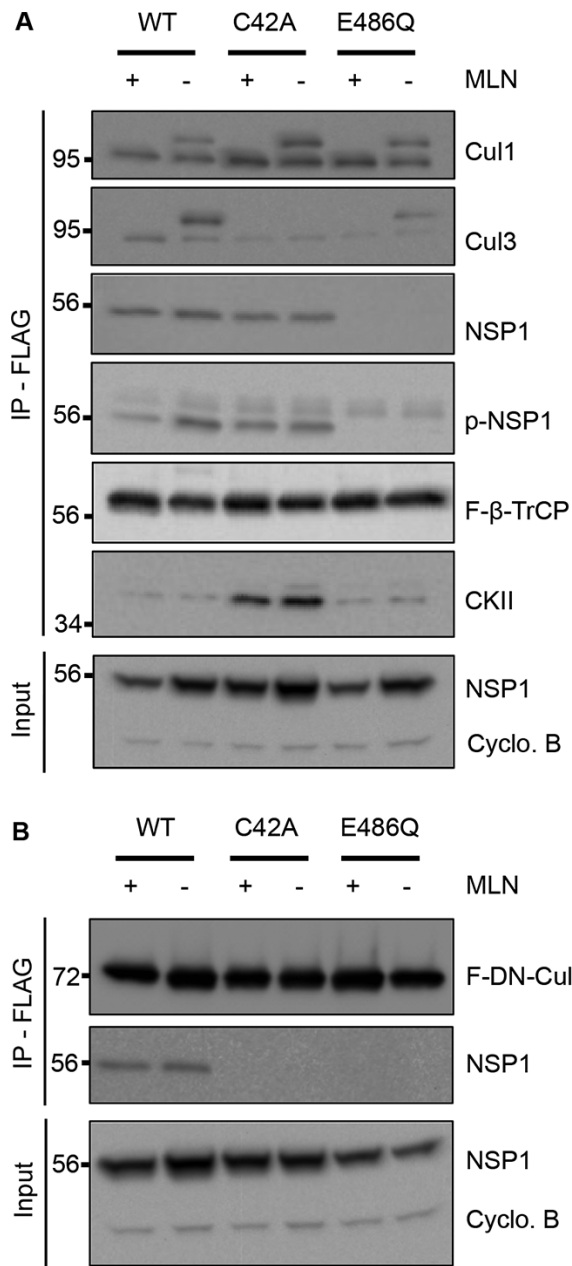


Figure 3-7. Effect of NSP1 phosphorylation on interactions with Cul3. HEK293T cells were transfected with vectors expressing WT or mutant C42A or E486Q OSU NSP1 and (A) FLAG-β-TrCP or (B) FLAG (F)-DN-Cul3. Transfected cells were mock treated or treated with the neddylation inhibitor MLN4964 (MLN). Lysates prepared from the cells at 24 h p.t. were incubated with anti-FLAG resin to immunoprecipitate (IP) complexes containing FLAG-tagged proteins. Input fractions and eluted proteins were analyzed by immunoblot assay with antibodies specific for Cul1, Cul3, NSP1, p-NSP1, FLAG, CKII α and cyclophilin B.

markedly increased by 6 h p.i. and remained high through at least 10 h p.i., suggesting a failure of β -TrCP to efficiently recruit and induce the degradation of I κ B in the infected cell. Notably, degradation of β -TrCP was not apparent until after 6 to 8 h p.i., well after significant accumulation of phosphorylated I κ B was observed. Thus, even though β -TrCP was present in infected cells at 6 to 8 h p.i., its presence was not correlated with the degradation of phosphorylated I κ B. These results raise the likelihood that β -TrCP degradation may not be the only mechanism used by NSP1 to inhibit I κ B degradation and NF- κ B activation. Instead, it is possible that NSP1 can accomplish these tasks simply by binding β -TrCP, thereby interfering with the ability of NF- κ B to interact with its I κ B target.

Discussion

In this study, we have determined that rotavirus NSP1 is phosphorylated and that this modification represents a critical initiating event in the interaction of NSP1 with β -TrCP and in the incorporation of NSP1 into Cul3-CRLs. (Fig. 3-9). Our analysis indicates that both serine residues in the OSU NSP1 ILD (DSGXS) undergo phosphorylation, mimicking phosphorylation of the two conserved serine residues of the I κ B degron. The NSP1 proteins of all tested rotaviruses containing an ILD were phosphorylated, regardless of the species origin of the virus or the species origin of the cell line used to grow the virus. The phosphorylated NSP1 proteins included those belonging to genotypes A1 and A2, representing the types of NSP1 genes found in nearly all rotaviruses causing disease in humans (3). NSP1 proteins with ILD motifs, whether transiently expressed in

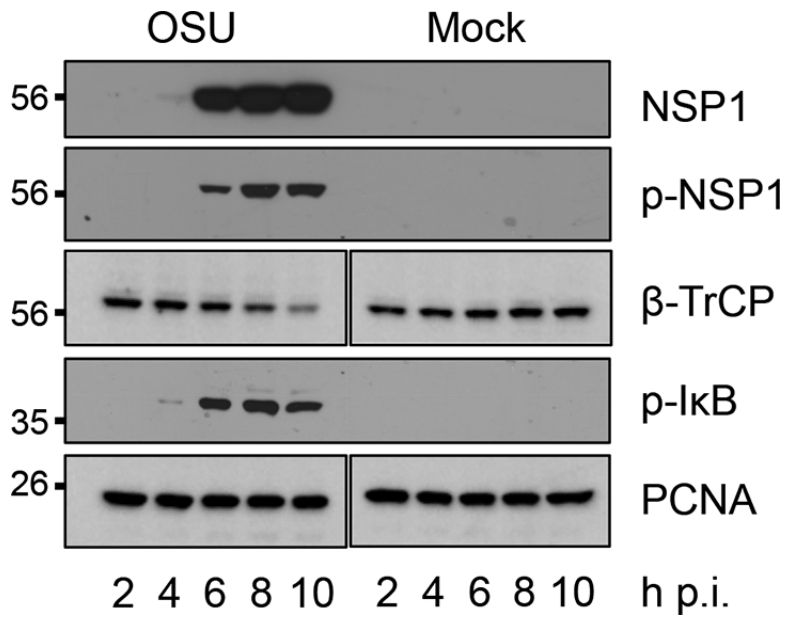


Figure 3-8. Accumulation of p-NSP1, β -TrCP, and p-I κ B during viral infection. HT29 cells were mock infected or infected with OSU rotavirus (MOI of 5) and harvested from 2 to 10 h p.i. Cellular lysates were resolved by gel electrophoresis and transferred onto nitrocellulose membranes. Blots were probed with antibodies specific for NSP1, p-NSP1, β -TrCP, p-I κ B, and PCNA.

cells transfected with CMV transcription vectors or expressed in rotavirus-infected cells, were phosphorylated. There was no evidence suggesting that other rotavirus gene products were necessary or affected NSP1 phosphorylation. Experiments performed with the NSP1 C42A mutant indicated that the protein's N-terminal RING region does not have a role in regulating ILD phosphorylation.

Phosphorylation assays carried out with small molecule inhibitors, siRNAs and mutagenized expression vectors all indicated that CKII, a ubiquitous constitutively-active serine-threonine kinase (230), was responsible for phosphorylation of the NSP1 ILD. Based on the time course experiment presented in Fig. 3-8, phosphorylated NSP1 is detected in OSU-infected cells at approximately the same time (6 h p.i.) that NSP1 begins to accumulate (Fig. 3-8). Thus, NSP1 is likely primed for interaction with β -TrCP soon after synthesis, in contrast to I κ B, which is dependent on activation of the upstream IKK signaling cascade to undergo phosphorylation (179). Indeed, by utilizing CKII, NSP1 can potentially undergo phosphorylation and target β -TrCP for degradation before pathogen recognition receptors of infected cells have triggered innate immune signaling pathways and I κ B phosphorylation. Our co-immunoprecipitation studies suggest that CKII not only phosphorylates the NSP1 ILD, but transiently binds to NSP1 at a step antibody, is not known. The source of the CKII kinase activity may be the COP9 signalsome (231), a multi-subunit protein complex responsible for deneddylating cullins and regulating CRL activity (232). Notably, NSP1 is not the only rotavirus protein known to be phosphorylated by a cellular kinase during virus replication. In particular, one of the major building blocks of rotavirus viroplasms (NSP5) undergoes extensive phosphorylation by CKI (72).

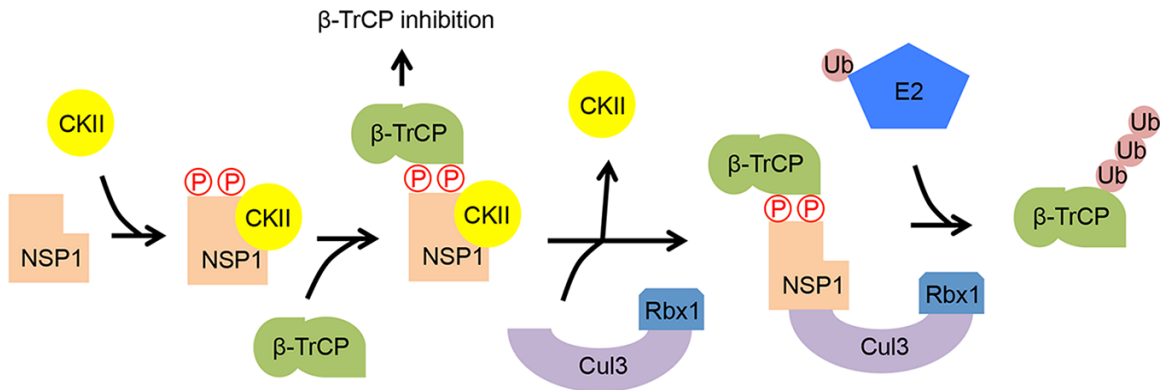


Figure 3-9. Predicted steps in the CKII-dependent incorporation of NSP1 into a Cul3 CRL. The constitutively-active kinase CKII interacts with NSP1, leading to phosphorylation of the NSP1 ILD. The affinity of β -TrCP for the phosphorylated degron results in the formation of an NSP1- β -TrCP-CKII complex. CKII is released as the NSP1- β -TrCP complex interacts with the CRL assembly intermediate Cul3 - RBx1. Recruitment of a charged E2 conjugating enzyme to Rbx1 results in the formation of a Cul3 CRL that causes the ubiquitination and proteasomal degradation of β -TrCP.

occurring prior to NSP1's incorporation into CRLs. Whether the entire CKII tetrameric complex (233) is bound to NSP1, or just the catalytically subunit recognized by the CKII

Our co-immunoprecipitation experiments suggest the CKII-NSP1- β -TrCP complex is a precursor of the Cul3-NSP1- β -TrCP complex, opening the possibility that interaction of Cul3 with NSP1 displaces CKII. Interestingly, the phosphorylation-defective NSP1 E486Q mutant does not form a complex with Cul3, supporting a hypothesis that phosphorylation of the NSP1 ILD triggers structural changes that must occur for the protein to bind Cul3. Whether the putative structural change results from just the phosphorylation of the ILD or also requires the binding of β -TrCP remains to be addressed. The NSP1 RING mutant C42A failed to form a complex with Cul3 complex, pointing to a key role for the RING in the incorporation of NSP1 into a CRL. The RING domain, including its C42 residue, is conserved among the NSP1 proteins of group A rotaviruses, regardless whether the protein targets β -TrCP or some other protein (e.g., IRF3) (234). The same RING domain is present in group C, D, and F rotaviruses (235), suggesting that the RING is a highly conserved structural feature necessary for formation of an NSP1 Cul3-CRL. Although the conserved RING domain suggests that the group C, D, and F rotaviruses incorporate into Cul3-CRLs like the group A rotaviruses, the group C, D, and F viruses lack a C-terminal ILD and thus are likely to target host proteins other than β -TrCP. The rotavirus RING domain is known to coordinate zinc binding (236); it may be the loss of this function and the subsequent failure to form zinc-stabilized fingers that prevents the NSP1 C42A mutant from binding to Cul3. There are multiple reports indicating that NSP1 is a single-stranded RNA-binding protein, with this activity

mapping to the RING domain (146, 236). Thus, NSP1 is likely a multifunctional protein with its RING residues contributing to more than one process.

Many animal group A rotaviruses (e.g., SA11-4F, RRV, EW, K9) encode NSP1 proteins that target IRF3 and other IRF proteins for degradation, instead of β -TrCP (137). The NSP1 of these viruses have a conserved C-terminal LL(I/L)S motif that mediates recognition of IRF3. The NSP1 LL(I/L)S motif is a mimic of the recognition motif pLxIS (p is hydrophobic) used by adaptor proteins of the IFN signaling pathway (STING, MAVS, and TRIF) to recognize IRF3 (237). Interestingly, the interaction of the adaptor protein with IRF3 requires phosphorylation of the serine residue in the pLxIS recognition motif by IKK kinase. In contrast, phosphorylation of its LL(I/L)S is not required for interaction of animal NSP1 proteins with IRF3, due to alternative contacts made between NSP1-IRF3 that do not involve the serine residue (212). As a result, NSP1 proteins targeting IRF3 need not undergo the same phosphorylation-dependent activation required by NSP1 proteins targeting β -TrCP. To avoid the assembly of functionless NSP1-CRLs, it seems likely that interactions of IRF3 with the C-terminal end of NSP1 would likely be necessary to induce structural changes enabling NSP1 to bind Cul3.

An important observation made in our experiments was that at relatively early times of infection with OSU rotavirus (6 to 8 h p.i.), phosphorylated I κ B accumulated despite approximately wild type levels of β -TrCP. Because β -TrCP is responsible for the degradation of I κ B, these results suggested that β -TrCP in the infected cell was being rendered inactive without undergoing degradation. This phenomenon could be explained by presuming that NSP1 can interfere with I κ B degradation simply by binding, and sequestering, β -TrCP. Alternatively, it could be that NSP1-mediated ubiquitination of β -

TrCP is the critical element that prevents β -TrCP and the SCF ^{β -TrCP} from targeting I κ B for ubiquitination and degradation. In this case, NSP1 could render β -TrCP inactive without requiring a long term sequestering interaction with NSP1.

Chapter 4:

Shutdown of interferon signaling by a viral-hijacked E3 ubiquitin ligase*

Kaitlin A. Davis, John T. Patton

The published manuscript may be accessed as follows:

<http://microbialcell.com/researcharticles/shutdown-of-interferon-signaling-by-a-viral-hijacked-e3-ubiquitin-ligase/>

KAD generated figures.

KAD and JTP wrote the manuscript.

*This article is prepared as a microreview commentary, and per guidelines by Microbial Cell, is written without the inclusion of references or citations.

Main text

Viruses manipulate cellular processes to create an environment favorable to replication. For most viruses, this includes subverting the expression of interferon (IFN), a signaling molecule that can stimulate production of a vast array of antiviral gene products. Rotavirus, a segmented double-stranded RNA virus that causes acute gastroenteritis in infants and young children, inhibits IFN expression through its nonstructural protein NSP1. This viral protein stifles IFN expression by inducing the degradation of host factors that are necessary for upregulating the activity of IFN genes. In the case of nearly all human and porcine rotavirus strains, NSP1 induces the ubiquitination-dependent proteasomal degradation of β -transducin repeat containing protein (β -TrCP), a host factor that plays an essential role in activating the IFN-transcription factor, NF- κ B. Key to the process is the presence of a decoy sequence (degron) at the C-terminus of NSP1 that causes β -TrCP to mistakenly bind NSP1 instead of its natural target, inhibitor-of-NF- κ B (I κ B). In a recent report published by Davis *et al* [2017; mBio 8(4) e01213-17], we describe molecular requirements that govern NSP1 recognition of β -TrCP, including an essential degron phosphorylation event, and the step-wise incorporation of NSP1 into hijacked cullin-RING E3 ligases (CRLs) that ubiquitinate and tag β -TrCP for degradation. Notably, although β -TrCP is chiefly recognized for its role as a master regulator of NF- κ B signaling and IFN expression, β -TrCP also controls the stability of checkpoint proteins implicated in numerous other cellular pathways with antiviral activities, including autophagy and apoptosis. Thus, the impact of NSP1 on creating an intracellular environment favorable to virus replication may extend well beyond the IFN signaling pathway.

Viruses have evolved a number of mechanisms to combat host antiviral responses in order to establish a pro-viral cellular environment. Many host antiviral responses rely on signaling cascades initiated by the production of IFN. To this end, rotavirus, a pathogen known to infect nearly all known mammalian and avian animal species, employs NSP1 as an IFN antagonist. NSP1 proteins encoded by various rotavirus strains share little sequence conservation except for the presence of a putative N-terminal RING domain and a C-terminal substrate-targeting domain. While the targeting domain of most human and porcine rotaviruses mediates the recruitment of β -TrCP by NSP1, the targeting domain of many animal strains (simian, murine, equine, etc.) mediates the recruitment of interferon-regulatory factors (e.g., IRF-3/-7). NSP1 binding to β -TrCP or IRF proteins is correlated with proteasomal degradation of these targets in the infected cell.

There is a growing body of data to suggest that NSP1 triggers the degradation of targets by hijacking a subset of E3 ubiquitin ligases, cullin-RING ligases (CRLs). Hijacked CRLs are presumed to direct the ubiquitination and proteasomal degradation of NSP1-bound targets. CRLs are large modular complexes that are minimally comprised of several key components: a cullin scaffold protein (Cul1, 2, 3, 4a, 4b, 5, 7), a RING-domain containing protein (Rbx1, 2), and a substrate adaptor that directs the CRL to the target protein. Through multiple experimental approaches, results have been obtained indicating that NSP1 associates with components of CRLs, including Cul3, which has led to the hypothesis that NSP1 functions as a substrate adaptor protein of a Cul3-CRL. A recent publication by Davis *et al* (2017) reveals the highly coordinated sequence of

events necessary for NSP1 recruitment of β -TrCP and the integration of the NSP1- β -TrCP complex into hijacked CRL complexes.

NSP1 proteins that target β -TrCP have within their C-termini the sequence DSGXS. This sequence is a molecular decoy of the degron sequence, DSG ϕ XS, contained in $\text{I}\kappa\text{B}$. During activation of IFN signaling pathways, the $\text{I}\kappa\text{B}$ degron undergoes phosphorylation by the serine-threonine kinase activity of $\text{I}\kappa\text{B}$ kinase (IKK), creating a phosphodegron that is recognized by β -TrCP (Fig. 1). Interaction of β -TrCP with the $\text{I}\kappa\text{B}$ phosphodegron leads to $\text{I}\kappa\text{B}$ degradation, which in turn frees NF- κB to translocate to the nucleus and upregulate IFN promoter activity. In a parallel manner, binding of β -TrCP to the C-terminal $\text{I}\kappa\text{B}$ -like degron of NSP1 is dependent on phosphorylation. As shown by Davis *et al* (2017), this phosphorylation event is not only required for binding of β -TrCP to NSP1 but is also essential for the subsequent incorporation of the NSP1- β -TrCP complex into a CRL (Fig. 2). Unlike the degron of $\text{I}\kappa\text{B}$, which is dependent on the inducible IKK for phosphorylation, the degron of NSP1 co-opts the use of the ubiquitously-active serine-threonine kinase CKII for phosphorylation. Use of this kinase potentially offers several benefits to the virus. Most notably, the NSP1 degron is activated without the need for a kinase, like IKK, that is regulated through an immune signaling pathway. Moreover, CKII is associated with CRL accessory components (e.g. the COP9 signalosome), possibly placing NSP1 in the constant presence of an activating kinase. Through the use of NSP1 mutants and CRL inhibitors, Davis *et al* (2017) obtained data showing that CKII remains associated with the NSP1- β -TrCP complex even after degron phosphorylation, creating the metastable

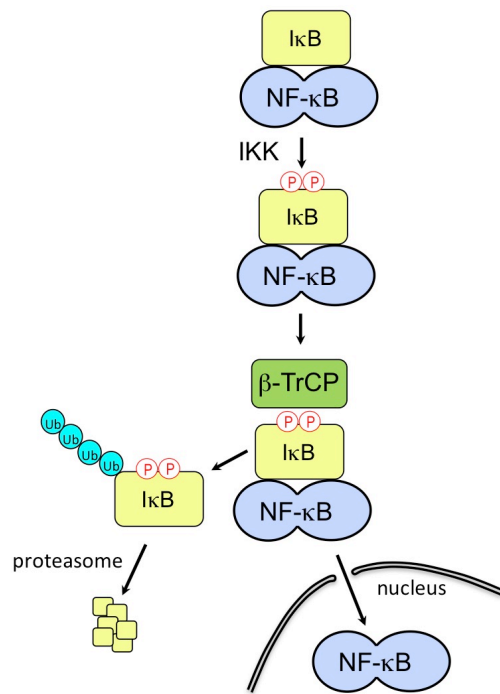


Figure 4-1. NF- κ B induction of interferon. When a host cell detects the presence of an invading pathogen, signaling cascades are induced which ultimately lead to interferon expression, triggering an anti-viral state in the affected cell. Upstream pathogen detection initiates signaling cascades that hinge on the activity of activatable kinases such as the I κ B kinase complex (IKK). A pool of inactive NF- κ B transcription factors exists in the cytoplasm, bound to the inhibitor, I κ B. Phosphorylation of I κ B by IKK leads to its recognition by components of an E3 ubiquitin ligase complex, SCF ^{β -TrCP}, leading to I κ B ubiquitination and degradation. NF- κ B, now free of its inhibitor, translocates to the nucleus and induces interferon expression.

NSP1-CKII- β -TrCP complex. Thus, CKII may have a role in the subsequent assembly of NSP1-CRLs that extends beyond NSP1 phosphorylation and activation.

In our Davis *et al* (2017) publication, we also present data indicating that the NSP1-CKII- β -TrCP complex interacts with Cul3 subunits, forming a Cul3-NSP1- β -TrCP complex. CKII was released at this step of the assembly process. The CRL3-NSP1- β -TrCP complex presumably binds a ubiquitin-charged E2 enzyme and its cullin component undergoes neddylation, initiating structural changes that facilitate transfer of ubiquitin to β -TrCP. Repeated cycles of binding and release of charged and uncharged E2s create a poly-ubiquitin chain on β -TrCP that is recognized by the proteasome. Interestingly, we found that mutation of the NSP1 RING domain (C42A) created a form of NSP1 that although capable of binding β -TrCP and CKII, could not bind Cul3. This finding raises the possibility that phosphorylation of the NSP1 κ B-like degron triggers a structural change that allows interaction of the N-terminal RING domain with Cul3. Considered together, our analyses indicate that formation of NSP1-CRLs is a highly ordered process, initiated by CKII-phosphorylation, followed by binding of β -TrCP, and ending with the incorporation of NSP1- β -TrCP complexes into a CRL through an interaction requiring participation of the NSP1 RING domain.

β -TrCP has many cellular targets besides κ B. These targets similarly contain phosphodegron motifs, and many serve as checkpoint proteins for cellular pathways that mediate antiviral activities beyond IFN induction. As one example, β -TrCP is responsible for degrading DEPTOR, the protein that binds to and regulates the activity of mTOR, a protein kinase that plays a major role in autophagocytic and apoptotic responses. In addition, β -TrCP has roles in regulating levels of IFN receptor (IFNAR1) in IFN-treated

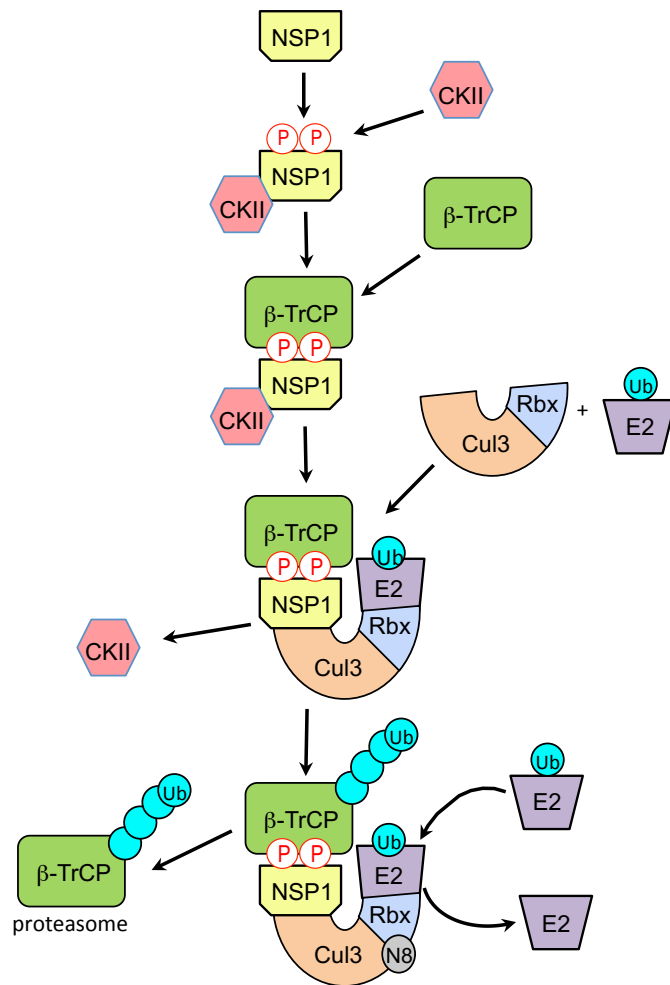


Figure 4-2. A model of NSP1-CRL assembly. Upon expression, NSP1 binds the constitutively active kinase CKII and undergoes phosphorylation of the C-terminal degron motif. The affinity of β -TrCP for phosphorylated NSP1 results in formation of an NSP1- β -TrCP-CKII complex. CKII is released as the NSP1- β -TrCP complex incorporates into the CRL assembly intermediate Cul3-Rbx1 and recruits a ubiquitin-charged E2 enzyme. Nedd8-activated CRLs facilitate ubiquitination of β -TrCP substrates, and multiple rounds of ubiquitination result in poly-ubiquitin chains that signal proteasomal degradation of β -TrCP.

cells, promoting maturation of the p105 precursor protein to the NF- κ B p50 subunit, and processing of the pro-apoptotic procaspase-3 into caspase 3. The diverse influence of β -TrCP on cellular pathways and antiviral responses, suggests that viral proteins - like NSP1 - that prevent β -TrCP activity affect the entire intracellular milieu and may shift the cellular atmosphere at multiple levels in favor of virus replication. Indeed, the positive implications of attacking β -TrCP on virus replication may explain why other viruses, such as HIV, vaccinia virus, and Epstein Barr virus also target this protein. Continued efforts to establish how NSP1 antagonizes β -TrCP activity will not only lead to a better understanding of the basis of rotavirus pathogenesis, but also provide insight into the structure and function of CRLs and the role that β -TrCP plays in promoting an antiviral intracellular environment.

Chapter 5:

Biochemical exploration of human and animal NSP1 proteins

Part 1: The pLxIS motif does not require phosphorylation for substrate engagement

Abstract

Rotavirus is a non-enveloped, double-stranded RNA virus responsible for significant disease worldwide. To combat host innate immune responses, rotaviruses encode non-structural protein 1 (NSP1), the product of genome segment 5, which is capable of inhibiting key interferon induction cascades. The NSP1 proteins of rotavirus species A cluster by both host and by preferred innate immune target proteins, specified within the C-terminus of the protein. Wa and OSU-like NSP1 proteins encode a phosphodegron motif (DSGIS) in this region to target cellular proteins in NF- κ B signaling cascades. SA11-like NSP1 proteins that target IRF3 for degradation instead conserve a C-terminal pLxIS motif that strongly resembles motifs utilized by MAVS, STING and TRIF proteins to bind IRF3. Because of this similarity, we sought to establish the relevance of this domain in NSP1 mediated IRF3 degradation. To understand the functional role of this conserved sequence, we examined the capacity of mutagenized NSP1s to degrade target IRFs or antagonize signaling, and have demonstrated a lack of dependence on any single phosphorylated residue. This is contrary to cellular interactions with the IRF3 dimerization domain, which requires phosphorylation. Successful interactions between NSP1 and IRF3 likely rely instead on the pLxIS leucine residue within the motif, demonstrating unusual folding and target interaction of this domain.

Introduction

Similar to what has been observed and reported for OSU-like proteins of human and porcine rotavirus strains, the SA11-like animal NSP1 proteins are thought to behave

as adaptor proteins of CRLs. Ding, et al. (144) and Lutz, et al (145) included NSP1 proteins from this group of proteins in their analyses, and data strongly supports that like OSU, these NSP1 proteins rely on the same or very similarly comprised cellular machinery to exert control over host signaling cascades. Unlike OSU related strains, these NSP1 proteins are associated with the degradation of IRF proteins.

Following detection of viral nucleic acids by cGAS (DNA) or RIG-I-like-receptors (RNA), signaling through the respective proteins STING and MAVS recruits kinases, such as IKK or TBK1, in order to activate NF- κ B or IRF3 (Figure 5-1) (106). TRIF can be similarly activated through upstream detection of lipopolysaccharide by TLR4. Activated RIG-I is known to facilitate oligomerization of MAVS, which results in recruitment of TRAF2, TRAF5, and TRAF6, and subsequently, activation of IKK and TBK1. This leads to phosphorylation of IRF3, and its subsequent dimerization and translocation to nucleus, leading to interferon induction. Activated TLR3 and TLR4 similarly signal through recruitment of TRIF to activate IKK and TBK1. While other innate immune sensing pathways result in activation of TBK1, IRF3 activation is only induced by pathways that signal through MAVS, STING, or TRIF. Recent data by Liu, et al. (237) demonstrates that these immune adaptor proteins are phosphorylated on a conserved pLxIS motif (where p is a hydrophilic residue, and x is any nonaromatic amino acid) by TBK1, and that this interaction recruits IRF3 to the complex, leading to its phosphorylation and subsequent dimerization and nuclear translocation.

While SA11-like NSP1 proteins do not contain an I κ B-like degron, they do contain a motif reminiscent of the pLxIS motif found in MAVS, TRIF, and STING. Because of the similarity of this domain to the known IRF-recruiting domain observed in

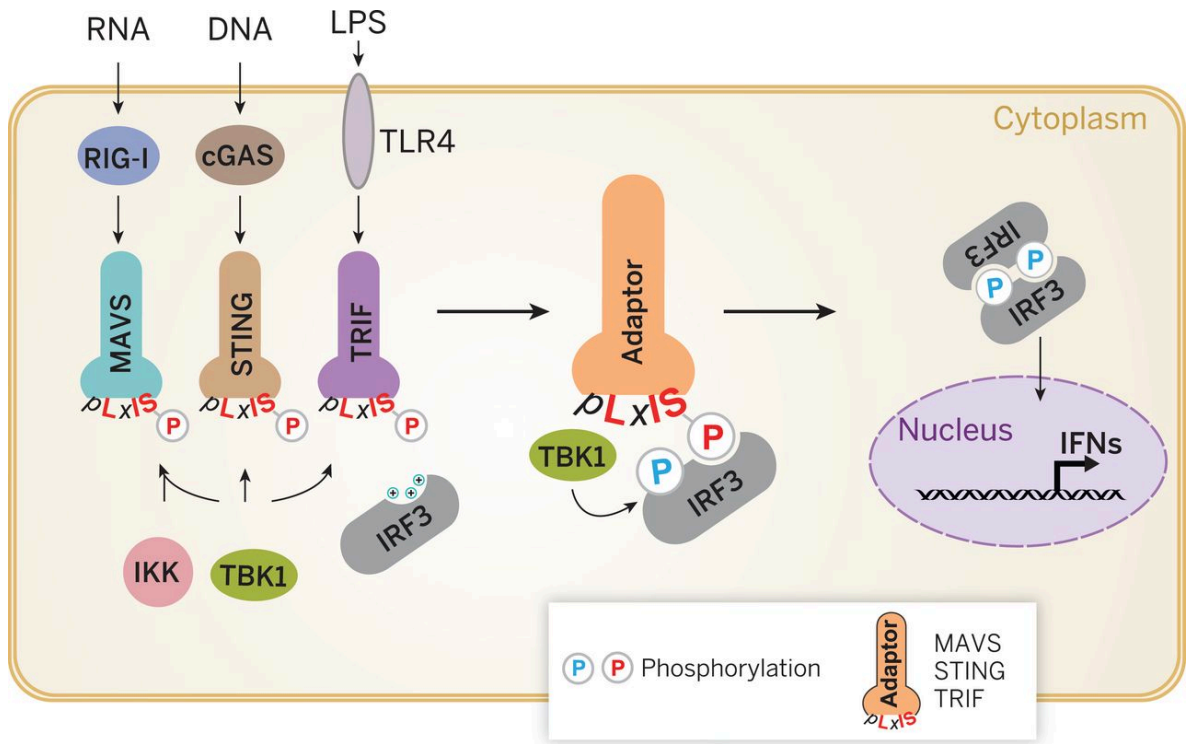


Figure 5-1. Activation of immune adaptor proteins and IRF3. Adapted from Liu, et al. (237). Following detection of foreign RNA, DNA, or lipopolysaccharide, MAVS, STING, and TRIF activate IKK and TBK1 kinases which subsequently phosphorylate these adaptor proteins on a conserved pLxIS motif. This phosphorylation recruits IRF3, which is activated by an analogous phosphorylation event.

		Δ C
Simian	SA11-4F	KNSGTLTEEFELLISNSEDDNE
Simian	SA11-5S	KNSGT
Simian	RRV	EEEGKLSEEEYELLISDSSEDD
Human	B4106	EEEGKLAEEYELLISDSSEDD
Lapine	30-96	EEEGRLAEEYELLISDSSEDD
Human	Ro1845	EEEGKISEEEYELLISDSSEDD
Canine	K9	EEEGKISEEEYELLISDSSEDDQ
Equine	L338	YEQGELSEEEYELLISDSGDDE
Equine	FI14	EKQGKLSEEEYDLLISDSDD
Murine	ETD	QEHGDLAEEFDLLLSSSDSDED
Bovine	UK	NKRNELIDEYDLELSDVE
Human	AK-13	NKRNDLMDEYSYELSDTE

Figure 5-2. C-terminal alignment of SA11-like NSP1 proteins. SA11-like strains harbor a conserved motif reminiscent of the adaptor sequence pLxIS. All full-length NSP1 proteins are proposed to interact with cullin-RING ligases via a conserved N-terminal RING domain, and to target host innate immune targets through a variable C-terminus. The conserved pLxIS motif occupies this location, much like phosphodegron motif of OSU-like NSP1 proteins.

cellular immune adaptor proteins, we sought to evaluate the relevance of the pLxIS motif in the ability of NSP1 proteins to antagonize IRF3 signaling cascades.

Materials & Methods

Cells. Human embryonic kidney HEK293T cells were grown in Dulbecco's modified Eagle's medium (DMEM) containing 10% fetal bovine serum (FBS; Gibco), 2 mM glutamine, and 1,000 units per ml each of penicillin and streptomycin.

Plasmids. The pLIC6 vector used for transient expression of wild-type and mutant forms of NSP1 has been described previously (138). Plasmids were grown in TOP10 *Escherichia coli* cells (Thermo, Fisher), purified using NucleoBond Xtra endotoxin-free plasmid purification kits (Clontech), and verified by sequencing. Plasmids were modified using ligation independent cloning (LIC) as described in Morelli, et al. (138). Briefly, mutations were introduced by outward PCR of original plasmids with suitable primers, and ORFs were PCR amplified with LIC-compatible primers. PCR fragments were then gel purified and treated with T4 DNA polymerase in the presence of dATP to generate LIC sticky ends. The treated insert and digested pLIC6 were mixed, incubated at 25°C for at least 20 min, and transformed into *Escherichia coli* strain TOP10.

Luciferase reporter assays. Transfection complexes (9.25 μ l Opti-MEM, 92 ng pLIC6-NSP1, 30 ng reporter construct, 3 ng pGL4.74[hRluc/TK] [Promega], 0.25 μ l Lipofectamine 2000) were prepared in triplicate according to the manufacturer's protocols and transferred to wells of a 96-well plate. An HEK293T cell suspension (90

ul; 1.1×10^6 cells/ml) was added to each well. Cells were treated at the time of transfection with 10 μ g/ml poly(I:C) (Sigma), and incubated for 40 hours. At appropriate time points, cells were lysed in 20 μ l $1\times$ passive lysis buffer (Promega), and luciferase activity was assessed with the Dual-Glo luciferase assay system (Promega), according to the manufacturer's instructions. Relative luciferase activity (NF- κ B stimulation) was calculated by normalizing measured firefly activity to Renilla luciferase activity. Data (mean \pm SD) are from one of three independent experiments.

Statistical analysis. Prism v6.3f (GraphPad Software) was used to perform statistical analyses of independent experiments. Data were analyzed with one-way analysis of variance (ANOVA) using Dunnett's multiple comparisons test.

Results

NSP1 proteins that encode a pLxIS motif inhibit IRF3 signaling. Work published by Liu, et al. demonstrates that interactions between IRF3 and innate immune adaptor proteins requires a pLxIS motif. By extrapolation, it was hypothesized that a similar motif within the C-terminus of NSP1 proteins may fulfill this requirement. To determine whether this motif has a role in IRF3 signaling inhibition, HEK293T cells were co-transfected with NSP1 expression plasmids (Figure 5-2) and luciferase reporter constructs driven by either IRF3 or TK promoters (Figure 5-3A, B). Transfected cells were stimulated with the cytokine TNF- α to induce IFN signaling cascades. The NSP1 constructs included in this experiment either had pLxIS motifs within their c-termini (SA11-4F, RRV, B4106, 30-96, Ro1845, K9, L338, FI14) or did not (SA11-4F Δ C, ETD,

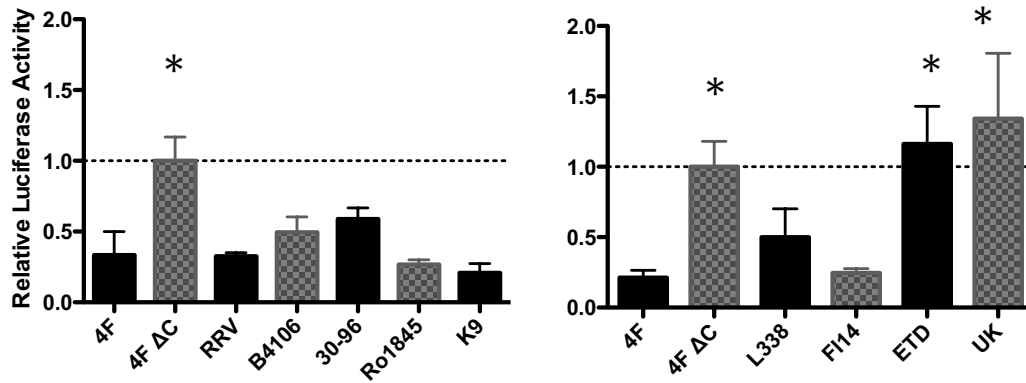


Figure 5-3. Effect of NSP1 expression on IRF3 promoter activity. HEK293T cells were cotransfected with NSP1 and IRF3 firefly and HSV-tk Renilla luciferase reporters. Cells were stimulated at the time of transfection with 10 μ g/ml poly(I:C). Relative luciferase activity was calculated at 40 h p.t. by normalizing firefly to Renilla luciferase activity. Samples were processed as part of two independent experiments. Data (mean \pm SD from representative experiments performed in triplicate) were analyzed by two-way ANOVA.

UK). Only those NSP1 proteins lacking pLxIS motifs failed to inhibit IRF3 signaling when stimulated with TNF- α . This result supports the hypothesis that the pLxIS has a role in mediating IRF3 signaling during rotavirus infection. This finding is supported by the inclusion of the C-terminally truncated SA11-4F Δ C construct; that this NSP1 protein has reduced activity when compared to its full-length counterpart implicates a specific role for the pLxIS motif. Interestingly, both NSP1 proteins that failed to inhibit luciferase expression contained pLxIS > pLxLS mutations.

To further explore the role of the C-terminal pLxIS motif in innate immune antagonism, constructs to express mutant C-terminal truncations were generated for each of the NSP1 proteins included in the previous experiment. Each protein was truncated directly proximal to the pLxIS motif, as indicated in Figure 5-2 (red bar). As in Figure 6, HEK293T cells were co-transfected with plasmids to express mutant or WT NSP1 proteins, in addition to luciferase expression constructs driven by an IRF3 or TK promoter. Compared to WT, most NSP1 proteins failed to inhibit IRF3 signaling when C-terminally truncated. Ro1845 and K9, rotavirus strains of canine origin, retained their ability to antagonize IRF3 signaling when truncated (Figure 5-4A, B). This experiment supports a role for the pLxIS motif in NSP1 innate immune antagonism. Furthermore, the inclusion of NSP1 strains from diverse species origins, including simian, human, canine, and equine strains, suggests that this motif may be utilized by rotavirus NSP1 regardless of host or virus species.

A terminal serine residue is not required for IRF3 antagonism. Liu, et al. found that phosphorylation of the terminal serine residue within the pLxIS motif was required for

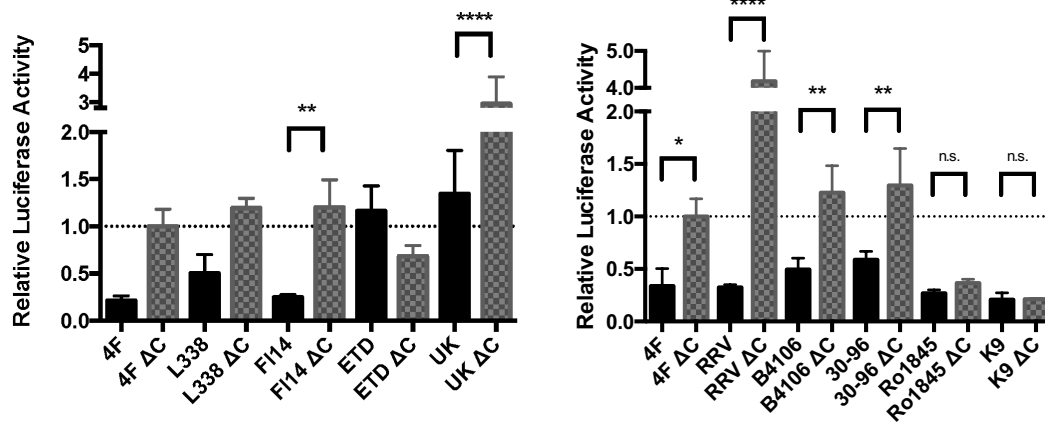


Figure 5-4. Effect of pLxIS truncations on NSP1-mediated IRF3 inhibition. HEK293T cells were cotransfected with wild-type or truncated NSP1 and IRF3 firefly and HSV-tk Renilla luciferase reporters. Cells were stimulated at the time of transfection with 10 μ g/ml poly(I:C). Relative luciferase activity was calculated at 40 h p.t. by normalizing firefly to Renilla luciferase activity. Data (mean \pm SD from one representative experiment performed in triplicate) were analyzed by two-way ANOVA

interactions between IRF3 and innate immune adaptor proteins. Additionally, Davis, et al. (148) recently published evidence demonstrating that OSU-like NSP1 proteins require phosphorylation of serine residues within a similar C-terminal motif to engage substrates within the NF- κ B signaling cascade. Therefore, it was hypothesized that SA11-like NSP1 proteins may also require phosphorylation prior to IRF3 binding. In order to evaluate the role of distinct residues within the pLxIS motif, plasmids to express mutant SA11-4F NSP1 proteins in which individual residues were changed to alanine were generated, including mutation of the terminal pLxIS serine residue, as well as a downstream proximal serine or glutamic acid residue. The ability of these mutant NSP1 proteins to antagonize IRF3 signaling was evaluated in HEK293T cells in which luciferase expression constructs had been co-transfected. Interestingly, each of these mutant SA11-4F NSP1 proteins retained their ability to disrupt IRF3 signaling. This finding suggests that unlike what has been reported for OSU NSP1, no individual residue tested within the pLxIS motif governs the ability of NSP1 to engage IRF3. The absence of a required serine residue also suggests that phosphorylation within this region may not govern the activity of NSP1. This data does not exclude the possibility that the isoleucine residue affects binding; both UK and ETD NSP1s have an isoleucine > leucine substitution, and are inactive in this context (Figure 5-4B).

Discussion

In this study, the role of a conserved, C-terminal pLxIS motif was evaluated in the ability of NSP1 to antagonize IRF3 signaling. Recent studies had identified pLxIS motifs within innate immune adaptor proteins MAVS, STING, and TRIF and demonstrated the

importance of this motif in the ability of these proteins to recruit the cellular kinase TBK1 and subsequently, cytoplasmic IRF3 transcription factors. These studies included biochemical, bioinformatic, and modeling techniques, and identified only residues within the pLxIS motif as contributing factors for target binding. Furthermore, it is intriguing that bound kinases serve two distinct purposes: first, to modify the immune adaptor protein, thus activating a motif for IRF3 interaction, and second, to efficiently modify bound IRF3 to swiftly activate without the need to form a secondary complex.

In the studies described here, we employed IRF3 promoter-driven dual luciferase assays to evaluate the ability of NSP1 proteins from numerous strains to antagonize signaling through this cascade. Including wild type, mutant, and truncated NSP1 proteins, these studies suggest that a conserved pLxIS motif is required for NSP1-mediated IRF3 signaling disruption and innate immune evasion. This finding is similar to the requirements observed for IRF3 binding to its known cellular binding partners, suggesting that NSP1 proteins may have evolved to mimic the conserved motif found within MAVS, TRIF, and STING. While the pLxIS motif within cellular proteins is phosphorylated, our data suggests that this NSP1 motif is not modified prior to IRF3 engagement.

Recently, Zhao, et al. (212) reported similar findings for SA11-like NSP1 proteins. Their study, too, finds that a pLxIS motif is required for NSP1 to facilitate IRF3 degradation, and show that phosphorylation is not required for this activity. They introduced the same S489A mutation and report that IFN- β promoter activity is unaffected, indicating that phosphorylation is not required. Furthermore, SPR binding data shows that NSP1 binding to IRF3 is unaffected by this change. Similar to our

assessment of defective ETD and UK NSP1 proteins, which include I486L mutations, Zhao, et al. report that an I488A mutation of SA11-4F NSP1 impairs IRF3 antagonism. Their modeling data suggest that both NSP1 and a phosphorylated NSP1 may bind IRF3 substrates in a similar manner regardless of modification.

The elimination of a required phosphorylation event may be beneficial for NSP1, several-fold. Because NSP1 can engage IRF3 without first requiring engagement by TBK1, the virus is able to produce antagonistic proteins that are active from conception; there are no down stream steps required to activate these proteins, thus avoiding a potential limiting step. Furthermore, by specifically avoiding TBK1 modification or engagement requirements, NSP1 does not rely upon activation of innate immune signaling cascades for modification. This allows NSP1 to exert control over these signaling molecules prior to and independently of required detection by any PRRs. This finding is somewhat in contrast to the noted requirement of OSU-like NSP1 proteins and their reliance upon a CKII-mediated modification for activation. Perhaps, as is observed for MAVS, TRIF, and STING, in which the activating step is one of two required phosphorylation events, OSU NSP1 engagement with CKII precedes another as yet unidentified downstream phosphorylation event. Like SA11-4F, OSU NSP1 avoids the use of an immune-activated kinase responsible for phosphorylation of the protein it mimics, and these studies do not rule out the possibility that an as yet unidentified cellular kinase, perhaps a ubiquitously active kinase such as CKII, may modify SA11-4F NSP1 and regulate its activity.

Part 3: Non-RVA NSP1 proteins have interferon antagonist activity

Abstract

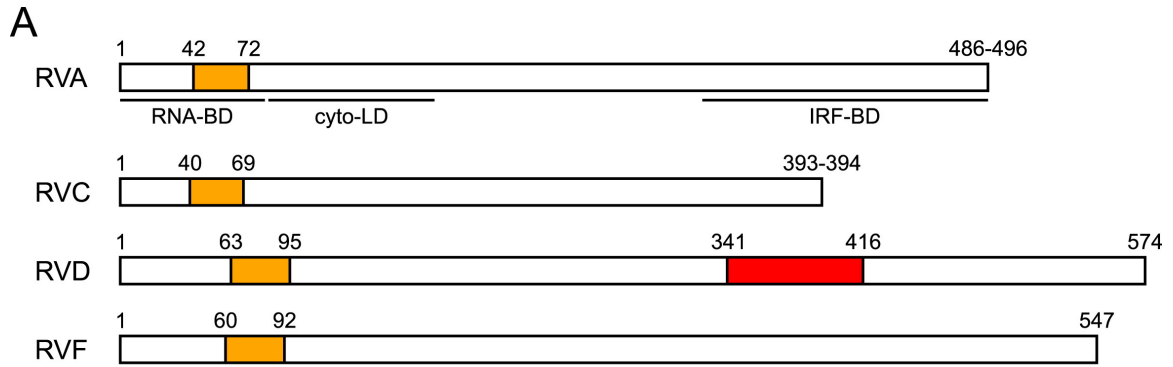
Rotavirus is a non-enveloped, segmented, double-stranded RNA virus that is responsible for significant gastrointestinal disease of both pediatric and veterinary concern. There are nine rotavirus species (RVA-RVI) currently recognized, of which RVA is responsible for the majority of infection in humans. To establish infection, a virus must initially circumvent the host innate immune response, and to combat this defense, RVA encodes at least two direct antagonists, NSP1 and VP3. RVA NSP1 is the product of genome segment 5 and mediates strain-specific degradation of cellular factors involved in the induction of interferon, a central innate immune effector whose expression established an antiviral state in the infected cell. NSP1 proteins conserve key structural and functional domains within and between rotavirus species, and cluster according to host, supporting a role for NSP1 in host range restriction. RVA NSP1, the most variable member of the viral proteome, conserves an N-terminal putative RING domain and targets specific host proteins through a variable C-terminus. RVC, RVD, and RVF NSP1 proteins also conserve an N-terminal RING domain, suggesting that they may function utilizing a similar mechanism. To understand how these non-RVA NSP1 proteins might antagonize host innate immunity, we examined their capacity to block interferon induction by targeting the NF- κ B, IRF3, and JAK/STAT pathways. NF- κ B, a transcription factor required for interferon induction, is activated by β -TrCP, a target of human and porcine RVA NSP1 activity. We have demonstrated that expression of RVD NSP1 prevents NF- κ B activation, but unlike RVA NSP1, does not induce the degradation of β -TrCP. None of the tested NSP1 proteins affected IRF signaling, a frequent target of

animal-derived RVA strains. The precise mechanism of action of these NSP1 proteins remains to be elucidated, and interestingly, we did not identify any targets of RVC or RVF NSP1 activity. Further exploration of critical protein domains and potential targets will shed light on the novel innate immune evasion strategy employed by non-RVA NSP1 proteins.

Introduction

While significant strides have been made in delineating the approach and mechanisms employed by Group A rotaviruses to disrupt immune responses and interferon induction, much less is known about NSP1 proteins from non-Group-A strains. Rotavirus Group C (RVC) are a pathogenic agent of piglets and adult pigs, and are sometimes found in adult humans, although human infections are often asymptomatic (238). Rotavirus Group D and Group F (RVC, RVF) are frequently found in avian species (239). These viral strains are difficult to culture in lab settings, and the associated hurdles have been difficult to surpass. However, the publication of whole genome sequences from viruses recovered from infected animals has improved accessibility in recent years (240).

While RVA NSP1 proteins have known roles in control of interferon and antiviral responses, the role of NSP1 proteins from non-Group A rotaviruses in viral innate immune antagonism is less clear. The activity of NSP1 proteins from RVC, RVD, and RVF strains has not been evaluated. Based on sequence homology, it is likely that these proteins share a domain composition and organization similar to what has been reported for Group A NSP1 proteins (Figure 5-5A). Briefly, RVA NSP1 proteins can be



B

RVA	Wa	L18943	42	CLDCCQHTDLTYCRGCTMYHVCQWCSQYGR--C	72
RVC	Bristol	AJ132204	40	CLNCLNECKVCPCDYCGIRHKCENCLNSD---C	69
RVD	05V0049	GU733447	63	CLTCGCFHNVYSCDFCSVNHICKSKQNYSDL	95
RVF	03V0568	JQ919999	60	CLSCGRVRSLFSCILCHVPHICHNCLSLNLLI	92

Figure 5-5. Non-Group A NSP1 predicted structural architecture, adapted from Morelli, et al. (115). (A) RVC, RVD, and RVF NSP1 proteins retain structural elements common to RVA NSP1 proteins, including a putative RING domain (gold). RVD NSP1 shares in common with avian RVA NSP1 proteins a domain of the transcription factor IIE alpha subunit (red). (B) The putative RING domains from RVA, RVC, RVD, and RVF NSP1 proteins possess similar spacing and predicted structure.

characterized as having three key domains: a N-terminal, RNA-binding putative RING domain (Figure 5-5B); a cytoskeleton-localization domain; and a C-terminal targeting domain. This same organization has been predicted for RVC, RVD, and RVF NSP1 proteins, using sequences from Bristol, 05V0049, and 03V0568 strains respectively, and thus these strains are sometimes referred to as having an Group A-like classification (115, 241, 242). While it is markedly shorter, RVC NSP1 is most closely related to Group A proteins (243). RVD NSP1 proteins are closely related to Group A avian NSP1 proteins, but these proteins contain an additional domain with TFIIE (Transcription Factor II E) homology, suggesting nucleic acid binding activity, that is not found in other NSP1 proteins.

Despite differences that appear between rotaviruses that have divergent host speciation, it has long been supported that diverse rotavirus lineages may serve promising roles as attenuated vaccine strains (244). However, widely utilized vaccines of either reassortant origin, while highly efficacious in developed countries, fail to protect to the same degree in developing regions of the world. To this end, it will be valuable to further explore how existing strains interact with innate immune responses. In this study, we sought to evaluate the role of NSP1 from RVC, RVD, and RVF viruses in immune antagonism and interferon induction.

Materials & Methods

Cells. Human embryonic kidney HEK293T cells were grown in Dulbecco's modified Eagle's medium (DMEM) containing 10% fetal bovine serum (FBS; Gibco), 2 mM glutamine, and 1,000 units per ml each of penicillin and streptomycin.

Plasmids. RVC (Bristol), RVD (05V0049), and RVF (03V0568) NSP1 sequences were synthesized by GenScript and cloned into PLIC6 expression vectors, as described in Morelli, et al. (138). Plasmids were generated in TOP10 *Escherichia coli* cells (Thermo, Fisher) and purified using an NucleoBond Xtra endotoxin-free plasmid purification kit (Clontech). All sequences were verified by sequencing.

Luciferase reporter assays. Transfection complexes (9.25 μ l Opti-MEM, 92 ng pLIC6-NSP1, 30 ng reporter construct [NF- κ B, Promega; IRF3, Marrio Barro], 3 ng pGL4.74[hRLuc/TK] [Promega], 0.25 μ l Lipofectamine 2000) were prepared in triplicate in compliance with the manufacturer's protocols and as described (Morelli mBio) and incubated in wells of a 96-well plate. HEK293T cells in DMEM (90 μ l; 1.1×10^6 cells/ml) were added to each well. For NF- κ B experiments, cells were treated for 4 h at 24 h p.t. in medium with 25 ng/ml TNF- α (PeproTech). For IRF3 experiments, cells were treated with 10 μ g/ml poly(I:C) (Sigma) at the time of transfection and incubated for 40 hours. At appropriate specified points, cells were lysed in $1\times$ passive lysis buffer (Promega) (20 μ l), and luminescence was assessed with the Dual-Glo luciferase assay system (Promega), according to the manufacturer's instructions. The relative luciferase activity (NF- κ B or IRF3 stimulation) was calculated by normalizing firefly luciferase activity to Renilla luciferase activity. Data (mean \pm SD) are from one representative independent experiment.

Immunoblot assay. Transfection complexes (94 μ l Opti-MEM [Gibco], 500 ng pLIC6-NSP1, 500 ng pLIC6F- β -TrCP, 2 μ l Lipofectamine 2000 [Life Technologies]) were

prepared according to the manufacturer's protocols and transferred to wells of a 12-well plate. A HEK293T cell suspension (900 μ l; 1.3×10^6 cells/ml) was added to each well. At 24 h p.t., cells were collected, washed once with phosphate-buffered saline (PBS [pH 7.4]), and lysed in a 100- μ l solution of 1 \times radioimmunoprecipitation assay (RIPA) buffer (150 mM NaCl, 50 mM Tris [pH 8.0], 1% Nonidet P-40, 0.5% sodium deoxycholate, 0.1% sodium dodecyl sulfate), 1 \times NuPAGE lithium dodecyl sulfate (LDS) sample buffer (Life Technologies), 25 mM dithiothreitol, 1 \times phosphatase inhibitor cocktail (1 mM each sodium fluoride, sodium orthovanadate, β -glycerophosphate, and sodium pyrophosphate), and 1 \times Complete EDTA-free protease inhibitor cocktail (Roche). Lysates were briefly sonicated, denatured by heating to 70°C, and electrophoresed on 10% Tris-Glycine gels (Invitrogen). Samples were transferred onto nitrocellulose membranes using an iBlot apparatus (Thermo, Fisher). Membranes were blocked by incubation in Blotto Solution (Thermo, Fisher) prior to incubation with primary antibody diluted in PBST (PBS with 0.02% Tween) with 5% milk solution. Membranes were washed with PBST before incubating with fluorophore-conjugated secondary antibody diluted in milk-PBST solution. Membranes were imaged on an Odyssey Classic and quantified using Image Studio Lite v3.1.4 (LI-COR Biosciences). Bands of interest were normalized to the loading control, PCNA.

Statistical analysis. Prism v6.3f (GraphPad Software) was used to perform statistical analyses of independent experiments. Data of each experiment were analyzed with one-way analysis of variance (ANOVA) using Dunnett's multiple comparisons test.

Results

RVC, RVD, and RVF NSP1 proteins contain neither an IRF- nor a β -TrCP-

targeting domain. NSP1 proteins differentially antagonize host signaling pathways in a manner that is often directly associated with C-terminal sequences and the presence of conserved interaction motifs (137). Minimally, these NSP1 interaction motifs can be characterized as indicative of IRF3 or β -TrCP binding, as has been observed for SA11-4F and OSU NSP1. To predict the activity of RVC (Bristol), RVD (05V0049), and RVF (03V0568) NSP1 proteins, the Eukaryotic Linear Motif resource (elm.eu.org) was used to identify potential binding sites. This effort was focused on sequences within the C-terminus of the protein, where Group A rotaviruses harbor the majority of their interaction motifs. This analysis indicated the absence of any known relevant binding sites within the NSP1 proteins tested. However, while interaction motifs of mammalian IRF3 and NF- κ B have been well characterized, less is known about the avian homologues of these proteins. Accordingly, this analysis does not rule out the possibility that an alternative motif mediates interactions with these proteins in chickens. Notably, RVD contained a pLxIS motif at residues 244-249 (TLDIS), but the location of this motif within the globular center of the protein makes it an unlikely candidate in IRF3 antagonism. These findings suggest that RVC, RVD, and RVF NSP1 proteins may target host signaling pathways in a manner that is different than what has been described for RVA NSP1 proteins, or alternatively, that they may have novel targets to mediate interferon antagonism.

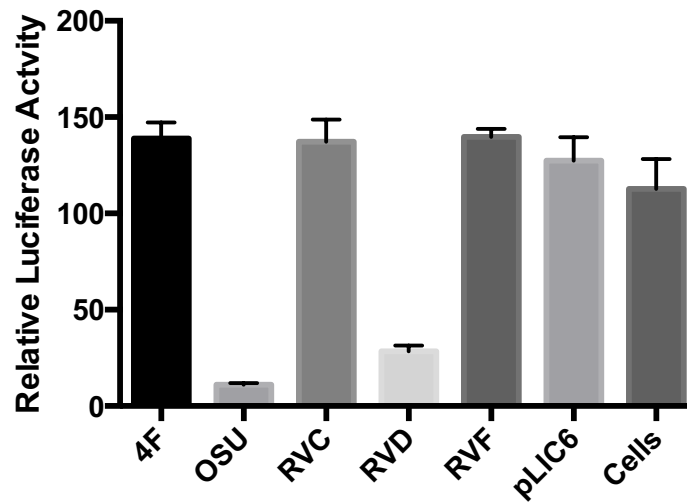


Figure 5-6. Effect of NSP1 expression on NF- κ B activation. Like OSU NSP1, RVD antagonizes NF- κ B activation. HEK293T cells were cotransfected with NSP1 and NF- κ B firefly and HSV-tk Renilla luciferase reporters. At 24 h p.t., cells were stimulated for 4 h with 25 ng/ml TNF- α . Relative luciferase activity was calculated by normalizing firefly to Renilla luciferase activity.

RVD NSP1 disrupts NF- κ B signaling. Despite the lack of any detectable substrate interaction motifs, we sought to experimentally evaluate whether RVC, RVD, or RVF were antagonists of canonical NSP1 target signaling cascades. Expression constructs containing NSP1 ORFs of each NSP1 were generated as described previously (138). To evaluate the capacity of non-Group A NSP1 proteins to block NF- κ B activation, HEK293T cells were co-transfected with NSP1 and NF- κ B luciferase reporter constructs. In addition to non-RVA NSP1 proteins, the well-characterized NSP1 proteins from simian SA11-4F and porcine OSU strains were included (Fig. 5-6). These NSP1 proteins are known antagonists of IRF3 and NF- κ B signaling, respectively, and do not possess the ability to target both respective pathways. In addition to OSU NSP1, RVD NSP1 markedly inhibited NF- κ B promoter activity, but SA11-4F, RVC, and RVF NSP1 proteins did not reduce activation compared to empty vector or mock transfected cells. RVD NSP1 lacks a known DSGIS motif that regulates interaction between OSU NSP1 and β -TrCP, so this data suggests that an alternative mechanism may be employed by RVD NSP1 to disrupt promoter activation.

OSU NSP1 primarily disrupts NF- κ B signaling cascades by facilitating proteasomal degradation of β -TrCP. However, OSU NSP1 may possess the ability to inhibit β -TrCP by simply binding, without necessarily inducing degradation (148). To evaluate whether RVD NSP1 similarly facilitates proteasomal degradation of β -TrCP, constructs to express RVD NSP1 and FLAG-tagged β -TrCP were co-transfected into HEK293T cells. The level of β -TrCP was assayed 24 h p.t. by quantitative immunoblot using anti-FLAG antibodies. As indicated in Fig. 5-7A, RVD NSP1 expression had no effect on FLAG- β -TrCP expression. Similarly, when levels of FLAG-IRF3 were assessed

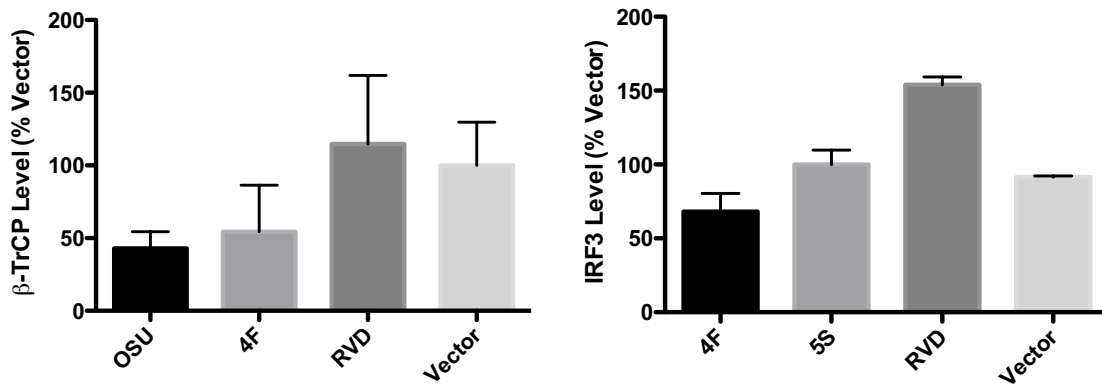


Figure 5-7. Quantification of NSP1 protein ability to facilitate degradation of β -TrCP or IRF3. HEK293T cells were cotransfected with NSP1 and (A) FLAG- β -TrCP or (B) FLAG-IRF3. At 24 h p.t., proteins were assayed by immunoblot. Intensity of anti-FLAG signal was normalized to PCNA, and the vector control was set to 100%.

in the presence of RVD NSP1, no degradation was observed (Fig. 5-7B). This data suggests that RVD NSP1 inhibits NF- κ B activation without also facilitating degradation of β -TrCP, and likely has no effect on IRF3 signaling cascades.

Neither RVC, RVD, nor RVF NSP1 restrict IRF3-mediated interferon induction.

Because both NF- κ B and IRF3 signaling cascades are important for the induction of interferon in chickens, we next investigated the ability of non-RVA NSP1 proteins to inhibit IRF3 signaling cascades. RVD NSP1 does not contain a canonical β -TrCP targeting domain, and yet our data show that this protein possesses the ability to antagonize NF- κ B signaling cascades. By extrapolation, it is possible that RVC, RVD, and RVF NSP1 proteins that do not contain canonical IRF3 targeting domains may also retain the ability to antagonize this signaling cascade. To evaluate this possibility, constructs to express individual NSP1 proteins were co transfected with an IRF3-driven luciferase reporter construct in HEK293T cells. While SA11-4F proteins sufficiently inhibited activation of the ISRE promoter, both SA11-5S and OSU NSP1 proteins were unable to disrupt this signaling cascade (Fig. 5-8). Similarly, RVC, RVD, and RVF NSP1 proteins did not inhibit ISRE activation. This data suggests that RVC, RVD, and RVF NSP1 proteins do not inhibit interferon induction by targeting IRF3 proteins, but this experiment does not rule out the possibility that they may behave differently in a non-human cell type.

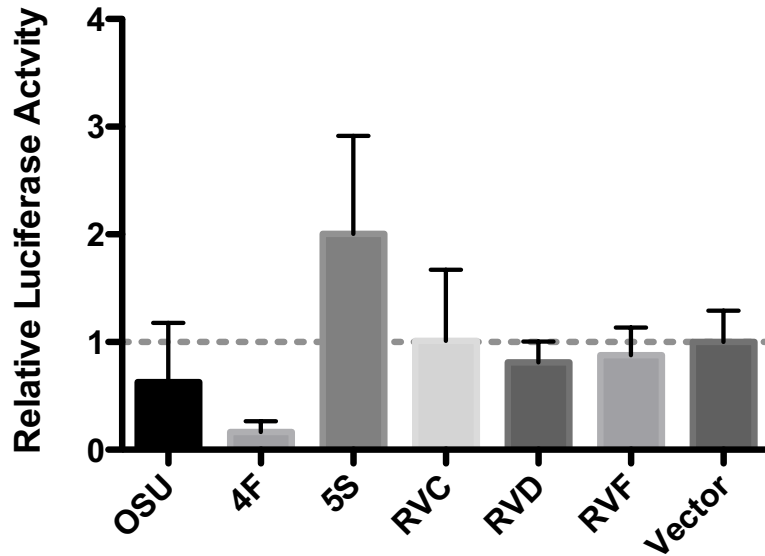


Figure 5-8. Effect of non-RVA NSP1 expression on IRF3 activation. Only SA11-4F NSP1 inhibits IRF3 signaling and ISRE activation. HEK293T cells were cotransfected with NSP1 and ISRE firefly and HSV-tk Renilla luciferase reporters. At 48 h p.t., cells were stimulated for 4 h with 10 ug/ml poly(I:C). Relative luciferase activity was calculated by normalizing firefly to Renilla luciferase activity.

RVD NSP1 antagonizes JAK/STAT signaling. Thus far, our data does not present a strong role for these non-RVA NSP1 proteins in inhibition of interferon induction. Thus, in addition to the canonical IRF3 and NF- κ B signaling cascades, we expanded our analysis to include paracrine and autocrine cascades. Cytokines released from activated cells to bind interferon receptors on its own surface (autocrine) or on a neighboring cell (paracrine) to amplify antiviral responses. This response activates the Janus kinase (JAK) and activator of transcription (STAT) pathway to induce interferon and interferon-stimulated genes. Activated JAK and TYR kinases phosphorylate STAT1 and STAT2, which in turn, assemble with IRF9 to form the ISGF3 (Interferon Stimulated Gene Factor 3) complex, which binds ISRE promoters in the nucleus to induce interferon (245). NSP1 proteins from the human strain Wa and the simian strain RRV are known to inhibit nuclear translocation of STAT proteins (246). To assess the possible role of non-Group A NSP1 proteins in JAK/STAT signaling, NSP1 expression plasmids were co-transfected into HEK293T cells with ISRE-driven luciferase constructs. Following treatment with Poly(I:C), only RVD NSP1 was able to inhibit JAK/STAT activation (Fig. 5-9). Neither OSU, SA11-4F, SA11-5S, RVC, nor RVF NSP1 proteins reduced activation below levels observed in vector- or mock-treated cells. NSP1 proteins from OSU and RVC strains appeared to increase activation more than 3-fold.

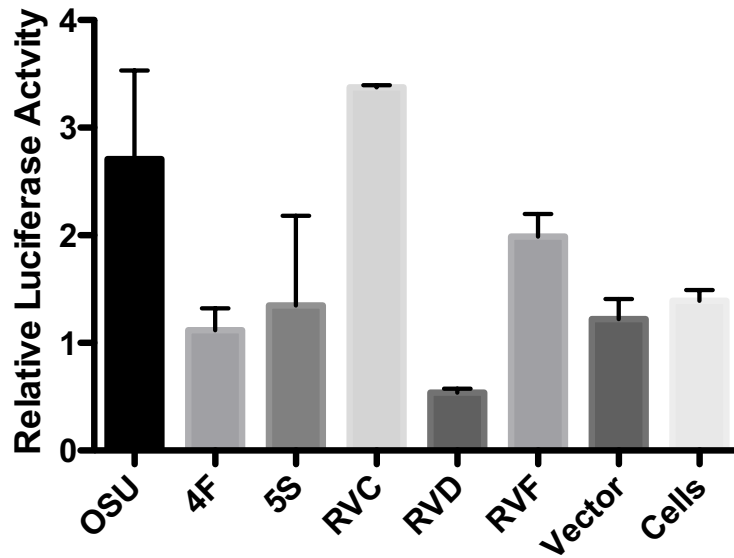


Figure 5-9. Effect of non-RAV NSP1 expression on JAK/STAT activation. RVD NSP1 inhibits JAK/STAT signaling. HEK293T cells were cotransfected with NSP1 and STAT firefly and HSV-tk Renilla luciferase reporters. At 4 h p.t., cells were stimulated with Interferon. At 24 h p.t., cells were assayed for luciferase activity.

Discussion

In the present study, we evaluated the ability of non-Group A NSP1 proteins to interfere with signaling cascades known to be common targets for Group A NSP1 proteins. These pathways included pro-interferon activation pathways mediated by IRF3, NF- κ B, and JAK/STAT. In dual luciferase assays, RVC and RVF NSP1 proteins failed to interfere with either IRF3 or NF- κ B promoter activity, suggesting that they do not have the same activity as known classes of RVA NSP1 proteins. Interestingly, RVC NSP1 expression appeared to increase activation of both JAK/STAT and IRF3 signaling cascades. RVD NSP1, however, was found to inhibit activation of JAK/STAT and NF- κ B signaling, and did so without facilitating degradation of either β -TrCP or IRF3. Expression of interferon β mRNA was not directly assessed in these experiments, but this data collection represents the first evidence that non-RVA NSP1 proteins may possess the ability to inhibit interferon induction cascades.

While NSP1 proteins are notoriously diverse with little sequence conservation between rotavirus groups and species, most NSP1 proteins conserve the N-terminal RING domain. Available NSP1 sequences primarily belong to viruses within group A, rotaviruses responsible for the majority of human disease. Non-RVA rotavirus strains have been identified as major disease causing pathogens in a number of non-human host species, but very few studies have been published describing the pathogenesis or molecular biology of these strains. These RVD and RVF virus groups are found avian species, while RVC causes infection in pigs, but only RVC is known to infect humans. Few sequences are available for non-Group A NSP1 proteins, but current analysis suggests that NSP1 proteins from RVC, RVD and RVF cluster with RVA sequences in

an RVA-like functional class (115). Furthermore, sequencing data suggests that these NSP1 proteins, like Group A NSP1 proteins, contain an analogous putative RING domain with similar spacing and predicted architecture: C-X₂-C-X₈-C-X₂-C-X₃-H-X-C-X₂-C-X₄-₇-C. While earlier reports define an RNA binding role for this region of the protein, more recent studies suggest a second biological role for this sequence conservation in mediating interactions with hijacked CRLs (148). This finding also points towards a shared mechanism governing NSP1 activity despite target protein identity or host species.

While non-RVA NSP1 proteins contain no readily identifiable targeting domains within their C-termini, as has been observed for RVA strains such as OSU and SA11-4F, it is possible that these proteins utilize as yet unidentified motifs within these regions towards this goal. While there appears to be little sequence variation in dimerization domains of IRF proteins specifically (237), diversity does exist in innate immune response proteins across species. Chickens, for example, do not encode a RIG-I protein (247), and thus are much more susceptible to avian influenza viruses to which ducks are resistant. RIG-I, too has been identified as a crucial PRR in mediating immune responses to rotavirus infection, so it is intriguing that RVD rotaviruses, an avian pathogen, has evolved to antagonize signaling cascades down stream of RIG-I activation. As individual pathogens evolve with a specific host, it is expected that their respective approach towards interferon antagonism may also narrow. It will be intriguing to examine the ability of non-human pathogens, such as RVD, RVC, and RVF rotaviruses, to antagonize immune responses across a panel of host species. Clearly, additional research is needed to fully evaluate the approaches utilized by the NSP1 proteins of these viruses, and to establish how they diverged evolutionarily with individual hosts.

Part 3: OSU rotavirus infection affects mTOR signaling through DEPTOR accumulation

Abstract

The F-box adaptor protein β -TrCP is responsible for specifying ubiquitination substrates of the cullin-RING ligase SCF ^{β -TrCP} (Skp1-Cul1-F-box). This process leads to directed proteasomal degradation of specific substrate proteins, and helps to regulate the stability of proteins involved in regulating a vast number of cellular pathways. These pathways are involved in cell cycle progression, innate immune response, as well as aspects of cell fate and survival. While many viruses are known to target β -TrCP and its activity as a means of inhibiting interferon expression, increasingly evidence suggests that β -TrCP control may provide added benefits to viruses, shaping an intracellular environment that promotes viral replication from a number of angles. To this end, we addressed whether rotavirus infection by the OSU strain resulted in observable changes in signaling of pathways under β -TrCP control, in addition to NF- κ B and interferon expression. We found that in multiple cell types, OSU infection results in increased levels of DEPTOR, an mTOR-associated protein that promotes autophagy. The constellation of mTOR associated proteins detected during rotavirus infection suggest that infected cells adopt a state of extended autophagy, and this intracellular environment may represent a generally pro-viral milieu promoted by the activities of diverse viral proteins from both RNA and DNA viruses.

Introduction

The mechanism by which human and porcine NSP1 proteins target β -TrCP for degradation has been well described by several groups, and the role of this protein as an interferon antagonist has been strongly established (137, 138, 148). β -TrCP, however, has roles that extend far beyond control of NF- κ B signaling and modulation of innate immune responses (248-252). While many publications exist describing control of this protein by viruses in diverse families, including HIV, Epstein Barr, and vaccinia viruses (150, 151), few studies have been published describing the impact of virus-altered β -TrCP activity on regulation of other cellular pathways.

β -TrCP functions as an F-box containing adaptor protein of cellular E3 ubiquitin ligases from the cullin-RING family (CRLs). Specifically, β -TrCP binds CRLs containing a cullin 1 (Cul1) scaffold protein, termed SCF ^{β -TrCP} after its critical components (Skp1-Cul1-F-box). As an integral component of the ubiquitin proteasome pathway, this protein complex targets proteins for ubiquitination and subsequent degradation. Substrate targeting is specified by β -TrCP adaptor proteins, and binding is mediated by affinity for a preferred phosphodegron sequence, DpSDGxxpS. Variations of this phosphodegron exist, typically with an insertion or deletion between phospho-serine residues. Human and porcine NSP1 proteins, for example, encode a conserved DSGIS phosphodegron sequence that is also found in cellular targets of β -TrCP, such as Nrf2, EpoR, and CREB-H (253-255).

Intriguingly, several known substrates of β -TrCP directly affect cell survival pathways, including DEPTOR (DEP-domain containing mTOR-interacting protein) (256), a negative regulator of mTOR signaling (257). As an mTOR inhibitor, DEPTOR is

involved in control of cellular homeostasis by regulating apoptosis and autophagy, however its complete role has not been defined. Furthermore, data suggests that DEPTOR can behave as either a negative or positive regulator of cell death, depending on cell and tissue contexts (257). DEPTOR exists in both mTORC1 and mTORC2 complexes, and when bound, inhibits mTOR kinase activity (258). Additionally, both DEPTOR and mTOR negatively regulate each other; DEPTOR downregulation increases mTOR activity, in turn, further reducing levels of DEPTOR. Active mTORC1 is highly reactive to intra- and extra-cellular stimuli, including growth factors and oxygen, by phosphorylating 4EBP1 and p70-S6K, leading to protein and lipid synthesis. Inhibition of mTORC1 leads to an apparent increase in mTORC2 signaling, leading to Akt phosphorylation, promoting cell survival pathways (257). The Akt pathway is highly active in some cancers, and its downstream targets are associated with proliferation (259) and the inhibition of apoptosis (260).

Because of its role in cell survival and because DEPTOR is regulated by β -TrCP activity, we assessed the impact of rotavirus infection on DEPTOR stability, and subsequent regulation of mTOR substrates. In this study, we found that DEPTOR levels increased during OSU infection, but not during infection with the bovine strain UK or with TNF- α activation. Analysis of mTORC1 and mTORC2 substrates, including Akt, 4E-BP1, and p70-S6, suggest that OSU infection results in preferential inhibition of mTORC1, while supporting mTORC2 activation and pro-survival signaling. This study supports a role for NSP1 as a regulator of intracellular environments resulting in a pro-viral setting that may be beneficial for many viral species.

Materials & Methods

Cells and viruses. Human colorectal HT29 cells were grown in McCoy's 5A (modified) medium containing 10% fetal bovine serum (FBS) (Gibco) and 1,000 units/ml penicillin-streptomycin. African green monkey fetal kidney (MA104) cells were grown in Medium M199 containing 10% FBS and penicillin-streptomycin. Rotaviruses were propagated and titered by plaque assay on MA104 cells as described previously (221). Prior to infection, rotaviruses were activated by treatment with 5 μ g per ml of porcine pancreas trypsin (type IX-S; Sigma-Aldrich) for 1 h at 37°C.

Antibodies. Rabbit polyclonal antibodies to viral proteins (simian SA11-4F VP6 protein, porcine OSU NSP1 protein) (137) and PCNA (Santa Cruz Biotech [SCB], sc-7907), DEPTOR (SCB, sc-398169) and p-I κ B (Cell Signaling Technology [CST], #9246) were used at 1:5,000 dilution. Antibodies to 4E-BP1 (CST, #9452), p-4E-BP1 (CST, #2855), Akt (CST, #4691), p-Akt (CST, #9271), mTOR (CST, #2983), p70-S6K (CST, #2708), and p-p70-S6K (CST, #9234) were used at a 1:1000 dilution. HRP-conjugated goat anti-rabbit IgG antibody (CST, #7074) and horse anti-mouse IgG antibody (CST, #7076) were used at 1:10,000 dilution.

Inhibitors. The protein kinase CKII inhibitor, 4,5,6,7-tetrabromobenzotriazole (TBB) (Tocris Bioscience) and the small molecule inhibitor of CRL neddylation, MLN4924 (Cayman Chemical), were prepared as 1 mM stocks in dimethyl sulfoxide (DMSO), which were stored at -20°C. TBB and MLN4924 were diluted in cell culture medium to final concentrations of 80 and 1 μ M, respectively, immediately prior to use. TNF- α

(Sigma) was dissolved in water at a concentration of 25 mg/ml and diluted in media to a final concentration of 25 ng/ml.

Viral infection. Near confluent monolayers of HT29 cells in 6-well tissue-culture plates were infected at an MOI of 5 with trypsin-activated rotavirus. After adsorption for one-hour, the virus inoculum was removed and cell monolayers were rinsed once with PBS. Monolayers were then incubated in serum-free McCoy's 5A (modified) or M199 medium until 8 h p.i. Lysates were prepared by washing monolayers with cold PBS and scraping cells into 0.25 ml lysis buffer (150 mM NaCl, 50 mM Tris-HCl, pH 7.4, 1% Triton X-100, with 1× Complete EDTA-free protease inhibitor cocktail). Lysates were incubated on ice for 30 min, gently mixed, and clarified by centrifugation for 10 min at 15,000 x g at 4°C.

Immunoblot assay. Protein samples were mixed with NuPAGE LDS sample buffer (Invitrogen) with 50 mM dithiothreitol (DTT), and denatured by heating to 70°C (10 min). Proteins were resolved by electrophoresis on pre-cast 10% Tris-glycine polyacrylamide gels (Novex). Molecular weight markers (EZ-Run, Fisher Scientific) were resolved in parallel to determine protein sizes. Proteins were transferred from gels onto nitrocellulose membranes using an iBlot dry transfer apparatus (ThermoFisher) according to the manufacturer's instructions. Membranes were blocked by incubating in 5% BSA dissolved in TBS-0.1% Tween-20 (TBST) prior to incubation with primary antibody diluted in BSA-TBST solution. Membranes were washed with TBST before incubating with HRP-conjugated secondary antibody diluted in BSA-TBST solution.

Membranes were washed with TBST and developed using Super Signal West Pico chemiluminescent substrate (Pierce). Immunoblots were imaged using the Azure Series c500 Infrared Imaging System.

Results

DEPTOR levels increase during OSU infection. To assess whether rotavirus infection influenced DEPTOR stability, infected cell lysates were assayed for the presence of DEPTOR proteins (Fig. 5-10). DEPTOR is a target of β -TrCP, and accordingly, a rotavirus strain that encodes an NSP1 capable of facilitating inhibition and proteasomal degradation of β -TrCP was chosen. HT-29 cells were infected with the porcine rotavirus strain OSU, or mock infected, and harvested every 2 h to 10 h p.i. By immunoblot analysis, DEPTOR levels in infected cells appeared to increase, and reach peak levels by 10 h p.i. This time point correlated with observable β -TrCP degradation (148). No DEPTOR was detected in mock-infected cells, or at early time points during infection. This data suggests that β -TrCP inhibition and degradation by NSP1 may facilitate accumulation of DEPTOR during rotavirus infection.

OSU-dependent DEPTOR accumulation correlated with viral replication. To further assess the association between rotavirus infection and DEPTOR accumulation, we addressed whether an increase in cellular DEPTOR levels was a result of interferon induction or activation of pro-inflammatory responses. To test this hypothesis, MA104 cells were infected with OSU or treated with TNF- α . Cell lysates were prepared and analyzed by western blot. Immunoblots probed for DEPTOR showed an increase in

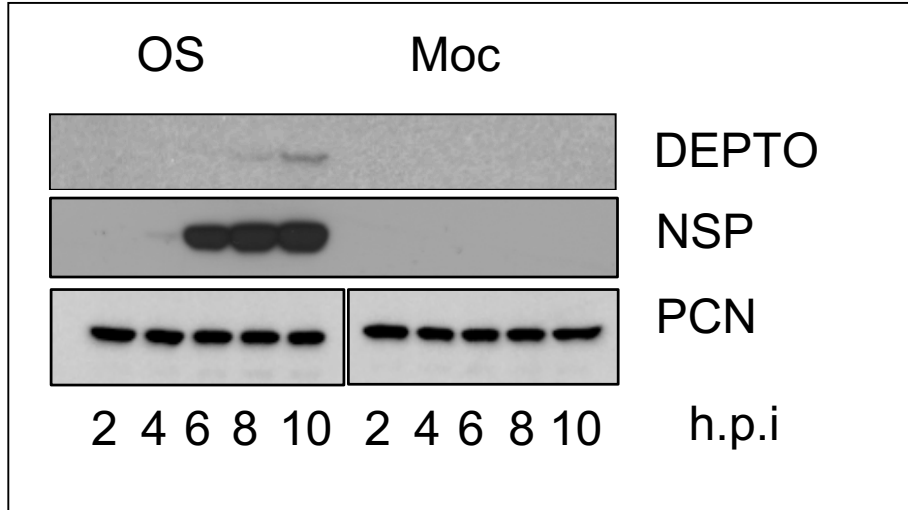


Figure 5-10. Accumulation of DEPTOR during OSU infection. HT29 cells were OSU- or mock-infected (MOI of 5) and harvested at 2 h intervals to 10 h p.i. Lysates were resolved by electrophoresis and transferred to nitrocellulose membranes. Blots were probed for antibodies specific for DEPTOR, NSP1, or PCNA.

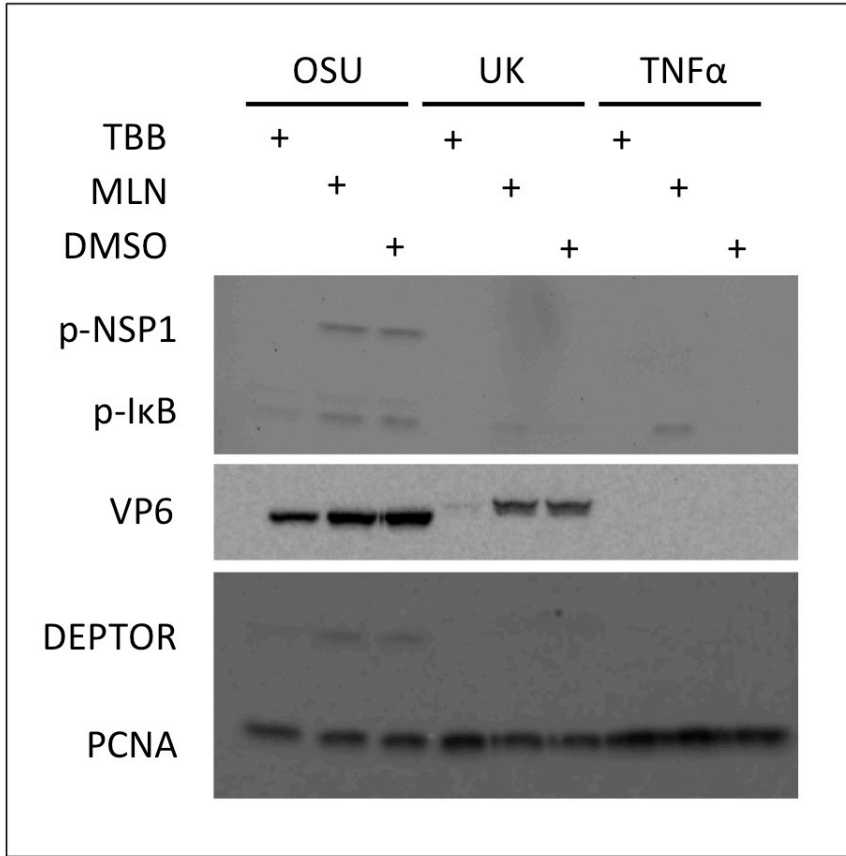


Figure 5-11. Effects of drug treatment on DEPTOR accumulation. MA104 cells were OSU- or UK- infected at an MOI of 5, or treated with TNF- α , and harvested at 8 h p.i. Lysates were resolved by electrophoresis and transferred to nitrocellulose membranes for immunoblotting with antibodies specific for p-I κ B and p-NSP1, VP6, DEPTOR, or PCNA.

protein levels following OSU infection, but not when cells were treated with TNF- α (Fig. 5-11). This result indicates that DEPTOR accumulation is likely a direct result of rotavirus infection. DEPTOR is a highly variable protein in that it is over expressed in some cancer cells and under expressed in others; that OSU infection resulted in increased DEPTOR levels in both human HT-29 colorectal cancer cells and simian MA104 kidney cells suggests that OSU induction of DEPTOR may not be a cell-line specific result. Interestingly, MA104 cells infected with the bovine UK virus did not induce DEPTOR accumulation. UK NSP1 proteins have only mild effects on β -TrCP stability, when compared to results obtained with OSU NSP1 proteins, which may account for this discrepancy.

To examine the role of NSP1 function on DEPTOR accumulation, protein levels were assessed in infected or TNF- α -treated cells following treatment with TBB or MLN (Fig. 5-11). NSP1 requires dual phosphorylation mediated by CKII to facilitate binding to β -TrCP; TBB is a small molecule inhibitor of CKII, thus inhibiting NSP1- β -TrCP interactions (148). MLN is a Nedd8 activating enzyme inhibitor that inhibits activation of assembled CRLs, preventing proteasomal degradation of CRL targets, such as β -TrCP (148). Compared to OSU-infected cells treated with DMSO, TBB reduced DEPTOR accumulation in OSU-infected cells. As measured by levels of VP6, OSU viral replication decreased in the presence of TBB. The observed decrease in DEPTOR levels may be due to compromised NSP1 activity, but we cannot rule out the possibility that DEPTOR levels are affected by a decrease in viral replication. MLN treatment appeared to have no effect on DEPTOR accumulation in OSU infected cells, but did affect levels of p-I κ B, a protein that is rapidly degraded by CRLs when β -TrCP is functional.

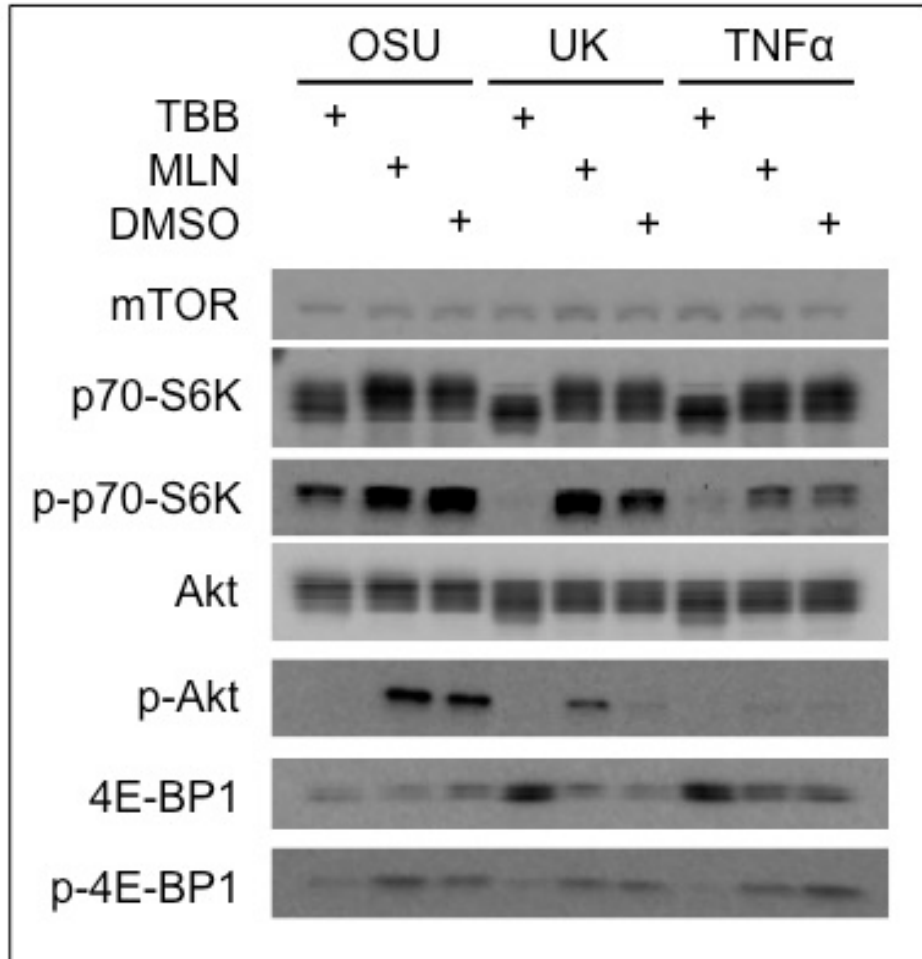


Figure 5-12. Effects of drug treatment and viral infection on mTOR signaling proteins. MA104 cells were OSU- or UK- infected at an MOI of 5, or treated with TNF- α , and harvested at 8 h p.i. Lyastes were resolved by electrophoresis and transferred to nitrocellulose membranes for immunoblotting with antibodies specific for mTOR, p70-S6K, p-p70-S6K, Akt, p-Akt, 4E-BP1, or p-4E-BP1.

Next, because rotavirus infection appears to affect DEPTOR levels, we assessed the impact of OSU or UK infection on autophagy by assessing markers of mTOR signaling. We included assessments of substrate proteins known to be markers of either mTORC1 and mTORC2 activity. p70-S6K is a substrate of active mTORC1 whereas Akt is a substrate of mTORC2. Active p-Akt is often associated with inhibition of mTORC1. While total levels of mTOR did not change upon infection with OSU or UK strains, or with TNF- α treatment, phosphorylation of p70-S6K increased during viral infection compared to TNF- α treatment, although to a lesser extent in the presence of UK compared to OSU (Fig. 5-12). p-Akt also increased during infection, and like p70-S6K, more p-Akt was observed during OSU infection compared to UK. Phosphorylation of both p70-S6K and Akt was inhibited in the presence of TBB, but our results cannot resolve whether this is a direct result of TBB, or if it is instead due to the TBB-mediated failure to activate NSP1 proteins. Together, this data suggests that rotavirus infection results in activation of mTORC1 and mTORC2, with stronger effects observed during OSU infection compared to the UK strain. Our results describe the balance of mTOR signaling at only a single time point during viral infection; these signaling cascades are highly dynamic and may be regulated differently at other time points.

To further examine the role of rotavirus infection on cell survival pathways, we assessed the effect of infection by OSU and UK on Akt signaling. Both OSU and UK infection resulted in increased levels of p-Akt, and to assess the activity of this protein, we examined levels and modification of 4E-BP1, a substrate of p-Akt. 4E-BP1 negatively regulates protein synthesis and can be inhibited by Akt-mediated phosphorylation. In these experiments, we observed no change in p-4E-BP1 levels, however, 4E-BP1 levels

appeared to increase with TBB treatment for UK-infected and TNF- α -treated cells, whereas levels remained low in TBB-treated OSU-infected cells.

Discussion

Rotavirus infection results in cell death and release of nascent virions through cell lysis. Activation of cell death pathways late in infection benefits spread of viral infection due to release of mature particles, but viral control of cell fate earlier in infection may benefit the pathogen by inhibiting premature cell death. To this end, little is known about how rotavirus may affect apoptosis or autophagy pathways, and if control of mTOR pathways is implicated in these activities. In these experiments, we have shown that infection with β -TrCP targeting rotavirus strains results in accumulation of DEPTOR, an mTOR regulatory protein, and that infection results in marked activation of mTORC1, mTORC2, and Akt signaling.

mTOR signaling and the balance between mTOR and Akt is somewhat paradoxical (261). It has been proposed that activities of each complex require inactivation of other components, as has been suggested for mTORC1 and mTORC2. Inactivation of mTORC1 can promote to the constitution of mTORC2, leading to phosphorylation of Akt. Activation of Akt is associated with active mTORC2 and inactive mTORC1 (262), however p-Akt can in turn increase the activity of mTORC1 in a negative feedback cycle. Activation of Akt promotes cell survival and activates autophagy, and this protein can be alternatively activated by TBK1 (263). It is not clear how individual activities are partitioned, and the complete network by which each signaling cascade influences the others.

A recent assessment of autophagy pathways during influenza infection has led to the proposal of a mechanism for viral control of expanded, lethal autophagy signaling cascades (264). Autophagy is activated during influenza infection, and helps avoid triggering apoptosis. In the absence of apoptosis, cells are described as undergoing a vastly expanded autophagy process. In this terminal autophagy cascade, activity of mTORC1, PI3K, and mTORC2 increase, as observed in highly phosphorylated p70-S6K populations that are regulated by mTORC2. Similar to our results, Datan, et al. also show an increase in p-Akt without changes to mTOR populations. Through timecourse analysis they demonstrate a more intricate network of how these pathways co-regulate one another. This signaling pattern is described as altered mTOR/p70-S6K signaling, and occurs during expanded lethal autophagy; inhibition of this process vastly decreases influenza titer.

Continued research is required to assess the complete functional role that autophagy signaling plays during rotavirus infection, and specifically, how the activity of NSP1 proteins may direct signal transduction through these cascades. The PI3K-Akt-mTOR axis has recently been reported to be an essential signaling cascade during rotavirus infection (265). Yin, et al. describe inhibition of viral replication achieved by rapamycin treatment, however the precise mechanism that the virus uses to harness this signaling cascade to its own advantage is not described. Our identification of an axis drawing from NSP1 activity through β -TrCP signaling and DEPTOR stability presents a novel mechanism of viral control. Our assessment is a single step towards describing these interactions in full detail.

Chapter 6:
Conclusions & Discussion

Viruses have evolved a vast set of complex approaches towards regulating innate immune responses, and yet, a surprising number of these approaches hinge upon altering the activity of a single protein: β -TrCP. β -TrCP is a key regulator of NF- κ B signaling, and by facilitating degradation of I κ B, the inhibitor of NF- κ B, promotes NF- κ B nuclear translocation and interferon induction. To this end, most human and porcine rotavirus strains encode NSP1 proteins capable of binding β -TrCP, inhibiting interferon induction and regulation of other β -TrCP substrates. NSP1 acts as a substrate adaptor protein of cellular CRLs, and by bridging both β -TrCP and a CRL, the protein facilitates proteasomal degradation of its β -TrCP target. Additional evidence supports the hypothesis that while observable β -TrCP degradation remains the gold standard in NF- κ B inhibition, binding by NSP1 may be sufficiently inhibitory. Inhibition of β -TrCP has clear implications in regulation of interferon induction pathways; however, β -TrCP controls the stability of additional targets beyond I κ B. That viruses co-opt control of this protein suggests there may be far reaching implications of β -TrCP activity that affect the intracellular environment to support productive viral replication.

In our studies of NSP1 function, we first sought to establish the determinants of β -TrCP-NSP1 binding and to identify cellular regulatory steps affecting these protein-protein interactions. NSP1 proteins are believed to interact with target proteins by specific C-terminal motifs, and analysis of β -TrCP-targeting NSP1 proteins reveals a conserved DSGIS motif with notable similarity to the DSG ϕ xS phosphodegron motif conserved within I κ B (138). With experimental techniques combining the use of phosphospecific antibodies, site directed mutagenesis, and phosphatase treatment, our data suggests that NSP1 proteins conserving this motif are indeed phosphorylated.

Furthermore, analysis of the surrounding degron context revealed a consensus sequence of CKII. With experiments utilizing mutagenesis, RNAi, and a small molecular inhibitor, our data demonstrates that phosphorylation is accomplished by CKII. When CKII was inhibited, we saw markedly reduced phosphorylation of NSP1 proteins, also suggesting that no other cellular kinase utilizes the NSP1 C-terminus as a substrate.

We next sought to assess the biological relevance of NSP1 phosphorylation by addressing NSP1 function in the presence or absence of C-terminal phosphorylation modifications. By immunoblot analyses, data demonstrates that unphosphorylated NSP1 proteins are not able to inhibit β -TrCP activity. Additionally, unphosphorylated NSP1 proteins are not able to facilitate direct interactions with β -TrCP target proteins, as assessed by immunoprecipitation experiments. Most surprising, however, was the apparent reliance of CRL incorporation on the phosphorylation of NSP1:

unphosphorylated NSP1 proteins, despite an intact RING domain, were unable to bind cellular Cul3. Together, this data suggests an ordered step-wise process governing NSP1-incorporation into cellular CRLs: (1) NSP1 is bound by CKII and phosphorylated, (2) phosphorylation of the degron motif leads to binding by β -TrCP target proteins, (3) the NSP1- β -TrCP complex associates with Cul3 CRLs via the N-terminal RING domain, releasing CKII, and (4) CRL incorporation leads to β -TrCP ubiquitination and degradation.

In our studies, we observed that NSP1 expression reaches peak levels near 4 h p.t., and that this time point also correlates with apparent inhibition of β -TrCP activity, as measured by accumulation of p-I κ B. Degradation of β -TrCP, however, does not occur until much later in infection. This data suggests that binding alone by NSP1 may be

enough to inhibit β -TrCP activity, either by sequestration or by ubiquitination independent of proteasomal degradation. Interestingly, experiments with an avian RVD NSP1 protein indicated that this NSP1 protein was capable of inhibiting NF- κ B signaling without facilitating degradation of β -TrCP. Together, this data suggests that this mechanism may represent an approach adopted by many viral proteins, both within the *Reoviridae* family, but also beyond, including vaccinia and Epstein Barr virus proteins.

To examine the extent to which mechanisms may be shared between rotavirus NSP1 proteins, we next focused our efforts on NSP1 proteins that share similar putative RING domains. Our experiments with RVA NSP1 proteins suggest that the RING domain bridges interactions with cullin scaffold proteins, whereas the C-terminus of the protein identifies substrates for binding and degradation. NSP1 proteins from groups A, C, D, and F all share a putative RING domain, but the activity of group C, D, and F NSP1 proteins as interferon antagonists has not been reported.

Studies from Ding, et al. and Lutz, et al. report that RVA NSP1 proteins interact with cullin proteins and adopt shared mechanisms regardless of substrate protein identity, so we assessed whether these non-group A NSP1 proteins had SA11-4F-like or OSU-like activity. Specifically, we examined the potential role of non-group A NSP1 proteins as antagonists of IRF, NF- κ B, and JAK/STAT signaling, beginning with an *in silico* analysis of the protein C-termini. Surprisingly, the NSP1 included in the study did not contain canonical C-terminal targeting motifs seen in Group A NSP1 proteins. Interestingly, only RVD NSP1 had NF- κ B antagonist activity, and was able to restrict promoter activation without facilitating degradation of β -TrCP. None of the NSP1

proteins tested were able to inhibit IRF3 signaling to the same extent that is observed by SA11-4F NSP1 proteins, and only RVD NSP1 was able to limit JAK/STAT signaling.

While additional studies are needed to describe in detail the role of non-RVA NSP1 proteins in interferon induction, our observations suggest that multiple NSP1 proteins from different strains may utilize a similar mechanism to target diverse targets. This work builds upon studies by Ding, et al. and Lutz, et al., who have extensively studied IRF3-targeting NSP1 proteins, such as those from SA11-4F viruses. However, no C-terminal modification was been reported for these NSP1 proteins. Our studies with OSU-like NSP1 proteins demonstrate that phosphorylation is required for both substrate and CRL engagement, suggesting that a conformational change may govern these binding interactions. To this end, we assessed whether the interaction between SA11-4F NSP1 and IRF3 was similarly governed by phosphorylation.

NSP1 proteins from SA11-4F-like strains have within their C-terminal substrate targeting domain a conserved pLxIS motif, that is likely a mimic of analogous motif utilized by immune adaptor proteins to engage IRF proteins. Cellular proteins containing pLxIS motifs are phosphorylated prior to IRF binding, but our *in silico* analysis of SA11-4F NSP1 identified no known cellular kinase consensus sequence in this region. Furthermore, mutations introduced within the pLxIS motif were unable to inhibit NSP1 antagonism of IRF3 promoter activation, including mutation of the terminal serine residue. These NSP1 proteins remained active when multiple mutations were introduced at once. Instead, our data indicates that these proteins likely forge interactions hinging upon contacts with the isoleucine residue, a finding supported by Liu, et al. in PNAS (237).

While SA11-4F NSP1 proteins do not appear to be phosphorylated within their C-terminal targeting domain, our findings do not rule out the possibility that other phosphorylation events affect the function of this protein. It is possible that SA11-4F NSP1 proteins adopt a conformation that allows them to engage targets and Cullin scaffold proteins effectively, and that OSU-like NSP1 proteins instead must undergo phosphorylation to catalyze appropriate folding. Additionally, it has been shown that phospho-mimetic mutations of OSU NSP1 proteins do not have the same activity of wildtype phosphorylated NSP1 proteins (138), suggesting that there may be chemical requirements for substrate binding specific to this interaction.

NSP1 is notoriously difficult to purify, but the suggestion that SA11-4F NSP1 proteins do not require context-specific modifications suggest the feasibility of experimentation with purified peptides. Experiments utilizing NSP1 peptides may be a useful tool to study specific protein-protein interactions, as was achieved by Liu, et al, to predict and study pLxIS binding to IRF3. This approach will likely be more challenging in studies of OSU NSP1 proteins, however. Phosphorylation of the DSGIS motif likely affects RING folding, and thus there seem to be long-range interactions between the N- and C-termini. Such a study would be particularly intriguing in studies of degron binding strength. The most common β -TrCP substrate phosphodegron, found within the phosphodegron domains of both I κ B and HIV Vpu, preserves a distance of three residues between the conserved residues of the essential serine doublet (DSG Φ XS). Vaccinia A49 increases this distance to four residues (DSG Φ XES), while OSU NSP1 instead opts for an abridged DSG Φ S motif. Reportedly, glutamic or aspartic acid replacement of serine residues increases binding strength for A49 but decreases binding for I κ B. Indeed,

phosphorylation and charge changes induce necessary conformational changes affecting distance within the I κ B degron to induce β -TrCP binding (266). The relative binding strength of the OSU NSP1 degron motif has not been established, and it has yet to be observed if this length modification confers a selective advantage for the virus in terms of target binding strength or other sources of regulation. It will be intriguing to examine why NSP1 has chosen to mimic a shortened version of this motif, as is found in CREB-H (253) and Nrf2 (267) over the degrons of other viral and cellular β -TrCP binding partners. The structure of a CREB-H- β -TrCP was recently published (253), and insights into this binding may provide a valuable framework by which to assess NSP1- β -TrCP complexes.

β -TrCP is targeted by many viral proteins outside the *Reoviridae* family, including vaccinia and Epstein-Barr viruses, suggesting that the benefits of β -TrCP manipulation may not be limited to rotavirus. To this end, we assessed whether β -TrCP inhibition resulted in changes in signaling patterns of other cascades known to be regulated by β -TrCP activity. Specifically, we found that DEPTOR, an mTOR-associated protein whose stability is regulated by β -TrCP, is stabilized during OSU infection, and that this observation held true in multiple cell types. OSU infection of both HT29 and MA104 cells lead to an increase in DEPTOR, and this effect was limited by the use of TBB, suggesting the increase may be due to NSP1 activity. UK, a rotavirus with an NSP1 with more mild effects on β -TrCP degradation, was unable to facilitate the same effects. Similarly, TNF- α treatment also did not result in DEPTOR accumulation.

Furthermore, immunoblot analysis of infected cell lysates suggest an mTOR signaling constellation consistent with extended autophagy also observed during

influenza infection. OSU infection caused an increase in phosphorylation of p70-S6K, Akt, and 4E-BP1. This phenotype may be indicative of viral control of expanded, lethal autophagy, a process that requires mTOR and p70-S6K and has been reported to support influenza replication (264). Perhaps this process, too, supports replication of rotavirus and indicates induction of an intracellular environment that is broadly pro-viral.

Progress in the rotavirus field has been long shaped by the lack of a flexible, whole-genome reverse genetics (RG) system. While the studies presented here were underway, the first report of a rotavirus RG system was published (77). The development of this system has significant impacts on the future of the rotavirus field; the introduction of this system would profoundly alter the course of action taken in the studies presented here. In our examination of NSP1, we have limited the assessment of protein activity to mechanisms of antiviral signaling control; however, this protein likely has many additional roles in infected cells. Of note, the putative RING domain has RNA-binding activity (146, 243), but the precise role this activity plays during replication is unknown. This domain has specific affinity for all rotavirus ssRNAs, suggesting that it may play a role in evasion of immune detection during replication. Because NSP1 is non-essential to rotavirus replication, the introduction of an RG system has particular value in the assessment of this protein compared to structural proteins or other essential enzymes. It is clear that the universal application of this system will have a great impact on our understanding of rotavirus biology; while strides have been made in the elucidation of the NSP1 functional landscape and its relationship to multiple aspects of cell biology, there are still many questions that remain unanswered.

References

1. **Flewett TH, Bryden AS, Davies H, Woode GN, Bridger JC, Derrick JM.** 1974. Relation between viruses from acute gastroenteritis of children and newborn calves. *Lancet* **2**:61-63.
2. **Adams WR, Kraft LM.** 1963. Epizootic diarrhea of infant mice: identification of the etiologic agent. *Science* **141**:359-360.
3. **Liu L, Johnson HL, Cousens S, Perin J, Scott S, Lawn JE, Rudan I, Campbell H, Cibulskis R, Li M, Mathers C, Black RE, Child Health Epidemiology Reference Group of WHO, Unicef.** 2012. Global, regional, and national causes of child mortality: an updated systematic analysis for 2010 with time trends since 2000. *Lancet* **379**:2151-2161.
4. **Tate JE, Burton AH, Boschi-Pinto C, Parashar UD, World Health Organization-Coordinated Global Rotavirus Surveillance N.** 2016. Global, Regional, and National Estimates of Rotavirus Mortality in Children <5 Years of Age, 2000-2013. *Clin Infect Dis* **62 Suppl 2**:S96-S105.
5. **Tate JE, Arora R, Bhan MK, Yewale V, Parashar UD, Kang G.** 2014. Rotavirus disease and vaccines in India: a tremendous public health opportunity. *Vaccine* **32 Suppl 1**:vii-xii.
6. **O'Ryan M, Linhares AC.** 2009. Update on Rotarix: an oral human rotavirus vaccine. *Expert Rev Vaccines* **8**:1627-1641.
7. **Cortes JE, Curns AT, Tate JE, Cortese MM, Patel MM, Zhou F, Parashar UD.** 2011. Rotavirus vaccine and health care utilization for diarrhea in U.S. children. *N Engl J Med* **365**:1108-1117.

8. **Vesikari T, Giaquinto C, Huppertz HI.** 2006. Clinical trials of rotavirus vaccines in Europe. *Pediatr Infect Dis J* **25**:S42-47.
9. **Vesikari T, Matson DO, Dennehy P, Van Damme P, Santosham M, Rodriguez Z, Dallas MJ, Heyse JF, Goveia MG, Black SB, Shinefield HR, Christie CD, Ylitalo S, Itzler RF, Coia ML, Onorato MT, Adeyi BA, Marshall GS, Gothefors L, Campens D, Karvonen A, Watt JP, O'Brien KL, DiNubile MJ, Clark HF, Boslego JW, Offit PA, Heaton PM, Rotavirus E, Safety Trial Study T.** 2006. Safety and efficacy of a pentavalent human-bovine (WC3) reassortant rotavirus vaccine. *N Engl J Med* **354**:23-33.
10. **Giaquinto C, Dominiak-Felden G, Van Damme P, Myint TT, Maldonado YA, Spoulou V, Mast TC, Staat MA.** 2011. Summary of effectiveness and impact of rotavirus vaccination with the oral pentavalent rotavirus vaccine: a systematic review of the experience in industrialized countries. *Hum Vaccin* **7**:734-748.
11. **O'Ryan M, Lucero Y, Linhares AC.** 2011. Rotarix(R): vaccine performance 6 years postlicensure. *Expert Rev Vaccines* **10**:1645-1659.
12. **Ramig RF.** 2004. Pathogenesis of intestinal and systemic rotavirus infection. *J Virol* **78**:10213-10220.
13. **Lecce JG, King MW.** 1978. Role of rotavirus (reo-like) in weanling diarrhea of pigs. *J Clin Microbiol* **8**:454-458.
14. **Estes MK, Morris AP.** 1999. A viral enterotoxin. A new mechanism of virus-induced pathogenesis. *Adv Exp Med Biol* **473**:73-82.

15. **Matthijssens J, Otto PH, Ciarlet M, Desselberger U, Van Ranst M, Johne R.** 2012. VP6-sequence-based cutoff values as a criterion for rotavirus species demarcation. *Arch Virol* **157**:1177-1182.
16. **Matthijssens J, Van Ranst M.** 2012. Genotype constellation and evolution of group A rotaviruses infecting humans. *Curr Opin Virol* **2**:426-433.
17. **Matthijssens J, Ciarlet M, Heiman E, Arijs I, Delbeke T, McDonald SM, Palombo EA, Iturriza-Gomara M, Maes P, Patton JT, Rahman M, Van Ranst M.** 2008. Full genome-based classification of rotaviruses reveals a common origin between human Wa-Like and porcine rotavirus strains and human DS-1-like and bovine rotavirus strains. *J Virol* **82**:3204-3219.
18. **Matthijssens J, Ciarlet M, McDonald SM, Attoui H, Banyai K, Brister JR, Buesa J, Esona MD, Estes MK, Gentsch JR, Iturriza-Gomara M, Johne R, Kirkwood CD, Martella V, Mertens PP, Nakagomi O, Parreno V, Rahman M, Ruggeri FM, Saif LJ, Santos N, Steyer A, Taniguchi K, Patton JT, Desselberger U, Van Ranst M.** 2011. Uniformity of rotavirus strain nomenclature proposed by the Rotavirus Classification Working Group (RCWG). *Arch Virol* **156**:1397-1413.
19. **Matthijssens J, Ciarlet M, Rahman M, Attoui H, Banyai K, Estes MK, Gentsch JR, Iturriza-Gomara M, Kirkwood CD, Martella V, Mertens PP, Nakagomi O, Patton JT, Ruggeri FM, Saif LJ, Santos N, Steyer A, Taniguchi K, Desselberger U, Van Ranst M.** 2008. Recommendations for the classification of group A rotaviruses using all 11 genomic RNA segments. *Arch Virol* **153**:1621-1629.

20. **Jayaram H, Estes MK, Prasad BV.** 2004. Emerging themes in rotavirus cell entry, genome organization, transcription and replication. *Virus Res* **101**:67-81.
21. **Estrozi LF, Settembre EC, Goret G, McClain B, Zhang X, Chen JZ, Grigorieff N, Harrison SC.** 2013. Location of the dsRNA-dependent polymerase, VP1, in rotavirus particles. *J Mol Biol* **425**:124-132.
22. **Rickgauer JP, Grigorieff N, Denk W.** 2017. Single-protein detection in crowded molecular environments in cryo-EM images. *Elife* **6**.
23. **McDonald SM, Patton JT.** 2011. Rotavirus VP2 core shell regions critical for viral polymerase activation. *J Virol* **85**:3095-3105.
24. **Trask SD, McDonald SM, Patton JT.** 2012. Structural insights into the coupling of virion assembly and rotavirus replication. *Nat Rev Microbiol* **10**:165-177.
25. **Trask SD, Ogden KM, Patton JT.** 2012. Interactions among capsid proteins orchestrate rotavirus particle functions. *Curr Opin Virol* **2**:373-379.
26. **Periz J, Celma C, Jing B, Pinkney JN, Roy P, Kapanidis AN.** 2013. Rotavirus mRNAs are released by transcript-specific channels in the double-layered viral capsid. *Proc Natl Acad Sci U S A* **110**:12042-12047.
27. **Lourenco S, Roy P.** 2011. In vitro reconstitution of Bluetongue virus infectious cores. *Proc Natl Acad Sci U S A* **108**:13746-13751.
28. **Prasad BV, Rothnagel R, Zeng CQ, Jakana J, Lawton JA, Chiu W, Estes MK.** 1996. Visualization of ordered genomic RNA and localization of transcriptional complexes in rotavirus. *Nature* **382**:471-473.
29. **Gridley CL, Patton JT.** 2014. Regulation of rotavirus polymerase activity by inner capsid proteins. *Curr Opin Virol* **9**:31-38.

30. **Rainsford EW, McCrae MA.** 2007. Characterization of the NSP6 protein product of rotavirus gene 11. *Virus Res* **130**:193-201.
31. **Tortorici MA, Shapiro BA, Patton JT.** 2006. A base-specific recognition signal in the 5' consensus sequence of rotavirus plus-strand RNAs promotes replication of the double-stranded RNA genome segments. *RNA* **12**:133-146.
32. **McDonald SM, Nelson MI, Turner PE, Patton JT.** 2016. Reassortment in segmented RNA viruses: mechanisms and outcomes. *Nat Rev Microbiol* **14**:448-460.
33. **Tortorici MA, Broering TJ, Nibert ML, Patton JT.** 2003. Template recognition and formation of initiation complexes by the replicase of a segmented double-stranded RNA virus. *J Biol Chem* **278**:32673-32682.
34. **Chizhikov V, Patton JT.** 2000. A four-nucleotide translation enhancer in the 3'-terminal consensus sequence of the nonpolyadenylated mRNAs of rotavirus. *RNA* **6**:814-825.
35. **Lawton JA, Estes MK, Prasad BV.** 2000. Mechanism of genome transcription in segmented dsRNA viruses. *Adv Virus Res* **55**:185-229.
36. **Gutierrez M, Isa P, Sanchez-San Martin C, Perez-Vargas J, Espinosa R, Arias CF, Lopez S.** 2010. Different rotavirus strains enter MA104 cells through different endocytic pathways: the role of clathrin-mediated endocytosis. *J Virol* **84**:9161-9169.
37. **Altan-Bonnet N.** 2017. Lipid Tales of Viral Replication and Transmission. *Trends Cell Biol* **27**:201-213.

38. **Isa P, Arias CF, Lopez S.** 2006. Role of sialic acids in rotavirus infection. *Glycoconj J* **23**:27-37.
39. **Lopez S, Arias CF.** 2006. Early steps in rotavirus cell entry. *Curr Top Microbiol Immunol* **309**:39-66.
40. **Hu L, Crawford SE, Czako R, Cortes-Penfield NW, Smith DF, Le Pendu J, Estes MK, Prasad BV.** 2012. Cell attachment protein VP8* of a human rotavirus specifically interacts with A-type histo-blood group antigen. *Nature* **485**:256-259.
41. **Huang P, Xia M, Tan M, Zhong W, Wei C, Wang L, Morrow A, Jiang X.** 2012. Spike protein VP8* of human rotavirus recognizes histo-blood group antigens in a type-specific manner. *J Virol* **86**:4833-4843.
42. **Ramani S, Cortes-Penfield NW, Hu L, Crawford SE, Czako R, Smith DF, Kang G, Ramig RF, Le Pendu J, Prasad BV, Estes MK.** 2013. The VP8* domain of neonatal rotavirus strain G10P[11] binds to type II precursor glycans. *J Virol* **87**:7255-7264.
43. **Imbert-Marcille BM, Barbe L, Dupe M, Le Moullac-Vaidye B, Besse B, Peltier C, Ruvoen-Clouet N, Le Pendu J.** 2014. A FUT2 gene common polymorphism determines resistance to rotavirus A of the P[8] genotype. *J Infect Dis* **209**:1227-1230.
44. **Guerrero CA, Bouyssounade D, Zarate S, Isa P, Lopez T, Espinosa R, Romero P, Mendez E, Lopez S, Arias CF.** 2002. Heat shock cognate protein 70 is involved in rotavirus cell entry. *J Virol* **76**:4096-4102.

45. **Zarate S, Cuadras MA, Espinosa R, Romero P, Juarez KO, Camacho-Nuez M, Arias CF, Lopez S.** 2003. Interaction of rotaviruses with Hsc70 during cell entry is mediated by VP5. *J Virol* **77**:7254-7260.
46. **Isa P, Realpe M, Romero P, Lopez S, Arias CF.** 2004. Rotavirus RRV associates with lipid membrane microdomains during cell entry. *Virology* **322**:370-381.
47. **Fleming FE, Bohm R, Dang VT, Holloway G, Haselhorst T, Madge PD, Deveryshetty J, Yu X, Blanchard H, von Itzstein M, Coulson BS.** 2014. Relative roles of GM1 ganglioside, N-acylneuraminic acids, and alpha2beta1 integrin in mediating rotavirus infection. *J Virol* **88**:4558-4571.
48. **Arias CF, Silva-Ayala D, Lopez S.** 2015. Rotavirus entry: a deep journey into the cell with several exits. *J Virol* **89**:890-893.
49. **Rodriguez JM, Chichon FJ, Martin-Forero E, Gonzalez-Camacho F, Carrascosa JL, Caston JR, Luque D.** 2014. New insights into rotavirus entry machinery: stabilization of rotavirus spike conformation is independent of trypsin cleavage. *PLoS Pathog* **10**:e1004157.
50. **Trask SD, Wetzel JD, Dermody TS, Patton JT.** 2013. Mutations in the rotavirus spike protein VP4 reduce trypsin sensitivity but not viral spread. *J Gen Virol* **94**:1296-1300.
51. **Kim IS, Trask SD, Babyonyshev M, Dormitzer PR, Harrison SC.** 2010. Effect of mutations in VP5 hydrophobic loops on rotavirus cell entry. *J Virol* **84**:6200-6207.

52. **Kaljot KT, Shaw RD, Rubin DH, Greenberg HB.** 1988. Infectious rotavirus enters cells by direct cell membrane penetration, not by endocytosis. *J Virol* **62**:1136-1144.
53. **Diaz-Salinas MA, Romero P, Espinosa R, Hoshino Y, Lopez S, Arias CF.** 2013. The spike protein VP4 defines the endocytic pathway used by rotavirus to enter MA104 cells. *J Virol* **87**:1658-1663.
54. **Sanchez-San Martin C, Lopez T, Arias CF, Lopez S.** 2004. Characterization of rotavirus cell entry. *J Virol* **78**:2310-2318.
55. **Silva-Ayala D, Lopez T, Gutierrez M, Perrimon N, Lopez S, Arias CF.** 2013. Genome-wide RNAi screen reveals a role for the ESCRT complex in rotavirus cell entry. *Proc Natl Acad Sci U S A* **110**:10270-10275.
56. **Henne WM, Buchkovich NJ, Emr SD.** 2011. The ESCRT pathway. *Dev Cell* **21**:77-91.
57. **Diaz-Salinas MA, Silva-Ayala D, Lopez S, Arias CF.** 2014. Rotaviruses reach late endosomes and require the cation-dependent mannose-6-phosphate receptor and the activity of cathepsin proteases to enter the cell. *J Virol* **88**:4389-4402.
58. **Ludert JE, Michelangeli F, Gil F, Liprandi F, Esparza J.** 1987. Penetration and uncoating of rotaviruses in cultured cells. *Intervirology* **27**:95-101.
59. **Abdelhakim AH, Salgado EN, Fu X, Pasham M, Nicastro D, Kirchhausen T, Harrison SC.** 2014. Structural correlates of rotavirus cell entry. *PLoS Pathog* **10**:e1004355.

60. **Lawton JA, Estes MK, Prasad BV.** 1997. Three-dimensional visualization of mRNA release from actively transcribing rotavirus particles. *Nat Struct Biol* **4**:118-121.
61. **Lu X, McDonald SM, Tortorici MA, Tao YJ, Vasquez-Del Carpio R, Nibert ML, Patton JT, Harrison SC.** 2008. Mechanism for coordinated RNA packaging and genome replication by rotavirus polymerase VP1. *Structure* **16**:1678-1688.
62. **Salgado EN, Upadhyayula S, Harrison SC.** 2017. Single-particle detection of transcription following rotavirus entry. *J Virol* doi:10.1128/JVI.00651-17.
63. **McClain B, Settembre E, Temple BR, Bellamy AR, Harrison SC.** 2010. X-ray crystal structure of the rotavirus inner capsid particle at 3.8 Å resolution. *J Mol Biol* **397**:587-599.
64. **Chen JZ, Settembre EC, Aoki ST, Zhang X, Bellamy AR, Dormitzer PR, Harrison SC, Grigorieff N.** 2009. Molecular interactions in rotavirus assembly and uncoating seen by high-resolution cryo-EM. *Proc Natl Acad Sci U S A* **106**:10644-10648.
65. **Libersou S, Siebert X, Ouldali M, Estrozi LF, Navaza J, Charpilienne A, Garnier P, Poncet D, Lepault J.** 2008. Geometric mismatches within the concentric layers of rotavirus particles: a potential regulatory switch of viral particle transcription activity. *J Virol* **82**:2844-2852.
66. **Estes MK, Cohen J.** 1989. Rotavirus gene structure and function. *Microbiol Rev* **53**:410-449.

67. **Aiyegbo MS, Sapparapu G, Spiller BW, Eli IM, Williams DR, Kim R, Lee DE, Liu T, Li S, Woods VL, Jr., Nannemann DP, Meiler J, Stewart PL, Crowe JE, Jr.** 2013. Human rotavirus VP6-specific antibodies mediate intracellular neutralization by binding to a quaternary structure in the transcriptional pore. *PLoS One* **8**:e61101.
68. **Stacy-Phipps S, Patton JT.** 1987. Synthesis of plus- and minus-strand RNA in rotavirus-infected cells. *J Virol* **61**:3479-3484.
69. **Ayala-Breton C, Arias M, Espinosa R, Romero P, Arias CF, Lopez S.** 2009. Analysis of the kinetics of transcription and replication of the rotavirus genome by RNA interference. *J Virol* **83**:8819-8831.
70. **Eichwald C, Rodriguez JF, Burrone OR.** 2004. Characterization of rotavirus NSP2/NSP5 interactions and the dynamics of viroplasm formation. *J Gen Virol* **85**:625-634.
71. **Jayaram H, Taraporewala Z, Patton JT, Prasad BV.** 2002. Rotavirus protein involved in genome replication and packaging exhibits a HIT-like fold. *Nature* **417**:311-315.
72. **Eichwald C, Jacob G, Muszynski B, Allende JE, Burrone OR.** 2004. Uncoupling substrate and activation functions of rotavirus NSP5: phosphorylation of Ser-67 by casein kinase 1 is essential for hyperphosphorylation. *Proc Natl Acad Sci U S A* **101**:16304-16309.
73. **Jiang X, Jayaram H, Kumar M, Ludtke SJ, Estes MK, Prasad BV.** 2006. Cryoelectron microscopy structures of rotavirus NSP2-NSP5 and NSP2-RNA complexes: implications for genome replication. *J Virol* **80**:10829-10835.

74. **Fabbretti E, Afrikanova I, Vascotto F, Burrone OR.** 1999. Two non-structural rotavirus proteins, NSP2 and NSP5, form viroplasm-like structures in vivo. *J Gen Virol* **80 (Pt 2):**333-339.
75. **Silvestri LS, Taraporewala ZF, Patton JT.** 2004. Rotavirus replication: plus-sense templates for double-stranded RNA synthesis are made in viroplasms. *J Virol* **78:**7763-7774.
76. **Carreno-Torres JJ, Gutierrez M, Arias CF, Lopez S, Isa P.** 2010. Characterization of viroplasm formation during the early stages of rotavirus infection. *Virology* **7:**350.
77. **Kanai Y, Komoto S, Kawagishi T, Nouda R, Nagasawa N, Onishi M, Matsuura Y, Taniguchi K, Kobayashi T.** 2017. Entirely plasmid-based reverse genetics system for rotaviruses. *Proc Natl Acad Sci U S A* **114:**2349-2354.
78. **Borodavka A, Ault J, Stockley PG, Tuma R.** 2015. Evidence that avian reovirus sigmaNS is an RNA chaperone: implications for genome segment assortment. *Nucleic Acids Res* **43:**7044-7057.
79. **Suzuki Y.** 2015. A candidate packaging signal of human rotavirus differentiating Wa-like and DS-1-like genomic constellations. *Microbiol Immunol* **59:**567-571.
80. **Li W, Manktelow E, von Kirchbach JC, Gog JR, Desselberger U, Lever AM.** 2010. Genomic analysis of codon, sequence and structural conservation with selective biochemical-structure mapping reveals highly conserved and dynamic structures in rotavirus RNAs with potential cis-acting functions. *Nucleic Acids Res* **38:**7718-7735.

81. **Borodavka A, Dykeman EC, Schrimpf W, Lamb DC.** 2017. Protein-mediated RNA folding governs sequence-specific interactions between rotavirus genome segments. *Elife* **6**.
82. **Patton JT, Gallegos CO.** 1988. Structure and protein composition of the rotavirus replicase particle. *Virology* **166**:358-365.
83. **Boudreaux CE, Kelly DF, McDonald SM.** 2015. Electron microscopic analysis of rotavirus assembly-replication intermediates. *Virology* **477**:32-41.
84. **Long CP, McDonald SM.** 2017. Rotavirus genome replication: Some assembly required. *PLoS Pathog* **13**:e1006242.
85. **Gallegos CO, Patton JT.** 1989. Characterization of rotavirus replication intermediates: a model for the assembly of single-shelled particles. *Virology* **172**:616-627.
86. **Taylor JA, O'Brien JA, Yeager M.** 1996. The cytoplasmic tail of NSP4, the endoplasmic reticulum-localized non-structural glycoprotein of rotavirus, contains distinct virus binding and coiled coil domains. *EMBO J* **15**:4469-4476.
87. **Trask SD, Dormitzer PR.** 2006. Assembly of highly infectious rotavirus particles recoated with recombinant outer capsid proteins. *J Virol* **80**:11293-11304.
88. **Tian P, Hu Y, Schilling WP, Lindsay DA, Eiden J, Estes MK.** 1994. The nonstructural glycoprotein of rotavirus affects intracellular calcium levels. *J Virol* **68**:251-257.
89. **Hyser JM, Utama B, Crawford SE, Broughman JR, Estes MK.** 2013. Activation of the endoplasmic reticulum calcium sensor STIM1 and store-

- operated calcium entry by rotavirus requires NSP4 viroporin activity. *J Virol* **87**:13579-13588.
90. **Crawford SE, Hyser JM, Utama B, Estes MK.** 2012. Autophagy hijacked through viroporin-activated calcium/calmodulin-dependent kinase kinase-beta signaling is required for rotavirus replication. *Proc Natl Acad Sci U S A* **109**:E3405-3413.
91. **Crawford SE, Estes MK.** 2013. Viroporin-mediated calcium-activated autophagy. *Autophagy* **9**:797-798.
92. **McNulty MS, Curran WL, McFerran JB.** 1976. The morphogenesis of a cytopathic bovine rotavirus in Madin-Darby bovine kidney cells. *J Gen Virol* **33**:503-508.
93. **Gardet A, Breton M, Fontanges P, Trugnan G, Chwetzoff S.** 2006. Rotavirus spike protein VP4 binds to and remodels actin bundles of the epithelial brush border into actin bodies. *J Virol* **80**:3947-3956.
94. **Arias CF, Romero P, Alvarez V, Lopez S.** 1996. Trypsin activation pathway of rotavirus infectivity. *J Virol* **70**:5832-5839.
95. **Angel J, Franco MA, Greenberg HB.** 2012. Rotavirus immune responses and correlates of protection. *Curr Opin Virol* **2**:419-425.
96. **Gonzalez AM, Azevedo MS, Jung K, Vlasova A, Zhang W, Saif LJ.** 2010. Innate immune responses to human rotavirus in the neonatal gnotobiotic piglet disease model. *Immunology* **131**:242-256.

97. **Wang Y, Dennehy PH, Keyserling HL, Tang K, Gentsch JR, Glass RI, Jiang B.** 2007. Rotavirus infection alters peripheral T-cell homeostasis in children with acute diarrhea. *J Virol* **81**:3904-3912.
98. **O'Neill LA, Bowie AG.** 2010. Sensing and signaling in antiviral innate immunity. *Curr Biol* **20**:R328-333.
99. **Wilkins C, Gale M, Jr.** 2010. Recognition of viruses by cytoplasmic sensors. *Curr Opin Immunol* **22**:41-47.
100. **Feng N, Sen A, Nguyen H, Vo P, Hoshino Y, Deal EM, Greenberg HB.** 2009. Variation in antagonism of the interferon response to rotavirus NSP1 results in differential infectivity in mouse embryonic fibroblasts. *J Virol* **83**:6987-6994.
101. **Randall RE, Goodbourn S.** 2008. Interferons and viruses: an interplay between induction, signalling, antiviral responses and virus countermeasures. *J Gen Virol* **89**:1-47.
102. **van Gent M, Gack MU.** 2017. Viral pathogenesis: Dengue virus takes on cGAS. *Nat Microbiol* **2**:17050.
103. **Sen A, Pruijssers AJ, Dermody TS, Garcia-Sastre A, Greenberg HB.** 2011. The early interferon response to rotavirus is regulated by PKR and depends on MAVS/IPS-1, RIG-I, MDA-5, and IRF3. *J Virol* **85**:3717-3732.
104. **Broquet AH, Hirata Y, McAllister CS, Kagnoff MF.** 2011. RIG-I/MDA5/MAVS are required to signal a protective IFN response in rotavirus-infected intestinal epithelium. *J Immunol* **186**:1618-1626.

105. **Chau TL, Gioia R, Gatot JS, Patrascu F, Carpentier I, Chapelle JP, O'Neill L, Beyaert R, Piette J, Chariot A.** 2008. Are the IKKs and IKK-related kinases TBK1 and IKK-epsilon similarly activated? *Trends Biochem Sci* **33**:171-180.
106. **Stetson DB, Medzhitov R.** 2006. Type I interferons in host defense. *Immunity* **25**:373-381.
107. **Wietek C, O'Neill LA.** 2007. Diversity and regulation in the NF-kappaB system. *Trends Biochem Sci* **32**:311-319.
108. **Honda K, Taniguchi T.** 2006. IRFs: master regulators of signalling by Toll-like receptors and cytosolic pattern-recognition receptors. *Nat Rev Immunol* **6**:644-658.
109. **Fitzgerald KA, McWhirter SM, Faia KL, Rowe DC, Latz E, Golenbock DT, Coyle AJ, Liao SM, Maniatis T.** 2003. IKKepsilon and TBK1 are essential components of the IRF3 signaling pathway. *Nat Immunol* **4**:491-496.
110. **Viatour P, Merville MP, Bours V, Chariot A.** 2005. Phosphorylation of NF-kappaB and I kappaB proteins: implications in cancer and inflammation. *Trends Biochem Sci* **30**:43-52.
111. **Douagi I, McInerney GM, Hidmark AS, Miriallis V, Johansen K, Svensson L, Karlsson Hedestam GB.** 2007. Role of interferon regulatory factor 3 in type I interferon responses in rotavirus-infected dendritic cells and fibroblasts. *J Virol* **81**:2758-2768.
112. **Pott J, Stockinger S, Torow N, Smoczek A, Lindner C, McInerney G, Backhed F, Baumann U, Pabst O, Bleich A, Hornef MW.** 2012. Age-

dependent TLR3 expression of the intestinal epithelium contributes to rotavirus susceptibility. *PLoS Pathog* **8**:e1002670.

113. **Deal EM, Jaimes MC, Crawford SE, Estes MK, Greenberg HB.** 2010. Rotavirus structural proteins and dsRNA are required for the human primary plasmacytoid dendritic cell IFN α response. *PLoS Pathog* **6**:e1000931.
114. **Hoshino Y, Saif LJ, Kang SY, Sereno MM, Chen WK, Kapikian AZ.** 1995. Identification of group A rotavirus genes associated with virulence of a porcine rotavirus and host range restriction of a human rotavirus in the gnotobiotic piglet model. *Virology* **209**:274-280.
115. **Morelli M, Ogden KM, Patton JT.** 2015. Silencing the alarms: Innate immune antagonism by rotavirus NSP1 and VP3. *Virology* **479-480**:75-84.
116. **Uzri D, Greenberg HB.** 2013. Characterization of rotavirus RNAs that activate innate immune signaling through the RIG-I-like receptors. *PLoS One* **8**:e69825.
117. **Silverman RH.** 2007. Viral encounters with 2',5'-oligoadenylate synthetase and RNase L during the interferon antiviral response. *J Virol* **81**:12720-12729.
118. **Silverman RH, Weiss SR.** 2014. Viral phosphodiesterases that antagonize double-stranded RNA signaling to RNase L by degrading 2-5A. *J Interferon Cytokine Res* **34**:455-463.
119. **Ogden KM, Hu L, Jha BK, Sankaran B, Weiss SR, Silverman RH, Patton JT, Prasad BV.** 2015. Structural basis for 2'-5'-oligoadenylate binding and enzyme activity of a viral RNase L antagonist. *J Virol* **89**:6633-6645.

120. **Ogden KM, Snyder MJ, Dennis AF, Patton JT.** 2014. Predicted structure and domain organization of rotavirus capping enzyme and innate immune antagonist VP3. *J Virol* **88**:9072-9085.
121. **Schneider RJ, Mohr I.** 2003. Translation initiation and viral tricks. *Trends Biochem Sci* **28**:130-136.
122. **Piron M, Vende P, Cohen J, Poncet D.** 1998. Rotavirus RNA-binding protein NSP3 interacts with eIF4GI and evicts the poly(A) binding protein from eIF4F. *EMBO J* **17**:5811-5821.
123. **Vende P, Piron M, Castagne N, Poncet D.** 2000. Efficient translation of rotavirus mRNA requires simultaneous interaction of NSP3 with the eukaryotic translation initiation factor eIF4G and the mRNA 3' end. *J Virol* **74**:7064-7071.
124. **Chung KT, McCrae MA.** 2011. Regulation of gene expression by the NSP1 and NSP3 non-structural proteins of rotavirus. *Arch Virol* **156**:2197-2203.
125. **Montero H, Arias CF, Lopez S.** 2006. Rotavirus Nonstructural Protein NSP3 is not required for viral protein synthesis. *J Virol* **80**:9031-9038.
126. **Arnold MM, Brownback CS, Taraporewala ZF, Patton JT.** 2012. Rotavirus variant replicates efficiently although encoding an aberrant NSP3 that fails to induce nuclear localization of poly(A)-binding protein. *J Gen Virol* **93**:1483-1494.
127. **Dutta D, Chattopadhyay S, Bagchi P, Halder UC, Nandi S, Mukherjee A, Kobayashi N, Taniguchi K, Chawla-Sarkar M.** 2011. Active participation of cellular chaperone Hsp90 in regulating the function of rotavirus nonstructural protein 3 (NSP3). *J Biol Chem* **286**:20065-20077.

128. **Contreras-Trevino HI, Reyna-Rosas E, Leon-Rodriguez R, Ruiz-Ordaz BH, Dinkova TD, Cevallos AM, Padilla-Noriega L.** 2017. Species A rotavirus NSP3 acquires its translation inhibitory function prior to stable dimer formation. *PLoS One* **12**:e0181871.
129. **Berkova Z, Crawford SE, Trugnan G, Yoshimori T, Morris AP, Estes MK.** 2006. Rotavirus NSP4 induces a novel vesicular compartment regulated by calcium and associated with viroplasm. *J Virol* **80**:6061-6071.
130. **Zhang M, Zeng CQ, Morris AP, Estes MK.** 2000. A functional NSP4 enterotoxin peptide secreted from rotavirus-infected cells. *J Virol* **74**:11663-11670.
131. **Bugarcic A, Taylor JA.** 2006. Rotavirus nonstructural glycoprotein NSP4 is secreted from the apical surfaces of polarized epithelial cells. *J Virol* **80**:12343-12349.
132. **Ball JM, Tian P, Zeng CQ, Morris AP, Estes MK.** 1996. Age-dependent diarrhea induced by a rotaviral nonstructural glycoprotein. *Science* **272**:101-104.
133. **Ge Y, Mansell A, Ussher JE, Brooks AE, Manning K, Wang CJ, Taylor JA.** 2013. Rotavirus NSP4 Triggers Secretion of Proinflammatory Cytokines from Macrophages via Toll-Like Receptor 2. *J Virol* **87**:11160-11167.
134. **Desselberger U.** 2014. Rotaviruses. *Virus Res* **190**:75-96.
135. **Hou Z, Huang Y, Huan Y, Pang W, Meng M, Wang P, Yang M, Jiang L, Cao X, Wu KK.** 2008. Anti-NSP4 antibody can block rotavirus-induced diarrhea in mice. *J Pediatr Gastroenterol Nutr* **46**:376-385.

136. **Arnold MM, Sen A, Greenberg HB, Patton JT.** 2013. The battle between rotavirus and its host for control of the interferon signaling pathway. *PLoS Pathog* **9**:e1003064.
137. **Arnold MM, Patton JT.** 2011. Diversity of interferon antagonist activities mediated by NSP1 proteins of different rotavirus strains. *J Virol* **85**:1970-1979.
138. **Morelli M, Dennis AF, Patton JT.** 2015. Putative E3 ubiquitin ligase of human rotavirus inhibits NF-kappaB activation by using molecular mimicry to target beta-TrCP. *MBio* **6**.
139. **Sen A, Feng N, Ettayebi K, Hardy ME, Greenberg HB.** 2009. IRF3 inhibition by rotavirus NSP1 is host cell and virus strain dependent but independent of NSP1 proteasomal degradation. *J Virol* **83**:10322-10335.
140. **Bhowmick R, Halder UC, Chattopadhyay S, Nayak MK, Chawla-Sarkar M.** 2013. Rotavirus-encoded nonstructural protein 1 modulates cellular apoptotic machinery by targeting tumor suppressor protein p53. *J Virol* **87**:6840-6850.
141. **Bagchi P, Nandi S, Chattopadhyay S, Bhowmick R, Halder UC, Nayak MK, Kobayashi N, Chawla-Sarkar M.** 2012. Identification of common human host genes involved in pathogenesis of different rotavirus strains: an attempt to recognize probable antiviral targets. *Virus Res* **169**:144-153.
142. **Nandi S, Chanda S, Bagchi P, Nayak MK, Bhowmick R, Chawla-Sarkar M.** 2014. MAVS protein is attenuated by rotavirus nonstructural protein 1. *PLoS One* **9**:e92126.

143. **Graff JW, Ettayebi K, Hardy ME.** 2009. Rotavirus NSP1 inhibits NFkappaB activation by inducing proteasome-dependent degradation of beta-TrCP: a novel mechanism of IFN antagonism. *PLoS Pathog* **5**:e1000280.
144. **Ding S, Mooney N, Li B, Kelly MR, Feng N, Loktev AV, Sen A, Patton JT, Jackson PK, Greenberg HB.** 2016. Comparative Proteomics Reveals Strain-Specific beta-TrCP Degradation via Rotavirus NSP1 Hijacking a Host Cullin-3-Rbx1 Complex. *PLoS Pathog* **12**:e1005929.
145. **Lutz LM, Pace CR, Arnold MM.** 2016. Rotavirus NSP1 Associates with Components of the Cullin RING Ligase Family of E3 Ubiquitin Ligases. *J Virol* **90**:6036-6048.
146. **Hua J, Chen X, Patton JT.** 1994. Deletion mapping of the rotavirus metalloprotein NS53 (NSP1): the conserved cysteine-rich region is essential for virus-specific RNA binding. *J Virol* **68**:3990-4000.
147. **Ikeda K, Inoue S.** 2012. TRIM proteins as RING finger E3 ubiquitin ligases. *Adv Exp Med Biol* **770**:27-37.
148. **Davis KA, Morelli M, Patton JT.** 2017. Rotavirus NSP1 Requires Casein Kinase II-Mediated Phosphorylation for Hijacking of Cullin-RING Ligases. *MBio* **8**.
149. **Tang W, Pavlish OA, Spiegelman VS, Parkhitko AA, Fuchs SY.** 2003. Interaction of Epstein-Barr virus latent membrane protein 1 with SCFHOS/beta-TrCP E3 ubiquitin ligase regulates extent of NF-kappaB activation. *J Biol Chem* **278**:48942-48949.

150. **Bour S, Perrin C, Akari H, Strebel K.** 2001. The human immunodeficiency virus type 1 Vpu protein inhibits NF-kappa B activation by interfering with beta TrCP-mediated degradation of Ikappa B. *J Biol Chem* **276**:15920-15928.
151. **Mansur DS, Maluquer de Motes C, Unterholzner L, Sumner RP, Ferguson BJ, Ren H, Strnadova P, Bowie AG, Smith GL.** 2013. Poxvirus targeting of E3 ligase beta-TrCP by molecular mimicry: a mechanism to inhibit NF-kappaB activation and promote immune evasion and virulence. *PLoS Pathog* **9**:e1003183.
152. **Mangeat B, Gers-Huber G, Lehmann M, Zufferey M, Luban J, Piguet V.** 2009. HIV-1 Vpu neutralizes the antiviral factor Tetherin/BST-2 by binding it and directing its beta-TrCP2-dependent degradation. *PLoS Pathog* **5**:e1000574.
153. **Decorsiere A, Mueller H, van Breugel PC, Abdul F, Gerossier L, Beran RK, Livingston CM, Niu C, Fletcher SP, Hantz O, Strubin M.** 2016. Hepatitis B virus X protein identifies the Smc5/6 complex as a host restriction factor. *Nature* **531**:386-389.
154. **Grove J, Marsh M.** 2011. The cell biology of receptor-mediated virus entry. *J Cell Biol* **195**:1071-1082.
155. **Walsh D, Mohr I.** 2011. Viral subversion of the host protein synthesis machinery. *Nat Rev Microbiol* **9**:860-875.
156. **Garcia-Sastre A.** 2017. Ten Strategies of Interferon Evasion by Viruses. *Cell Host Microbe* **22**:176-184.
157. **Deshaies RJ, Joazeiro CA.** 2009. RING domain E3 ubiquitin ligases. *Annu Rev Biochem* **78**:399-434.

158. **Pickart CM, Eddins MJ.** 2004. Ubiquitin: structures, functions, mechanisms. *Biochim Biophys Acta* **1695**:55-72.
159. **Komander D, Rape M.** 2012. The ubiquitin code. *Annu Rev Biochem* **81**:203-229.
160. **Berndsen CE, Wolberger C.** 2014. New insights into ubiquitin E3 ligase mechanism. *Nat Struct Mol Biol* **21**:301-307.
161. **Huibregtse JM, Scheffner M, Beaudenon S, Howley PM.** 1995. A family of proteins structurally and functionally related to the E6-AP ubiquitin-protein ligase. *Proc Natl Acad Sci U S A* **92**:5249.
162. **Wenzel DM, Klevit RE.** 2012. Following Ariadne's thread: a new perspective on RBR ubiquitin ligases. *BMC Biol* **10**:24.
163. **Petroski MD, Deshaies RJ.** 2005. Function and regulation of cullin-RING ubiquitin ligases. *Nat Rev Mol Cell Biol* **6**:9-20.
164. **Petroski MD, Deshaies RJ.** 2005. In vitro reconstitution of SCF substrate ubiquitination with purified proteins. *Methods Enzymol* **398**:143-158.
165. **Skaar JR, Pagan JK, Pagano M.** 2013. Mechanisms and function of substrate recruitment by F-box proteins. *Nat Rev Mol Cell Biol* **14**:369-381.
166. **Furukawa M, He YJ, Borchers C, Xiong Y.** 2003. Targeting of protein ubiquitination by BTB-Cullin 3-Roc1 ubiquitin ligases. *Nat Cell Biol* **5**:1001-1007.
167. **Kamura T, Maenaka K, Kotshiba S, Matsumoto M, Kohda D, Conaway RC, Conaway JW, Nakayama KI.** 2004. VHL-box and SOCS-box domains

- determine binding specificity for Cul2-Rbx1 and Cul5-Rbx2 modules of ubiquitin ligases. *Genes Dev* **18**:3055-3065.
168. **Yen HC, Elledge SJ.** 2008. Identification of SCF ubiquitin ligase substrates by global protein stability profiling. *Science* **322**:923-929.
169. **Pan ZQ, Kentsis A, Dias DC, Yamoah K, Wu K.** 2004. Nedd8 on cullin: building an expressway to protein destruction. *Oncogene* **23**:1985-1997.
170. **Hao B, Oehlmann S, Sowa ME, Harper JW, Pavletich NP.** 2007. Structure of a Fbw7-Skp1-cyclin E complex: multisite-phosphorylated substrate recognition by SCF ubiquitin ligases. *Mol Cell* **26**:131-143.
171. **Wu G, Xu G, Schulman BA, Jeffrey PD, Harper JW, Pavletich NP.** 2003. Structure of a beta-TrCP1-Skp1-beta-catenin complex: destruction motif binding and lysine specificity of the SCF(beta-TrCP1) ubiquitin ligase. *Mol Cell* **11**:1445-1456.
172. **Lyapina S, Cope G, Shevchenko A, Serino G, Tsuge T, Zhou C, Wolf DA, Wei N, Shevchenko A, Deshaies RJ.** 2001. Promotion of NEDD-CUL1 conjugate cleavage by COP9 signalosome. *Science* **292**:1382-1385.
173. **Wu S, Zhu W, Nhan T, Toth JI, Petroski MD, Wolf DA.** 2013. CAND1 controls in vivo dynamics of the cullin 1-RING ubiquitin ligase repertoire. *Nat Commun* **4**:1642.
174. **Pierce NW, Lee JE, Liu X, Sweredoski MJ, Graham RL, Larimore EA, Rome M, Zheng N, Clurman BE, Hess S, Shan SO, Deshaies RJ.** 2013. Cand1 promotes assembly of new SCF complexes through dynamic exchange of F box proteins. *Cell* **153**:206-215.

175. **Merlet J, Burger J, Gomes JE, Pintard L.** 2009. Regulation of cullin-RING E3 ubiquitin-ligases by neddylation and dimerization. *Cell Mol Life Sci* **66**:1924-1938.
176. **Mahon C, Krogan NJ, Craik CS, Pick E.** 2014. Cullin E3 ligases and their rewiring by viral factors. *Biomolecules* **4**:897-930.
177. **Hartmann T, Xu X, Kronast M, Muehlich S, Meyer K, Zimmermann W, Hurwitz J, Pan ZQ, Engelhardt S, Sarikas A.** 2014. Inhibition of Cullin-RING E3 ubiquitin ligase 7 by simian virus 40 large T antigen. *Proc Natl Acad Sci U S A* **111**:3371-3376.
178. **Pazhouhandeh M, Dieterle M, Marrocco K, Lechner E, Berry B, Brault V, Hemmer O, Kretsch T, Richards KE, Genschik P, Ziegler-Graff V.** 2006. F-box-like domain in the poliovirus protein P0 is required for silencing suppressor function. *Proc Natl Acad Sci U S A* **103**:1994-1999.
179. **Hinz M, Arslan SC, Scheidereit C.** 2012. It takes two to tango: IkappaBs, the multifunctional partners of NF-kappaB. *Immunol Rev* **246**:59-76.
180. **Kanarek N, Ben-Neriah Y.** 2012. Regulation of NF-kappaB by ubiquitination and degradation of the IkappaBs. *Immunol Rev* **246**:77-94.
181. **Spencer E, Jiang J, Chen ZJ.** 1999. Signal-induced ubiquitination of IkappaBalpha by the F-box protein Slimb/beta-TrCP. *Genes Dev* **13**:284-294.
182. **Hoffmann A, Natoli G, Ghosh G.** 2006. Transcriptional regulation via the NF-kappaB signaling module. *Oncogene* **25**:6706-6716.
183. **Kainulainen M, Lau S, Samuel CE, Hornung V, Weber F.** 2016. NSs Virulence Factor of Rift Valley Fever Virus Engages the F-Box Proteins

- FBXW11 and beta-TRCP1 To Degrade the Antiviral Protein Kinase PKR. *J Virol* **90**:6140-6147.
184. **Xia C, Vijayan M, Pritzl CJ, Fuchs SY, McDermott AB, Hahm B.** 2015. Hemagglutinin of Influenza A Virus Antagonizes Type I Interferon (IFN) Responses by Inducing Degradation of Type I IFN Receptor 1. *J Virol* **90**:2403-2417.
185. **Margottin F, Bour SP, Durand H, Selig L, Benichou S, Richard V, Thomas D, Strebel K, Benarous R.** 1998. A novel human WD protein, h-beta TrCp, that interacts with HIV-1 Vpu connects CD4 to the ER degradation pathway through an F-box motif. *Mol Cell* **1**:565-574.
186. **Sugden SM, Pham TN, Cohen EA.** 2017. HIV-1 Vpu Downmodulates ICAM-1 Expression, Resulting in Decreased Killing of Infected CD4⁺ T Cells by NK Cells. *J Virol* **91**.
187. **Willey RL, Maldarelli F, Martin MA, Strebel K.** 1992. Human immunodeficiency virus type 1 Vpu protein induces rapid degradation of CD4. *J Virol* **66**:7193-7200.
188. **Lama J, Mangasarian A, Trono D.** 1999. Cell-surface expression of CD4 reduces HIV-1 infectivity by blocking Env incorporation in a Nef- and Vpu-inhibitable manner. *Curr Biol* **9**:622-631.
189. **Pham TN, Lukhele S, Hajjar F, Routy JP, Cohen EA.** 2014. HIV Nef and Vpu protect HIV-infected CD4⁺ T cells from antibody-mediated cell lysis through down-modulation of CD4 and BST2. *Retrovirology* **11**:15.

190. **Weiss A, Littman DR.** 1994. Signal transduction by lymphocyte antigen receptors. *Cell* **76**:263-274.
191. **Levesque K, Zhao YS, Cohen EA.** 2003. Vpu exerts a positive effect on HIV-1 infectivity by down-modulating CD4 receptor molecules at the surface of HIV-1-producing cells. *J Biol Chem* **278**:28346-28353.
192. **Desimmie BA, Smith JL, Matsuo H, Hu WS, Pathak VK.** 2017. Identification of a tripartite interaction between the N-terminus of HIV-1 Vif and CBFbeta that is critical for Vif function. *Retrovirology* **14**:19.
193. **Guo Y, Dong L, Qiu X, Wang Y, Zhang B, Liu H, Yu Y, Zang Y, Yang M, Huang Z.** 2014. Structural basis for hijacking CBF-beta and CUL5 E3 ligase complex by HIV-1 Vif. *Nature* **505**:229-233.
194. **Stanley DJ, Bartholomeeusen K, Crosby DC, Kim DY, Kwon E, Yen L, Cartozo NC, Li M, Jager S, Mason-Herr J, Hayashi F, Yokoyama S, Krogan NJ, Harris RS, Peterlin BM, Gross JD.** 2012. Inhibition of a NEDD8 Cascade Restores Restriction of HIV by APOBEC3G. *PLoS Pathog* **8**:e1003085.
195. **Kirui J, Mondal A, Mehle A.** 2016. Ubiquitination up-regulates influenza virus polymerase function. *J Virol* doi:10.1128/JVI.01829-16.
196. **Su WC, Chen YC, Tseng CH, Hsu PW, Tung KF, Jeng KS, Lai MM.** 2013. Pooled RNAi screen identifies ubiquitin ligase Itch as crucial for influenza A virus release from the endosome during virus entry. *Proc Natl Acad Sci U S A* **110**:17516-17521.

197. **Desai TM, Marin M, Chin CR, Savidis G, Brass AL, Melikyan GB.** 2014. IFITM3 restricts influenza A virus entry by blocking the formation of fusion pores following virus-endosome hemifusion. *PLoS Pathog* **10**:e1004048.
198. **Huotari J, Meyer-Schaller N, Hubner M, Stauffer S, Katheder N, Horvath P, Mancini R, Helenius A, Peter M.** 2012. Cullin-3 regulates late endosome maturation. *Proc Natl Acad Sci U S A* **109**:823-828.
199. **Schrofelbauer B, Hakata Y, Landau NR.** 2007. HIV-1 Vpr function is mediated by interaction with the damage-specific DNA-binding protein DDB1. *Proc Natl Acad Sci U S A* **104**:4130-4135.
200. **Romani B, Baygloo NS, Hamidi-Fard M, Aghasadeghi MR, Allahbakhshi E.** 2016. HIV-1 Vpr Protein Induces Proteasomal Degradation of Chromatin-associated Class I HDACs to Overcome Latent Infection of Macrophages. *J Biol Chem* **291**:2696-2711.
201. **Ahn J, Vu T, Novince Z, Guerrero-Santoro J, Ropic-Otrin V, Gronenborn AM.** 2010. HIV-1 Vpr loads uracil DNA glycosylase-2 onto DCAF1, a substrate recognition subunit of a cullin 4A-ring E3 ubiquitin ligase for proteasome-dependent degradation. *J Biol Chem* **285**:37333-37341.
202. **Wu Y, Zhou X, Barnes CO, DeLucia M, Cohen AE, Gronenborn AM, Ahn J, Calero G.** 2016. The DDB1-DCAF1-Vpr-UNG2 crystal structure reveals how HIV-1 Vpr steers human UNG2 toward destruction. *Nat Struct Mol Biol* **23**:933-940.

203. **Hofmann H, Logue EC, Bloch N, Daddacha W, Polsky SB, Schultz ML, Kim B, Landau NR.** 2012. The Vpx lentiviral accessory protein targets SAMHD1 for degradation in the nucleus. *J Virol* **86**:12552-12560.
204. **Sharifi HJ, Furuya AK, Jellinger RM, Nekorchuk MD, de Noronha CM.** 2014. Cullin4A and cullin4B are interchangeable for HIV Vpr and Vpx action through the CRL4 ubiquitin ligase complex. *J Virol* **88**:6944-6958.
205. **Soucy TA, Smith PG, Milhollen MA, Berger AJ, Gavin JM, Adhikari S, Brownell JE, Burke KE, Cardin DP, Critchley S, Cullis CA, Doucette A, Garnsey JJ, Gaulin JL, Gershman RE, Lublinsky AR, McDonald A, Mizutani H, Narayanan U, Olhava EJ, Peluso S, Rezaei M, Sintchak MD, Talreja T, Thomas MP, Traore T, Vyskocil S, Weatherhead GS, Yu J, Zhang J, Dick LR, Claiborne CF, Rolfe M, Bolen JB, Langston SP.** 2009. An inhibitor of NEDD8-activating enzyme as a new approach to treat cancer. *Nature* **458**:732-736.
206. **Lo SC, Hannink M.** 2006. CAND1-mediated substrate adaptor recycling is required for efficient repression of Nrf2 by Keap1. *Mol Cell Biol* **26**:1235-1244.
207. **Schmidt MW, McQuary PR, Wee S, Hofmann K, Wolf DA.** 2009. F-box-directed CRL complex assembly and regulation by the CSN and CAND1. *Mol Cell* **35**:586-597.
208. **Goldenberg SJ, Cascio TC, Shumway SD, Garbutt KC, Liu J, Xiong Y, Zheng N.** 2004. Structure of the Cand1-Cul1-Roc1 complex reveals regulatory mechanisms for the assembly of the multisubunit cullin-dependent ubiquitin ligases. *Cell* **119**:517-528.

209. **Kawakami T, Chiba T, Suzuki T, Iwai K, Yamanaka K, Minato N, Suzuki H, Shimbara N, Hidaka Y, Osaka F, Omata M, Tanaka K.** 2001. NEDD8 recruits E2-ubiquitin to SCF E3 ligase. *EMBO J* **20**:4003-4012.
210. **Sakata E, Yamaguchi Y, Miyauchi Y, Iwai K, Chiba T, Saeki Y, Matsuda N, Tanaka K, Kato K.** 2007. Direct interactions between NEDD8 and ubiquitin E2 conjugating enzymes upregulate cullin-based E3 ligase activity. *Nat Struct Mol Biol* **14**:167-168.
211. **Bornstein G, Ganoth D, Hershko A.** 2006. Regulation of neddylation and deneddylation of cullin1 in SCFSkp2 ubiquitin ligase by F-box protein and substrate. *Proc Natl Acad Sci U S A* **103**:11515-11520.
212. **Zhao B, Shu C, Gao X, Sankaran B, Du F, Shelton CL, Herr AB, Ji JY, Li P.** 2016. Structural basis for concerted recruitment and activation of IRF-3 by innate immune adaptor proteins. *Proc Natl Acad Sci U S A* **113**:E3403-3412.
213. **Ramirez PW, DePaula-Silva AB, Szaniawski M, Barker E, Bosque A, Planelles V.** 2015. HIV-1 Vpu utilizes both cullin-RING ligase (CRL) dependent and independent mechanisms to downmodulate host proteins. *Retrovirology* **12**:65.
214. **Sugden SM, Bego MG, Pham TN, Cohen EA.** 2016. Remodeling of the Host Cell Plasma Membrane by HIV-1 Nef and Vpu: A Strategy to Ensure Viral Fitness and Persistence. *Viruses* **8**:67.
215. **Matheson NJ, Sumner J, Wals K, Rapiteanu R, Weekes MP, Vigan R, Weinelt J, Schindler M, Antrobus R, Costa AS, Frezza C, Clish CB, Neil SJ, Lehner PJ.** 2015. Cell Surface Proteomic Map of HIV Infection Reveals

- Antagonism of Amino Acid Metabolism by Vpu and Nef. *Cell Host Microbe* **18**:409-423.
216. **Kainulainen M, Habjan M, Hubel P, Busch L, Lau S, Colinge J, Superti-Furga G, Pichlmair A, Weber F.** 2014. Virulence factor NSs of rift valley fever virus recruits the F-box protein FBXO3 to degrade subunit p62 of general transcription factor TFIIH. *J Virol* **88**:3464-3473.
217. **Tao T, Zhou CJ, Wang Q, Chen XR, Sun Q, Zhao TY, Ye JC, Wang Y, Zhang ZY, Zhang YL, Guo ZJ, Wang XB, Li DW, Yu JL, Han CG.** 2017. Rice black streaked dwarf virus P7-2 forms a SCF complex through binding to *Oryza sativa* SKP1-like proteins, and interacts with GID2 involved in the gibberellin pathway. *PLoS One* **12**:e0177518.
218. **Mukai R, Ohshima T.** 2016. Enhanced Stabilization of MCL1 by the Human T-Cell Leukemia Virus Type 1 bZIP Factor Is Modulated by Blocking the Recruitment of Cullin 1 to the SCF Complex. *Mol Cell Biol* **36**:3075-3085.
219. **Gilson T, Blanchette P, Ballmann MZ, Papp T, Penzes JJ, Benko M, Harrach B, Branton PE.** 2016. Using the E4orf6-Based E3 Ubiquitin Ligase as a Tool To Analyze the Evolution of Adenoviruses. *J Virol* **90**:7350-7367.
220. **Lechner E, Achard P, Vansiri A, Potuschak T, Genschik P.** 2006. F-box proteins everywhere. *Curr Opin Plant Biol* **9**:631-638.
221. **Arnold M, Patton JT, McDonald SM.** 2009. Culturing, storage, and quantification of rotaviruses. *Curr Protoc Microbiol* **Chapter 15**:Unit 15C 13.
222. **Mahbub Alam M, Kobayashi N, Ishino M, Naik TN, Taniguchi K.** 2006. Analysis of genetic factors related to preferential selection of the NSP1 gene

- segment observed in mixed infection and multiple passage of rotaviruses. *Arch Virol* **151**:2149-2159.
223. **Alkalay I, Yaron A, Hatzubai A, Orian A, Ciechanover A, Ben-Neriah Y.** 1995. Stimulation-dependent I kappa B alpha phosphorylation marks the NF-kappa B inhibitor for degradation via the ubiquitin-proteasome pathway. *Proc Natl Acad Sci U S A* **92**:10599-10603.
224. **Dinkel H, Van Roey K, Michael S, Kumar M, Uyar B, Altenberg B, Milchevskaya V, Schneider M, Kuhn H, Behrendt A, Dahl SL, Damerell V, Diebel S, Kalman S, Klein S, Knudsen AC, Mader C, Merrill S, Staudt A, Thiel V, Welti L, Davey NE, Diella F, Gibson TJ.** 2016. ELM 2016--data update and new functionality of the eukaryotic linear motif resource. *Nucleic Acids Res* **44**:D294-300.
225. **Flotow H, Graves PR, Wang AQ, Fiol CJ, Roeske RW, Roach PJ.** 1990. Phosphate groups as substrate determinants for casein kinase I action. *J Biol Chem* **265**:14264-14269.
226. **Meggio F, Pinna LA.** 2003. One-thousand-and-one substrates of protein kinase CK2? *FASEB J* **17**:349-368.
227. **Pinna LA, Ruzzene M.** 1996. How do protein kinases recognize their substrates? *Biochim Biophys Acta* **1314**:191-225.
228. **Sarno S, Reddy H, Meggio F, Ruzzene M, Davies SP, Donella-Deana A, Shugar D, Pinna LA.** 2001. Selectivity of 4,5,6,7-tetrabromobenzotriazole, an ATP site-directed inhibitor of protein kinase CK2 ('casein kinase-2'). *FEBS Lett* **496**:44-48.

229. **Soucy TA, Smith PG, Rolfe M.** 2009. Targeting NEDD8-activated cullin-RING ligases for the treatment of cancer. *Clin Cancer Res* **15**:3912-3916.
230. **Litchfield DW.** 2003. Protein kinase CK2: structure, regulation and role in cellular decisions of life and death. *Biochem J* **369**:1-15.
231. **Uhle S, Medalia O, Waldron R, Dumdey R, Henklein P, Bech-Otschir D, Huang X, Berse M, Sperling J, Schade R, Dubiel W.** 2003. Protein kinase CK2 and protein kinase D are associated with the COP9 signalosome. *EMBO J* **22**:1302-1312.
232. **Wei N, Deng XW.** 2003. The COP9 signalosome. *Annu Rev Cell Dev Biol* **19**:261-286.
233. **Niefind K, Guerra B, Ermakowa I, Issinger OG.** 2001. Crystal structure of human protein kinase CK2: insights into basic properties of the CK2 holoenzyme. *EMBO J* **20**:5320-5331.
234. **Mitchell DB, Both GW.** 1990. Conservation of a potential metal binding motif despite extensive sequence diversity in the rotavirus nonstructural protein NS53. *Virology* **174**:618-621.
235. **Bremont M, Chabanne-Vautherot D, Vannier P, McCrae MA, Cohen J.** 1990. Sequence analysis of the gene (6) encoding the major capsid protein (VP6) of group C rotavirus: higher than expected homology to the corresponding protein from group A virus. *Virology* **178**:579-583.
236. **Brottier P, Nandi P, Bremont M, Cohen J.** 1992. Bovine rotavirus segment 5 protein expressed in the baculovirus system interacts with zinc and RNA. *J Gen Virol* **73 (Pt 8)**:1931-1938.

237. **Liu S, Cai X, Wu J, Cong Q, Chen X, Li T, Du F, Ren J, Wu YT, Grishin NV, Chen ZJ.** 2015. Phosphorylation of innate immune adaptor proteins MAVS, STING, and TRIF induces IRF3 activation. *Science* **347**:aaa2630.
238. **Nilsson M, Svenungsson B, Hedlund KO, Uhnöo I, Lagergren A, Akre T, Svensson L.** 2000. Incidence and genetic diversity of group C rotavirus among adults. *J Infect Dis* **182**:678-684.
239. **Dhama K, Saminathan M, Karthik K, Tiwari R, Shabbir MZ, Kumar N, Malik YS, Singh RK.** 2015. Avian rotavirus enteritis - an updated review. *Vet Q* **35**:142-158.
240. **Niira K, Ito M, Masuda T, Saitou T, Abe T, Komoto S, Sato M, Yamasato H, Kishimoto M, Naoi Y, Sano K, Tuchiaka S, Okada T, Omatsu T, Furuya T, Aoki H, Katayama Y, Oba M, Shirai J, Taniguchi K, Mizutani T, Nagai M.** 2016. Whole genome sequences of Japanese porcine species C rotaviruses reveal a high diversity of genotypes of individual genes and will contribute to a comprehensive, generally accepted classification system. *Infect Genet Evol* **44**:106-113.
241. **Phan TG, Vo NP, Boros A, Pankovics P, Reuter G, Li OT, Wang C, Deng X, Poon LL, Delwart E.** 2013. The viruses of wild pigeon droppings. *PLoS One* **8**:e72787.
242. **Trojanar E, Otto P, Johne R.** 2009. The first complete genome sequence of a chicken group A rotavirus indicates independent evolution of mammalian and avian strains. *Virology* **386**:325-333.

243. **Hua J, Mansell EA, Patton JT.** 1993. Comparative analysis of the rotavirus NS53 gene: conservation of basic and cysteine-rich regions in the protein and possible stem-loop structures in the RNA. *Virology* **196**:372-378.
244. **Kapikian AZ, Hoshino Y, Chanock RM, Perez-Schael I.** 1996. Jennerian and modified Jennerian approach to vaccination against rotavirus diarrhea using a quadrivalent rhesus rotavirus (RRV) and human-RRV reassortant vaccine. *Arch Virol Suppl* **12**:163-175.
245. **Fink K, Grandvaux N.** 2013. STAT2 and IRF9: Beyond ISGF3. *JAKSTAT* **2**:e27521.
246. **Holloway G, Dang VT, Jans DA, Coulson BS.** 2014. Rotavirus inhibits IFN-induced STAT nuclear translocation by a mechanism that acts after STAT binding to importin-alpha. *J Gen Virol* **95**:1723-1733.
247. **Barber MR, Aldridge JR, Jr., Webster RG, Magor KE.** 2010. Association of RIG-I with innate immunity of ducks to influenza. *Proc Natl Acad Sci U S A* **107**:5913-5918.
248. **Fuchs SY, Spiegelman VS, Kumar KG.** 2004. The many faces of beta-TrCP E3 ubiquitin ligases: reflections in the magic mirror of cancer. *Oncogene* **23**:2028-2036.
249. **Lau AW, Fukushima H, Wei W.** 2012. The Fbw7 and betaTRCP E3 ubiquitin ligases and their roles in tumorigenesis. *Front Biosci (Landmark Ed)* **17**:2197-2212.

250. **Seo E, Kim H, Kim R, Yun S, Kim M, Han JK, Costantini F, Jho EH.** 2009. Multiple isoforms of beta-TrCP display differential activities in the regulation of Wnt signaling. *Cell Signal* **21**:43-51.
251. **Ohsaki K, Oishi K, Kozono Y, Nakayama K, Nakayama KI, Ishida N.** 2008. The role of {beta}-TrCP1 and {beta}-TrCP2 in circadian rhythm generation by mediating degradation of clock protein PER2. *J Biochem* **144**:609-618.
252. **Putters J, Slotman JA, Gerlach JP, Strous GJ.** 2011. Specificity, location and function of betaTrCP isoforms and their splice variants. *Cell Signal* **23**:641-647.
253. **Cuadrado A.** 2015. Structural and functional characterization of Nrf2 degradation by glycogen synthase kinase 3/beta-TrCP. *Free Radic Biol Med* **88**:147-157.
254. **Meyer L, Deau B, Forejtnikova H, Dumenil D, Margottin-Goguet F, Lacombe C, Mayeux P, Verdier F.** 2007. beta-Trcp mediates ubiquitination and degradation of the erythropoietin receptor and controls cell proliferation. *Blood* **109**:5215-5222.
255. **Cheng Y, Gao WW, Tang HM, Deng JJ, Wong CM, Chan CP, Jin DY.** 2016. beta-TrCP-mediated ubiquitination and degradation of liver-enriched transcription factor CREB-H. *Sci Rep* **6**:23938.
256. **Wang Z, Zhong J, Gao D, Inuzuka H, Liu P, Wei W.** 2012. DEPTOR ubiquitination and destruction by SCF(beta-TrCP). *Am J Physiol Endocrinol Metab* **303**:E163-169.
257. **Catena V, Fanciulli M.** 2017. Deptor: not only a mTOR inhibitor. *J Exp Clin Cancer Res* **36**:12.

258. **Peterson TR, Laplante M, Thoreen CC, Sancak Y, Kang SA, Kuehl WM, Gray NS, Sabatini DM.** 2009. DEPTOR is an mTOR inhibitor frequently overexpressed in multiple myeloma cells and required for their survival. *Cell* **137**:873-886.
259. **Vivanco I, Sawyers CL.** 2002. The phosphatidylinositol 3-Kinase AKT pathway in human cancer. *Nat Rev Cancer* **2**:489-501.
260. **Zhang H, Chen J, Zeng Z, Que W, Zhou L.** 2013. Knockdown of DEPTOR induces apoptosis, increases chemosensitivity to doxorubicin and suppresses autophagy in RPMI-8226 human multiple myeloma cells in vitro. *Int J Mol Med* **31**:1127-1134.
261. **Vadlakonda L, Dash A, Pasupuleti M, Anil Kumar K, Reddanna P.** 2013. The Paradox of Akt-mTOR Interactions. *Front Oncol* **3**:165.
262. **Breuleux M, Klopfenstein M, Stephan C, Doughty CA, Barys L, Maira SM, Kwiatkowski D, Lane HA.** 2009. Increased AKT S473 phosphorylation after mTORC1 inhibition is rictor dependent and does not predict tumor cell response to PI3K/mTOR inhibition. *Mol Cancer Ther* **8**:742-753.
263. **Weidberg H, Elazar Z.** 2011. TBK1 mediates crosstalk between the innate immune response and autophagy. *Sci Signal* **4**:pe39.
264. **Datan E, Shirazian A, Benjamin S, Matassov D, Tinari A, Malorni W, Lockshin RA, Garcia-Sastre A, Zakeri Z.** 2014. mTOR/p70S6K signaling distinguishes routine, maintenance-level autophagy from autophagic cell death during influenza A infection. *Virology* **452-453**:175-190.

265. **Yin Y, Dang W, Zhou X, Xu L, Wang W, Cao W, Chen S, Su J, Cai X, Xiao S, Peppelenbosch MP, Pan Q.** 2017. PI3K-Akt-mTOR axis sustains rotavirus infection via the 4E-BP1 mediated autophagy pathway and represents an antiviral target. *Virulence* doi:10.1080/21505594.2017.1326443:1-16.
266. **Yazdi S, Naumann M, Stein M.** 2017. Double phosphorylation-induced structural changes in the signal-receiving domain of IkappaBalpha in complex with NF-kappaB. *Proteins* **85**:17-29.
267. **Hayes JD, Chowdhry S, Dinkova-Kostova AT, Sutherland C.** 2015. Dual regulation of transcription factor Nrf2 by Keap1 and by the combined actions of beta-TrCP and GSK-3. *Biochem Soc Trans* **43**:611-620.
268. **Zhou Z, Xu C, Chen P, Liu C, Pang S, Yao X, Zhang Q.** 2015. Stability of HIB-Cul3 E3 ligase adaptor HIB Is Regulated by Self-degradation and Availability of Its Substrates. *Sci Rep* **5**:12709.
269. **Galan JM, Peter M.** 1999. Ubiquitin-dependent degradation of multiple F-box proteins by an autocatalytic mechanism. *Proc Natl Acad Sci U S A* **96**:9124-9129.
270. **Okada AK, Teranishi K, Lobo F, Isas JM, Xiao J, Yen K, Cohen P, Langen R.** 2017. The Mitochondrial-Derived Peptides, HumaninS14G and Small Humanin-like Peptide 2, Exhibit Chaperone-like Activity. *Sci Rep* **7**:7802.

Appendix. Evidence of NSP1 or β -TrCP ubiquitination

Introduction

Cullin-RING ligases (CRLs) are subject to multiple levels of regulation, including localization and availability of substrates or other key components. One role of cullin-associated and neddylation dissociated 1 (Cand1) is to act as an exchange factor for adaptor proteins that allows assembly processes to bias towards adaptors for which substrates are available (174). Once adaptors have integrated into formed CRLs, however, their stability is highly dependent on the availability of substrates (268, 269). F-box adaptor proteins, in particular, appear to be an unstable protein population and readily undergo autophosphorylation when assembled onto CRLs. The HIB adaptor protein of Cul3 CRLs, for example, rapidly auto-ubiquitinates when substrates are in short supply (268).

The rotavirus protein NSP1 likely acts to facilitate degradation of host antiviral proteins by acting as a substrate adaptor protein of Cul3 CRLs (148). While several studies support a role for NSP1 as a member of a cellular CRL (144, 145, 270), many of these data are based upon interpretation of co-immunoprecipitation experiments. NSP1 cannot be easily purified, so *in vitro* analyses of this proteins behavior are difficult to perform. However, if indeed NSP1 behaves as an adaptor subunit of a hijacked CRL, there may be evidence of ubiquitination of the protein, as is observed as the cell regulates adaptor subunits of CRLs. To this end, we sought to evaluate the ubiquitination status of NSP1 proteins by several techniques, both in the context of infected cells and for exogenously expressed proteins.

Materials and methods

Cells and viruses. Human colorectal HT29 cells were grown in McCoy's 5A (modified) medium containing 10% fetal bovine serum (FBS) (Gibco) and penicillin-streptomycin. Rotaviruses were propagated and titered by plaque assay on MA104 cells as described by Arnold et al (221). Prior to infection, rotaviruses were activated by treatment with 5 μ g per ml of porcine pancreas trypsin (type IX-S; Sigma-Aldrich) for 1 h at 37°C.

Antibodies. Rabbit polyclonal antibodies to porcine OSU NSP1 protein (137) and PCNA (Santa Cruz Biotech [SCB], sc-7907), rabbit monoclonal antibody to β -TrCP (Cell Signaling Technology [CST], #11984S), and mouse monoclonal antibodies to I κ B (CST, #4814) and p-I κ B (CST, #9246) were used at 1:5,000 dilution. HRP-conjugated goat anti-rabbit IgG antibody (CST, #7074) and horse anti-mouse IgG antibody (CST, #7076) were used at 1:10,000 dilution.

Inhibitors. The protein kinase CKII inhibitor, 4,5,6,7-tetrabromobenzotriazole (TBB) (Tocris Bioscience) was prepared as 1 mM stocks in dimethyl sulfoxide (DMSO) and stored at -20°C. TBB was diluted in cell culture medium to a final concentration of 80 μ M prior to use. MG132 (Sigma) was dissolved in DMSO and diluted in media to a final concentration of 15 μ M.

Viral infection. Nearly confluent monolayers of HT29 cells in 10 cm² tissue-culture dishes were infected at an MOI of 5 with trypsin-activated rotavirus. After a one-hour adsorption incubation, the inoculum was removed and cells were rinsed with PBS. Cell

monolayers were then maintained in serum-free McCoy's 5A (modified) medium until specified time of harvest. Lysates were prepared by washing monolayers with cold PBS and scraping cells into 0.5 ml RIPA lysis buffer. Lysates were incubated on ice for 10 min, gently mixed, and clarified by centrifugation for 10 min at 15,000 x g at 4°C.

Immunoblot assay. Protein samples were mixed with NuPAGE LDS sample buffer (Invitrogen) containing 50 mM dithiothreitol (DTT), denatured by heating to 70°C for 10 min, and resolved by electrophoresis on pre-cast 10% Tris-glycine polyacrylamide gels (Novex). Molecular weight ladders (SeeBlue Plus2, Invitrogen) were resolved in parallel. Proteins were transferred from gels onto nitrocellulose membranes via the iBlot dry transfer apparatus (ThermoFisher) according to the manufacturer's protocol. Membranes were blocked by incubation in 5% Carnation dry milk in PBS-0.2% Tween-20 (PBST) prior to incubation with primary antibody diluted in milk-PBST. Membranes were washed with PBST before incubation with HRP-conjugated secondary antibody in milk-PBST. Membranes were washed with PBST and developed using Super Signal West Pico chemiluminescent substrate (Pierce). Signal was detected by exposing membranes to BioExcell X-ray film.

Immunoprecipitation. Nearly confluent monolayers of HT29 cells in 10-cm² dishes were infected as described above. At 4 h p.t., cells were treated with MG132 or DMSO. At 8 h p.t., cells were scraped, rinsed twice in PBS, and disrupted by resuspension in IP lysis buffer (150 mM NaCl, 50 mM Tris-HCl, pH 7.4, 1% Triton X-100, with 1× Complete EDTA-free protease inhibitor cocktail). After incubation on ice for 1 h, cellular

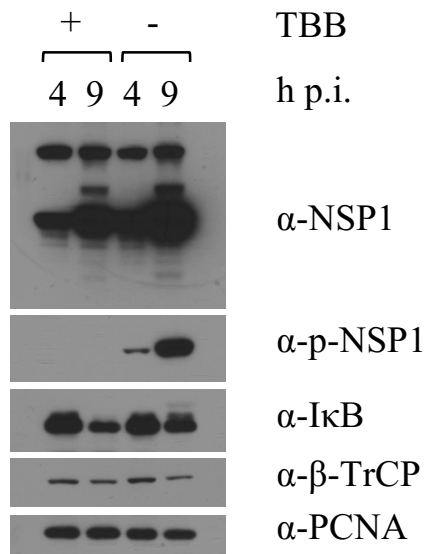


Figure A-1. Long exposure of immunoblot for proteins in infected cell lysate, including high molecular weight NSP1. Adapted from Davis, et al. (148). HT29 cells infected with OSU at an MOI of 5, were treated with TBB or DMSO at 2 h p.i. At 4 and 9 h p.i., cells were collected and lysed, and proteins were resolved by electrophoresis and examined by immunoblot assay. Altered cropping of the top panel reveals a high molecular weight bound by anti-NSP1 antibody at 9 h p.i., both in the presence and absence of TBB.

debris were removed by centrifugation at 14,000 x g for 10 min. Clarified lysates were incubated with primary antibody overnight at 4°C with nutation. Fifty µl of a slurry of protein A/G magnetic beads (Pierce) were pre-rinsed 3-times with IP wash buffer (150 mM NaCl, 50 mM Tris-HCl, pH 7.4), and added to clarified cell lysates. After 2 h incubation at 25°C with nutation, beads were recovered using a BioRad Surebeads magnetic stand and rinsed 3 times with IP wash buffer. Protein was released from beads by nutation in IP elution buffer (0.1 M glycine, pH 3.0) for 5 min at 4°C. Eluted proteins were analyzed by gel electrophoresis and immunoblot analysis.

Results and discussion

In our assessment of NSP1 activity and the reliance of this protein on CKII modification in order to engage substrates, we examined NSP1 accumulation in OSU infected cells. By western blot, NSP1 levels increase from 4 to 9 h p.i. (Fig A-1). Interestingly, immunoblotting with anti-OSU NSP1 primary antibody revealed an expected band at 56 kDa, as well as a higher molecular weight band that only appeared late in infection when blots were extensively exposed to film. The high molecular weight band appeared both in the presence and absence of TBB. This result suggests that OSU NSP1 acquires a modification late in infection and is not dependent on NSP1 interaction with substrate proteins.

To assess whether the suggested NSP1 modification was ubiquitination, we infected HT29 cells with OSU rotavirus, and treated infected cells with MG132. Immunoprecipitation experiments were the performed by recovering β-TrCP and bound complexes from infected cell lysates using anti-β-TrCP antibodies bound to magnetic

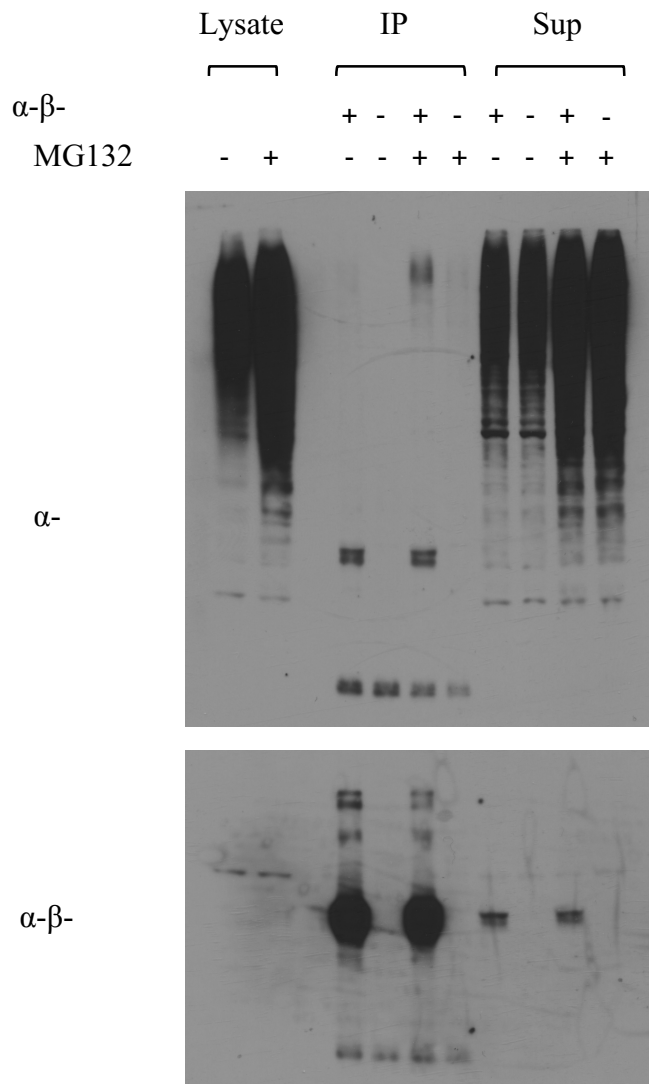


Figure A-2. Detection of ubiquitinated substrates in complex with β -TrCP. OSU-infected HT29 cells were lysed and immunoprecipitated with anti- β -TrCP antibody bound to magnetic beads. Control experiments were done in the absence of β -TrCP antibody. Whole cell lysates, immunoprecipitant (IP) fractions, and supernatant (Sup) fractions were assessed in parallel by immunoblot using anti-ubiquitin (Ub) or anti- β -TrCP antibodies.

beads (Fig. A-2). As a control, primary antibody was omitted from some samples. Whole cell lysates, immunoprecipitant (IP) fractions, and supernatant fractions were resolved by electrophoresis and transferred to nitrocellulose membranes for immunoblot analysis. Membranes were then probed for ubiquitin or for β -TrCP. Anti-ubiquitin blots show a strong band at approximately 56 kDa in IP fractions. A high molecular weight band can be seen in the IP fraction from MG132-treated samples, suggesting polyubiquitination. Whole cell lysates as well as supernatant fractions show large high molecular weight smears. Blots probed for β -TrCP indicate a strong band of approximately 56 kDa in IP fractions as well as in supernatant fractions.

Because β -TrCP and NSP1 form complexes with one another during infection, and because these proteins are comparable in size, the band appearing in anti-ubiquitin probed IP samples could represent either protein. However, while no shift is observable in anti- β -TrCP immunoblots of infected cell lysates, a high molecular weight band is observed when probed with anti-OSU NSP1 antibodies. Together, this data suggests that NSP1 may auto-ubiquitinate in a fashion that is known to be characteristic of cellular CRL substrate proteins.

Curriculum Vitae
Kaitlin A. Davis

Education:

- 2007-2011: B.S., Neuroscience
University of California, Los Angeles (UCLA); Los Angeles, CA, USA
- 2012-2017: PhD, Biology
Program in Cell, Molecular, Developmental Biology, and Biophysics
NIH/Johns Hopkins Graduate Partnership Program
Johns Hopkins University; Baltimore, MD, USA

Experience:

- 2006-2010: Undergraduate Research Assistant/Intern
Lawrence Berkeley National Laboratory; Emeryville, CA (2006-2007)
Mentors: Drs. John Dueber, Chris Anderson, Jay Keasling
Focus: Addressable bacterial communication via conjugation
UCLA Brain Research Institute, Neurotrauma Lab; Los Angeles, CA
(2007-2009)
Mentors: Drs. Neil Harris and David Hovda
Focus: Recovery and neuroplasticity following traumatic brain
injury
KineMed, Inc.; Emeryville, CA (2008)
Mentor: Dr. Shubha Shankaran
Focus: Neural plasticity following chronic antidepressant drug
therapies
NIH/NIAID, Prion Biochemistry Section, Laboratory of Persistent Viral
Diseases; Hamilton, MT (2009)
Mentor: Dr. Byron Caughey
Focus: Determinants of *in vitro* conversion of recombinant prion
protein
UCLA Laboratory of Neuroendocrinology; Los Angeles, CA (2009-2010)
Mentor: Dr. Paul Micevych
Focus: Estradiol-triggered calcium release in hypothalamic
neurons
UCSF Institute for Neurodegenerative Diseases; San Francisco, CA
(2010)
Mentors: Drs. Sina Ghaemmaghami and Stanley Prusiner
Focus: *In vitro* generation of infectious prion protein from naïve
brain homogenate
- 2011-2012: Post-Baccalaureate Fellow
NIH/NIAAA, Laboratory of Molecular Physiology, Section on Cellular
Biophotonics; Rockville, MD
Mentor: Dr. Steven Vogel
Focus: Monitoring of CaMKII oligomerization states and
autophosphorylation

2012-Present PhD Graduate Student – NIH/Johns Hopkins University
Mentor: Dr. John T. Patton
Focus: Innate immune antagonism by rotavirus NSP1

Honors and Awards:

2007: Association for Women in Science Scholarship
2009: Undergraduate Student Intramural Research Training Award (IRTA), NIH
2011-2012: Post-Baccalaureate Intramural Research Training Award (IRTA), NIH
2012-2015: Pre-Doctoral Intramural Research Training Award (IRTA), NIH
2015: General Registration & Travel Award, 12th Annual Double-Stranded RNA Virus Symposium; Bill and Melinda Gates Foundation, Global Health Grant Number OPP1095046
2016: Avrum Gudelsky Graduate Student Award, UMD
2016-2017: Visiting Scientist at Janelia Farm, Howard Hughes Medical Institute
2017: ASV Travel and Registration Award, 2017
2017: Indiana University Selected Speaker Award, 3rd Place, Microbiology Annual Retreat

Professional Associations:

2016-Present: Student Member, American Society for Virology

Teaching and Mentoring Experience:

2013: Johns Hopkins University, Department of Biology Teaching Assistant Cell Biology Lab, Spring 2013
2014: Johns Hopkins University, Department of Biology Teaching Assistant Biochemistry Lab, Fall 2014
2015-2017: Mentor to UMD Undergraduate Student Research Assistants Morgan Driver (Spring 2016, Fall 2017, Spring 2017); Elizabeth Martinez (Fall 2015, Spring 2016); Ariana Braganza (Fall 2015)
2016-2017: Mentor to UMD Doctoral Students Asha Ann Philip (2016-2017); Chantal Ama Abgemabiese (2017)

Formal Oral Presentations:

2016: A hijacker takes the keys: activation of rotavirus NSP1 by CK2
Kaitlin A. Davis, John T. Patton
University of Maryland 13th Annual Virology Retreat; College Park, MD
2016: Activation of the rotavirus interferon antagonist NSP1 by CK2 phosphorylation
Kaitlin A. Davis, Marco Morelli, John T. Patton
UMD Veterinary Medicine Departmental Seminar; College Park, MD
2016: CK2 mediates phosphorylation of the β -TrCP targeting domain in rotavirus OSU NSP1
Kaitlin A. Davis, Marco Morelli, John T. Patton
American Society for Virology Annual Meeting; Blacksburg, VA

- 2017: Rotavirus NSP1 as a phosphorylated substrate adaptor of hijacked cullin-RING ligases
Kaitlin A. Davis, Marco Morelli, John T. Patton
 American Society for Virology Annual Meeting; Madison, WI
- 2017: Rotavirus NSP1 Requires Phosphorylation for Hijacking of Cullin-RING Ligases
Kaitlin A. Davis, John T. Patton
 Indiana University Annual Microbiology Retreat; Nashville, IN

Poster Presentations & Meeting Abstracts:

- 2013: Characterization of calmodulin kinase II inhibitor protein (CaMKIIN) by FPPA
 Jithesh V. Veetil, **Kaitlin A. Davis**, Henry L. Puhl III, Tuan A. Nguyen, Pabak Sarkar, Steven S. Vogel
 Biophysical Society Annual Meeting; Biophysical Journal, 2013
- 2013: Reducing the number of subunits in the CAMKII α holoenzyme alters catalytic domain pairing, diffusion time, and T286 autophosphorylation
 Pabak Sarkar, **Kaitlin A. Davis**, Tuan A. Nguyen, Jithesh V. Veetil, Henry L. Puhl, Steven S. Vogel
 Biophysical Society Annual Meeting; Biophysical Journal, 2013
- 2014: Positive cooperativity and T286 autophosphorylation is observed in a dimeric mutant of calcium/calmodulin dependent protein kinase II α
 Pabak Sarkar, **Kaitlin A. Davis**, Tuan A. Nguyen, Jithesh V. Veetil, Henry L. Puhl, Steven S. Vogel
 Biophysical Society Annual Meeting; Biophysical Journal, 2014
- 2014: Characterization of calcium-calmodulin kinase II inhibitor protein (CaMKIIN) by fluorescence polarization and fluctuation analysis
 Jithesh V. Veetil, **Kaitlin A. Davis**, Henry L. Puhl III, Tuan A. Nguyen, Pabak Sarkar, Steven S. Vogel
 Biophysical Society Annual Meeting; Biophysical Journal, 2014
- 2014: Development of rapid and quantitative methods to identify small molecule inhibitors of flavivirus budding
Kaitlin A. Davis, Richard J. Kuhn, Theodore C. Pierson
 NIH Graduate Partnership Program Annual Symposium; Bethesda, MD
- 2014: Context-dependent cleavage at the C-prM junction by the West Nile virus NS2B/3 protease modulates the efficiency of virus assembly and release
 Laura A. VanBlargan, **Kaitlin A. Davis**, Kimberly A. Dowd, Theodore C. Pierson
 ASV Annual Meeting; CO
- 2015: Context-dependent cleavage by the West Nile virus protease modulates the efficiency of virus assembly
 Laura A. VanBlargan, Kimberly A. Dowd, **Kaitlin A. Davis**, Theodore C. Pierson
 NIH Graduate Partnership Program Annual Symposium; Bethesda, MD
- 2015: Covert changes in CaMKII holoenzyme structure identified for activation

- and subsequent interactions
Tuan A. Nguyen, Pabak Sarkar, Jitesh V. Veetil, **Kaitlin A. Davis**, Henry L. Puhl, Steven S. Vogel
Biophysical Society Annual Meeting; Biophysical Journal, 2015
- 2015: NSP1 of rotavirus SA11-4F-like strains may not target IRFs for degradation through a C-terminal pLxIS motif
Kaitlin A. Davis, Marco Morelli, John T. Patton
12th Annual dsRNA Viruses Symposium; Goa, India
- 2015: NSP1 of group D rotaviruses inhibits NF- κ B activation without targeting β -TrCP for degradation
Kaitlin A. Davis, Marco Morelli, John T. Patton
12th Annual dsRNA Viruses Symposium; Goa, India
- 2016: Deciphering CaMKII multimerization using holoenzyme assembly mutants, FCS, and concurrent homo- and hetero-FRET analysis
Pabak Sarkar, Jithesh V. Veetil, **Kaitlin A. Davis**, Henry L. Puhl III, Tuan A. Nguyen, Steven S. Vogel
Biophysical Society Annual Meeting; Biophysical Journal, 2016
- 2017: Rotavirus NSP1 as a phosphorylated substrate adaptor of Cullin RING ligases
Kaitlin A. Davis, Marco Morelli, John T. Patton
Experimental Biology; Chicago, IL
- 2017: Rotavirus NSP1 requires CKII-mediated phosphorylation for hijacking of Cullin-RING ligases
Kaitlin A. Davis, Marco Morelli, John T. Patton
Gordon Research Conference, Viruses & Cells; Lucca (Barga), Italy

Publications:

Tuan A. Nguyen, Pabak Sarkar, Jithesh V. Veetil, **Kaitlin A. Davis**, Henry L. Puhl III, Steven S. Vogel (2015). Covert changes in CaMKII holoenzyme structure identified for activation and subsequent interactions. *Biophysical Journal*. 108(9):2158-2170.

Laura A. VanBlargan, **Kaitlin A. Davis**, Kimberly A. Dowd, Janet Smith, Theodore T. Pierson (2015). Context-dependent cleavage of the capsid protein by the West Nile virus protease modulates the efficiency of virus assembly. *Journal of Virology*. 89(16):8632-42.

Pabak Sarkar, **Kaitlin A. Davis**, Henry L. Puhl III, Jithesh V Veetil, Tuan A. Nguyen, Steven S. Vogel (2017). Deciphering CaMKII multimerization using fluorescence correlation spectroscopy, and homo-FRET analysis. *Biophysical Journal*. 112(6):1270-1281.

Kaitlin A. Davis, Marco Morelli, John T. Patton (2017). Rotavirus NSP1 requires CKII-mediated phosphorylation for hijacking of cullin-RING ligases. *mBio*. 8(4) e01213-17.

Kaitlin A. Davis, John T. Patton. (2017). Shutdown of interferon signaling by a viral-hijacked E3 ubiquitin ligase. *Microbial Cell*. (11): 387-389.

Kaitlin A. Davis, John T. Patton (2017). Cullin-RING ligases and viral adaptors: novel repurposing of a familiar tool. *Journal of General Virology* (submitted)